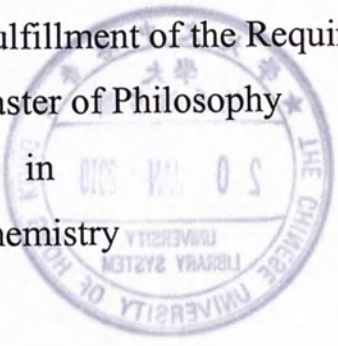


**Synthesis, Structural Characterization and Electrochemistry of 13-
Vertex Carboranes and Their Radical Anions**

FU, Xiaodu

A Thesis Submitted in Partial Fulfillment of the Requirements for the
Degree of Master of Philosophy
in
Chemistry



© The Chinese University of Hong Kong
July 2008

The Chinese University of Hong Kong holds the copyright of this thesis. Any person(s) intending to use a part or whole of the materials in this thesis in a proposed publication must seek copyright release from the Dean of the Graduate School.



Assessment Committee:

Professor Thomas Chung Wai Mak, Chair

Professor Kin Shing Chan, Committee Member

Professor Zuowei Xie, Research Supervisor

Professor Zhenyang Lin, External Examiner

To my Father!

獻給我的父親！

Acknowledgement

I would like to express my sincere thanks to my supervisor, Professor Zuowei XIE, for his guidance, encouragement, and help during my study in the past two years. He is responsible for involving me in the fascinating research of carborane chemistry and helping me complete writing of this dissertation as well as the challenging research that lies behind it.

I would like to thank Ms. Hoi-Shan CHAN for the determination of single-crystal X-ray structures, Mr. Chi-Chung LEE for mass spectra measurement and Prof. Hung-Kay LEE for the measurement of EPR spectra.

I am also grateful to my group mates, Dr. Liang DENG, Dr. Hao SHEN, Ms. Dongmei LIU, Mr. Jian ZHANG, Ms. Mei-Mei SIT, Ms. Zaozao QIU, Mr. Shikuo REN and Ms. Jingnan CHEN for their helpful discussion and suggestions.

I also thank my friends and staffs of the Department of Chemistry and Graduate School for their help and supports during the course of my study.

I am greatly indebted to The Chinese University of Hong Kong for the award of a Postgraduate Studentship and to the Hong Kong Research Grants Council for the financial support.

Abstract

Boranes and carboranes with odd skeletal electron counts are rare. This work describes one-electron reduction of 13-vertex carboranes by group 1 metal. Several carborane radical anions, $[1,2-(\text{CH}_2)_3-1,2-\text{C}_2\text{B}_{11}\text{H}_{11}][\text{Na}(18\text{-crown-6})(\text{THF})_2]$ (**III-1**), $[1,2-(\text{CH}_2)_3-3\text{-Ph-}1,2-\text{C}_2\text{B}_{11}\text{H}_{10}][\text{Na}(18\text{-crown-6})(\text{THF})_2]$ (**III-2**), $[1,2-(\text{CH}_2)_4-1,2-\text{C}_2\text{B}_{11}\text{H}_{11}][\text{Na}(18\text{-crown-6})(\text{THF})_2]$ (**III-3**) and $[1,2-(\text{CH}_2)_4-3\text{-Ph-}1,2-\text{C}_2\text{B}_{11}\text{H}_{10}][\text{Na}(18\text{-crown-6})(\text{THF})_2]$ (**III-4**) with $2n+3$ framework electrons were prepared and structurally characterized by single-crystal X-ray analyses. They fall between the two well-established and abundant closed $2n+2$ (*closo*) and open $2n+4$ (*nido*) structural systems. The results may imply that larger cages would enhance the thermodynamical stability of clusters with $2n+3$ systems.

摘要

含有奇数骨架电子的硼烷和碳硼烷是非常稀少的。本文描述了使用碱金属对 13 顶点超级碳硼烷进行还原，来合成具有 $2n+3$ 骨架电子的碳硼烷自由基阴离子 $[1,2-(\text{CH}_2)_3-1,2-\text{C}_2\text{B}_{11}\text{H}_{11}][\text{Na}(18\text{-crown-6})(\text{THF})_2]$ **(III-1)**， $[1,2-(\text{CH}_2)_3-3\text{-Ph-}1,2-\text{C}_2\text{B}_{11}\text{H}_{10}][\text{Na}(18\text{-crown-6})(\text{THF})_2]$ **(III-2)**， $[1,2-(\text{CH}_2)_4-1,2-\text{C}_2\text{B}_{11}\text{H}_{11}][\text{Na}(18\text{-crown-6})(\text{THF})_2]$ **(III-3)** 和 $[1,2-(\text{CH}_2)_4-3\text{-Ph-}1,2-\text{C}_2\text{B}_{11}\text{H}_{10}][\text{Na}(18\text{-crown-6})(\text{THF})_2]$ **(III-4)**，并对其结构使用 X-ray 单晶衍射进行了测定。此类含 $2n+3$ 电子的簇合物正好落在已经有大量实例的 $2n+2$ (封闭式) 和 $2n+4$ (鸟巢式) 结构体系之间，而 $2n+3$ 电子体系的簇合物之前从未被成功合成，虽然先前对碳硼烷电化学的研究表明此类化学物应当存在。本文的研究表明大的笼状体系可以增加含 $2n+3$ 电子簇合物的热力学稳定性。

Abbreviation	
br	broad
ⁿ BuLi	<i>n</i> -butyl lithium
CAd	carbon-atom-adjacent
CAP	carbon-atom-apart
d	doublet (NMR)
dd	doublet of doublets (NMR)
m	multiplet (NMR)
s	singlet (NMR)
t	triplet (NMR)
DME	dimethoxyethane
Et	ethyl
Et ₂ O	diethyl ether
IR	infrared spectroscopy
NMR	nuclear magnetic resonance spectroscopy
M	metal
Me	methyl
MS	mass spectrometry
Ph	phenyl
TBAF	tetrabutylammonium fluoride
THF	tetrahydrofuran
xs	excess

List of Compounds

Compd. No.	Compound Formula	Page No.
I-1	1,2-(CH ₂) ₃ -1,2-C ₂ B ₁₀ H ₁₀	25
I-2	1,2-(CH ₂) ₄ -1,2-C ₂ B ₁₀ H ₁₀	25
I-3	1,2-(CH ₂ CH=CHCH ₂)-1,2-C ₂ B ₁₀ H ₁₀	25
I-4	1,2-[<i>o</i> -C ₆ H ₄ (CH ₂) ₂]-1,2-C ₂ B ₁₀ H ₁₀	25
I-5	1,2-Me ₂ Si(CH ₂) ₂ -1,2-C ₂ B ₁₀ H ₁₀	25
I-6	1,2-[1-CH ₃ -(C=CHCH ₂)]-1,2-C ₂ B ₁₀ H ₁₀	33
I-7	1,2-[1-CH ₃ -3-Ph-(C=CHCH)]-1,2-C ₂ B ₁₀ H ₁₀	33
I-8	1,2-{1',4'-[EtC=C(Et)-C(Et)=CEt]}-1,2-C ₂ B ₁₀ H ₁₀	33
I-9	1,2-[1,8-C ₁₀ H ₆ (CH ₂) ₂]-1,2-C ₂ B ₁₀ H ₁₀	60
I-10	1,2-(1-methyl-2,5-cyclohexadiene-1,4-diyl)-1,2-C ₂ B ₁₀ H ₁₀	61
II-1	1,2-(CH ₂) ₃ -1,2-C ₂ B ₁₁ H ₁₁	26
II-2	1,2-(CH ₂) ₃ -3-Ph-1,2-C ₂ B ₁₁ H ₁₀	26
II-3	1,2-(CH ₂) ₄ -1,2-C ₂ B ₁₁ H ₁₁	26
II-4	1,2-(CH ₂) ₄ -3-Ph-1,2-C ₂ B ₁₁ H ₁₀	26
II-5	1,2-(CH ₂ CH=CHCH ₂)-1,2-C ₂ B ₁₁ H ₁₁	26
II-6	1,2-(CH ₂ CH=CHCH ₂)-3-Ph-1,2-C ₂ B ₁₁ H ₁₀	26
II-7	1,2-[<i>o</i> -C ₆ H ₄ (CH ₂) ₂]-1,2-C ₂ B ₁₁ H ₁₁	26
II-8	1,2-Me ₂ Si(CH ₂) ₂ -1,2-C ₂ B ₁₁ H ₁₁	26
II-9	1,2-Me ₂ -1,2-C ₂ B ₁₁ H ₁₁	26
II-10	1,6-Me ₂ -1,6-C ₂ B ₁₁ H ₁₁	26
II-11	1,2-Me ₂ -3-Ph-1,2-C ₂ B ₁₁ H ₁₀	26
III-1	[1,2-(CH ₂) ₃ -1,2-C ₂ B ₁₁ H ₁₁][Na(18-crown-6)(THF) ₂]	36

III-2	[1,2-(CH ₂) ₃ -3-Ph-1,2-C ₂ B ₁₁ H ₁₀][Na(18-crown-6)(THF) ₂]	36
III-3	[1,2-(CH ₂) ₄ -1,2-C ₂ B ₁₁ H ₁₁][Na(18-crown-6)(THF) ₂]	36
III-4	[1,2-(CH ₂) ₄ -3-Ph-1,2-C ₂ B ₁₁ H ₁₀][Na(18-crown-6)(THF) ₂]	37
IV-7	[1,2-{ <i>o</i> -C ₆ H ₄ (CH ₂)(CH)}-1,2-C ₂ B ₁₁ H ₁₁][Li(THF) ₄]	46

List of Figures

Fig. No.	Compd. No.	Content	Page No.
1.1		Cage frameworks based on a 12-vertex icosahedral cluster	1
1.2		Typical three-center two-electron bonds involved in borane clusters	1
1.3		Structure of known polyhedral $C_2B_nH_{n+2}$ molecules	2
2.1		Stick representation of the chemical shifts and relative intensities in the $^{11}B\{^1H\}$ spectra of compound II-1 to II-11	29
2.2	II-4	Molecular structure of 1,2-(CH ₂) ₄ -3-Ph-1,2-C ₂ B ₁₁ H ₁₀	30
2.3	II-6	Molecular structure of 1,2-(CH ₂ CH=CHCH ₂)-3-Ph-1,2-C ₂ B ₁₁ H ₁₀	31
2.4	I-7	Molecular structure of 1,2-[1-CH ₃ -3-Ph-(C=CHCH)]-1,2-C ₂ B ₁₀ H ₁₀	34
3.1		EPR spectra of III-1 in solid state and THF solution and of III-2 , III-3 and III-4 in THF solution.	38
3.2		UV-Vis Spectra of III-1 , III-2 , III-3 , III-4 and II-2	40
3.3	III-1	Molecular structure of $[(CH_2)_3C_2B_{11}H_{11}]^{\bullet-}$ in III-1	41
3.4	III-3	Molecular structure of [1,2-(CH ₂) ₄ -1,2-C ₂ B ₁₁ H ₁₁][Na(18-crown-6)(THF) ₂]	43
3.5	III-4	Molecular structure of [1,2-(CH ₂) ₄ -3-Ph-1,2-C ₂ B ₁₁ H ₁₁][Na(18-crown-6)(THF) ₂]	43
3.6	IV-7	Molecular structure of [1,2-{ <i>o</i> -C ₆ H ₄ (CH ₂)(CH)}-1,2-C ₂ B ₁₁ H ₁₁][Li(THF) ₄]	47

4.1	I-1	Cyclic voltammograms of I-1 in MeCN/0.1M Bu ₄ NPF ₆ recorded at 100 mV/s	53
4.2	I-2	Cyclic voltammograms of I-2 in MeCN/0.1M Bu ₄ NPF ₆ recorded at 100 mV/s	54
4.3	I-3	Cyclic voltammograms of I-3 in MeCN/0.1M Bu ₄ NPF ₆ recorded at 100 mV/s	55
4.4	I-4	Cyclic voltammograms of I-4 in MeCN/0.1M Bu ₄ NPF ₆ recorded at 100 mV/s	56
4.5	I-6	Cyclic voltammograms of I-6 in MeCN/0.1M Bu ₄ NPF ₆ recorded at 100 mV/s	57
4.6	I-7	Cyclic voltammograms of I-7 in MeCN/0.1M Bu ₄ NPF ₆ recorded at 100 mV/s	58
4.7	I-8	Cyclic voltammograms of I-8 in MeCN/0.1M Bu ₄ NPF ₆ recorded at 100 mV/s	59
4.8	I-9	Cyclic voltammograms of I-9 in MeCN/0.1M Bu ₄ NPF ₆ recorded at 100 mV/s	60
4.9	I-10	Cyclic voltammograms of I-10 in MeCN/0.1M Bu ₄ NPF ₆ recorded at 100 mV/s	61
4.10	II-1	Cyclic voltammograms of II-1 in MeCN/0.1M Bu ₄ NPF ₆ recorded at 100 mV/s	63
4.11	II-2	Cyclic voltammograms of II-2 in MeCN/0.1M Bu ₄ NPF ₆ recorded at 100 mV/s	64
4.12	II-3	Cyclic voltammograms of II-3 in MeCN/0.1M Bu ₄ NPF ₆ recorded at 100 mV/s	65
4.13	II-4	Cyclic voltammograms of II-4 in MeCN/0.1M Bu ₄ NPF ₆	66

		recorded at 100 mV/s	
4.14	II-5	Cyclic voltammograms of II-5 in MeCN/0.1M Bu ₄ NPF ₆ recorded at 100 mV/s	67
4.15	II-6	Cyclic voltammograms of II-6 in MeCN/0.1M Bu ₄ NPF ₆ recorded at 100 mV/s	68
4.16	II-7	Cyclic voltammograms of II-7 in MeCN/0.1M Bu ₄ NPF ₆ recorded at 100 mV/s	69
4.17	II-8	Cyclic voltammograms of II-8 in MeCN/0.1M Bu ₄ NPF ₆ recorded at 100 mV/s	70
4.18	II-9	Cyclic voltammograms of II-9 in MeCN/0.1M Bu ₄ NPF ₆ recorded at 100 mV/s	71
4.19	II-10	Cyclic voltammograms of II-10 in MeCN/0.1M Bu ₄ NPF ₆ recorded at 100 mV/s	72
4.20	II-11	Cyclic voltammograms of II-11 in MeCN/0.1M Bu ₄ NPF ₆ recorded at 100 mV/s	73

Contents

Acknowledgement	I
Abstract (in English)	II
Abstract (in Chinese)	III
Abbreviation	IV
List of Compounds	V
List of Figures	VII
Contents	X
Chapter 1 Introduction	1
1.1 Carboranes	1
1.2 C,C'-Linked 12-Vertex Carborane Anions	10
1.3 13-Vertex <i>closo</i> -Carboranes	13
1.4 13-Vertex <i>nido</i> -Carborane Salts and 14-Vertex <i>closo</i> -Carboranes	16
1.5 Carborane Radical Anions	19
1.6 Our Objectives	23
Chapter 2 13-Vertex Carboranes	24
2.1 Synthesis and Characterization of 13-Vertex <i>closo</i> -Carboranes	24
2.2 Molecular Structures of II-4 and II-6	30
2.3 Attempts to prepare 13-vertex carboranes with propenyl bridges	33
2.4 Summary	35
Chapter 3 13-Vertex Carborane Radical Anions	36
3.1 Synthesis	36
3.2 Structures	41
3.3 Synthesis and Structure of a monoanionic salt	46

3.4 Summary	50
Chapter 4 Electrochemical Study of 12- and 13-Vertex <i>closo</i> -Carboranes	51
4.1 Electrochemical Study of 12-Vertex Carboranes	51
4.2 Electrochemical Study of 13-Vertex Supercarboranes	61
4.3 Summary	74
Chapter 5 Conclusion	75
Chapter 6 Experimental Section	77
References	93
Appendix	
I. Publication Based on the Research Findings	103
II. Crystal Data and Summary of Data Collection and Refinement	104
III. X-ray crystallographic data in CIF (electronic form)	

Chapter 1. Introduction

1.1. Carboranes

Carboranes are a class of boron cluster compounds with one or more polyhedral boron vertices replaced by carbon which have been known since the 1960s.¹ These electron-deficient neutral compounds are classified as *closo*-, *nido*-, *arachno*-, and *hypho*-, etc.² according to the number of skeletal electrons. Their structures are related to each other as the *closo*-species adopts closed polyhedral structure with all faces triangulated whereas those of the *nido*-, *arachno*-, and *hypho*-compounds can be viewed by sequential removal of one, two, and three vertices from the *closo*-ones, respectively. Figure 1.1 demonstrates their relationships.

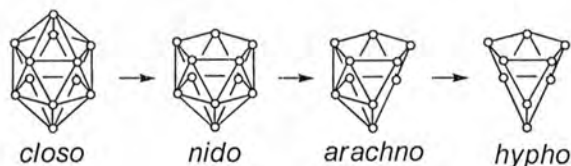


Figure 1.1. Cage frameworks based on a 12-vertex icosahedral cluster.

As the classical two-center bond concept is inadequate for electron-deficient situations, the bonding structure of such molecules can be written by employing the concept of three-center two-electron bonding, in which three atoms are linked by a single pair of electrons.³ In these clusters several types of three-center two-electron bonds may be involved, as shown in Figure 1.2.

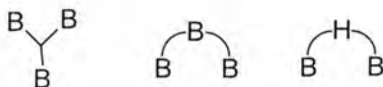


Figure 1.2. Typical three-center two-electron bonds involved in borane clusters.

1.1.1. Structure and Synthesis of *closo*-Carboranes

The *closo*-carboranes ($C_2B_nH_{n+2}$) are the oldest and most investigated ones in the carborane family.^{4,5} As earlier as 1960s, the *closo*-carboranes of the general formula $C_2B_nH_{n+2}$ were known for $n = 3$ to 10.^{4a} Figure 1.3 shows the geometries of these molecules. The preparative routes to these compounds vary as the cluster sizes differ. The small carboranes $C_2B_nH_{n+2}$ ($n = 3$ to 5) are normally formed *via* high-energy combination of volatile boranes and alkynes in electric discharge or flash reactions.^{1,6} Other methods such as conversion of *nido*-carboranes to *closo*-carboranes,⁷ reactions of alkylboranes with alkynes,⁸ dehalogenation of alkylhaloboranes with alkali metals, were also reported.⁹

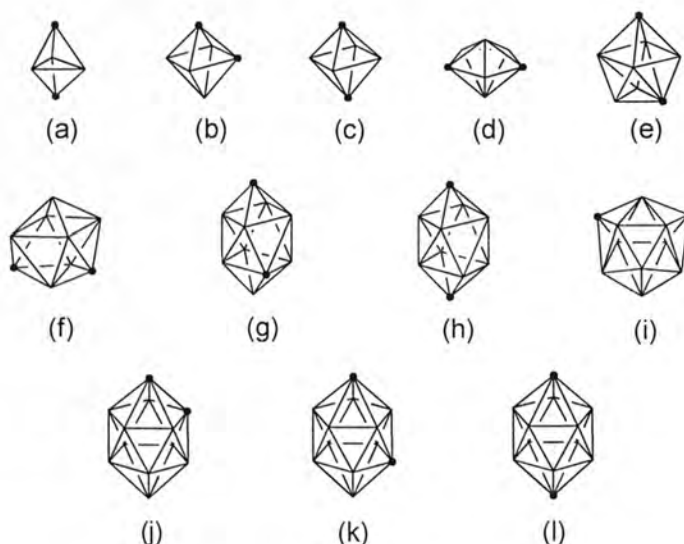
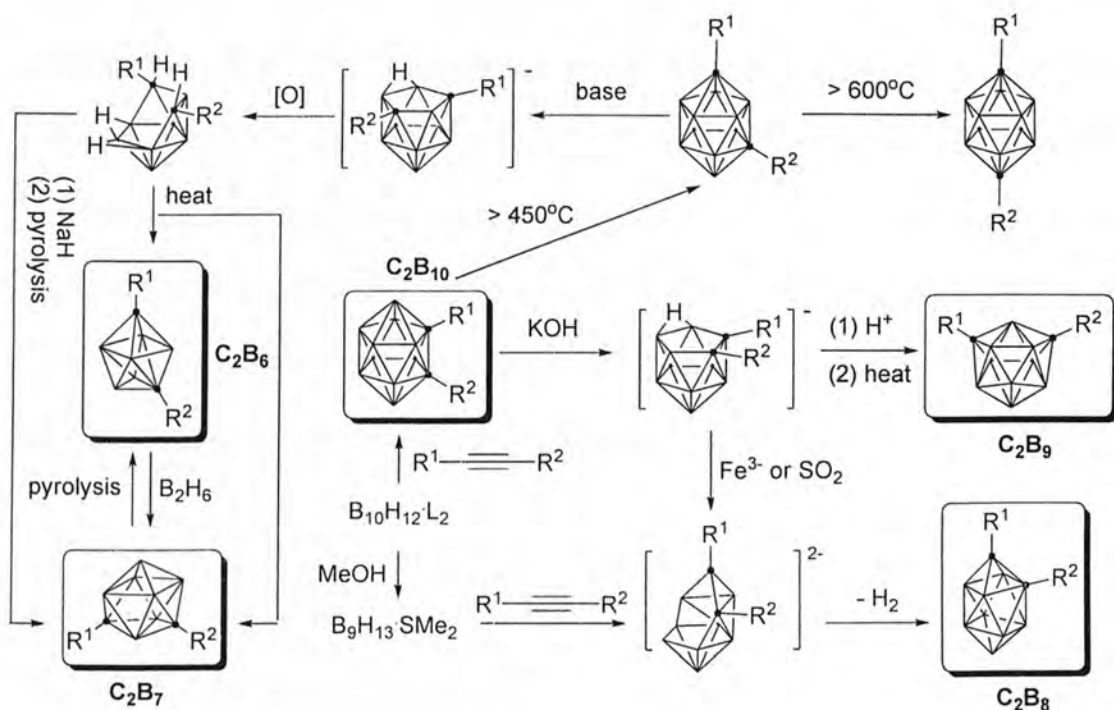


Figure 1.3. Structure of known polyhedral $C_2B_nH_{n+2}$ molecules. (a) 1,5- $C_2B_3H_5$. (b) 1,2- $C_2B_4H_6$. (c) 1,6- $C_2B_4H_6$. (d) 2,4- $C_2B_5H_7$. (e) 1,7- $C_2B_6H_8$. (f) 4,5- $C_2B_7H_9$. (g) 1,6- $C_2B_8H_{10}$. (h) 1,10- $C_2B_8H_{10}$. (i) 2,3- $C_2B_9H_{11}$. (j) 1,2- $C_2B_{10}H_{12}$. (k) 1,7- $C_2B_{10}H_{12}$. (l) 1,12- $C_2B_{10}H_{12}$.

The intermediate *closo*-carboranes $C_2B_nH_{n+2}$ ($n = 6$ to 9) are usually prepared by the degradation of icosahedral carboranes $R_2C_2B_{10}H_{10}$, which can be readily synthesized through the reaction of $B_{10}H_{12}L_2$ with alkynes, as shown in Scheme

1.1.¹⁰ The icosahedral carboranes $R_2C_2B_{10}H_{10}$ are attacked by strong Lewis bases to yield $R_2C_2B_9H_{10}^-$ ions. Protonation of the ions followed by pyrolysis yields the 11-vertex 1,8-*closo*- $R_2C_2B_9H_9$.¹¹

Scheme 1.1. Synthetic method of *closo*- o - $C_2B_nH_{n+2}$ ($n = 6$ to 10).

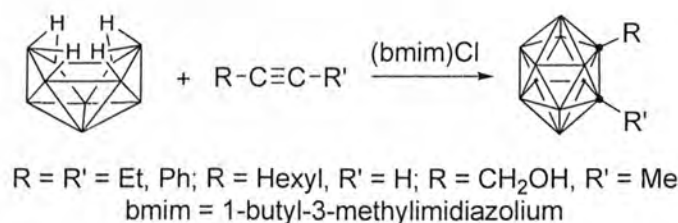


Degradation of 1,8-*closo*- $R_2C_2B_9H_9$ or oxidation of 1,7- $R_2C_2B_9H_{10}^-$ ions produces an open-cage structure of 1,3- $R_2C_2B_7H_{11}$. The pyrolysis of 1,3- $R_2C_2B_7H_{11}$ yields a mixture of 8-vertex carborane 1,7- $R_2C_2B_6H_6$, 9-vertex carborane 1,7- $R_2C_2B_7H_7$, and 10-vertex carborane 1,6- $R_2C_2B_8H_8$.¹² On the other hand, the 10-vertex carboranes 1,2- $R_2C_2B_8H_8$ can be prepared by thermal or base-induced dehydrogenation of *nido*-carboranes 7,8- $R_2C_2B_9H_{10}^-$, which are obtained either through sequential deboration of 12-vertex o - $R_2C_2B_{10}H_{10}$ or by acetylene insertion to $B_9H_{13} \cdot SMe_2$.¹³ The 9-vertex carboranes 1,7- $R_2C_2B_7H_7$ can also be prepared in a relatively high yield by pyrolysis of the sodium salt of 1,3- $R_2C_2B_7H_{11}$ in

diphenylether.¹² Good yields of 8-vertex carboranes $R_2C_2B_6H_6$ are also obtained from the pyrolysis of pure 1,3- $R_2C_2B_7H_{11}$ in vacuum.¹²

As mentioned above, *ortho*-carboranes (o - $R_2C_2B_{10}H_{10}$) are normally synthesized by a two-step process starting from decaborane $B_{10}H_{14}$.¹⁰ The reactions involve *in situ* formation of the $B_{10}H_{12}L_2$ adduct followed by alkyne insertion. The typical yields of this method for terminal alkynes range from 6 to 75%, whereas much lower yields are given or even no reaction takes place for many internal alkynes. Recently, Sneddon and co-workers reported an improved method for the synthesis of 1,2-disubstituted *o*-carboranes by direct reaction of $B_{10}H_{14}$ or 6- R - $B_{10}H_{13}$ with terminal or internal alkynes in ionic liquid in high yields (Scheme 1.2).¹⁴

Scheme 1.2. Synthesis of *o*-carboranes in ionic liquid.



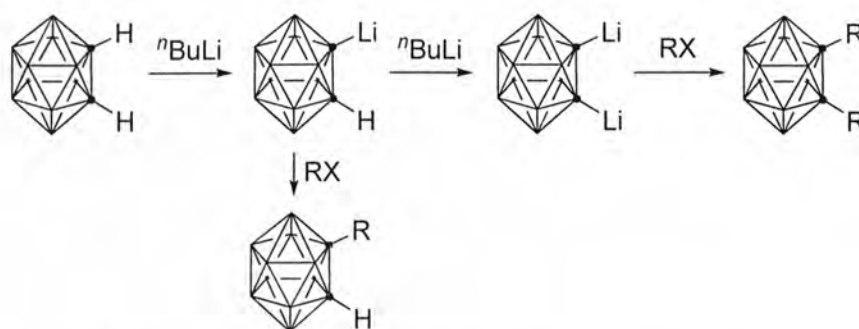
1.1.2. *o*-Carboranes

In the field of boranes and heteroboranes, the chemistry of *o*-carboranes is extensively investigated, owing to commercial availability. There are six types of important reactions for *o*-carboranes: (1) deprotonation and introduction of functional groups at the cage CH vertices; (2) electrophilic substitution at the cage BH vertices; (3) base-promoted removal of BH vertex from the cage to form *nido*-species; (4) reduction of the cage to form *nido*- and *arachno*-species; (5) thermal rearrangement; and (6) preparation of supercarboranes from *nido*- and *arachno*-species.

The *o*-carborane unit displays strong electron-withdrawing characters with respect to substituents attached to the carbon atoms. The mildly acidic C-H bonds in

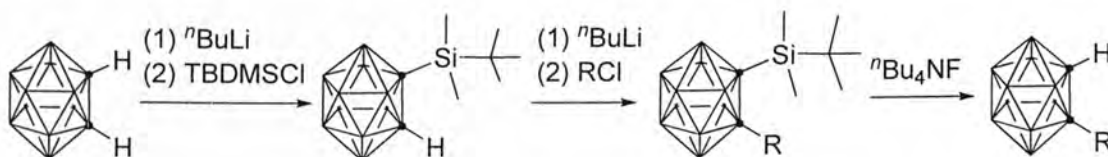
o-carborane (with the pK_a value of ~ 23) react easily with strong bases such as $n\text{BuLi}$, PhLi to form C-monolithio-*o*-carborane or C,C'-dilithio-*o*-carborane, which can be converted into the corresponding mono- or di-organosubstituted products (Scheme 1.3).¹⁶ The synthesis of a mono-C-substituted *o*-carborane is a difficult problem due to the disproportionation of monolithio-*o*-carborane which leads to the undesired disubstituted product.^{16b}

Scheme 1.3. Functionalization of *o*-carborane on the CH vertices.



Hawthorne et al. proposed to protect one carbon atom of *o*-carborane by *tert*-butyldimethylsilyl (TBDMS), as the reactions between mono- or dilithio-*o*-carborane with TBDMSCl only give monosubstituted product and the TBDMS group can be easily removed in the further deprotection step, which makes the synthesis of mono-substituted *o*-carborane facile (Scheme 1.4).¹⁷ The easy functionalization of the cage CH vertices results in the emergence of numerous carborane derivatives which made the further application possible.^{4a}

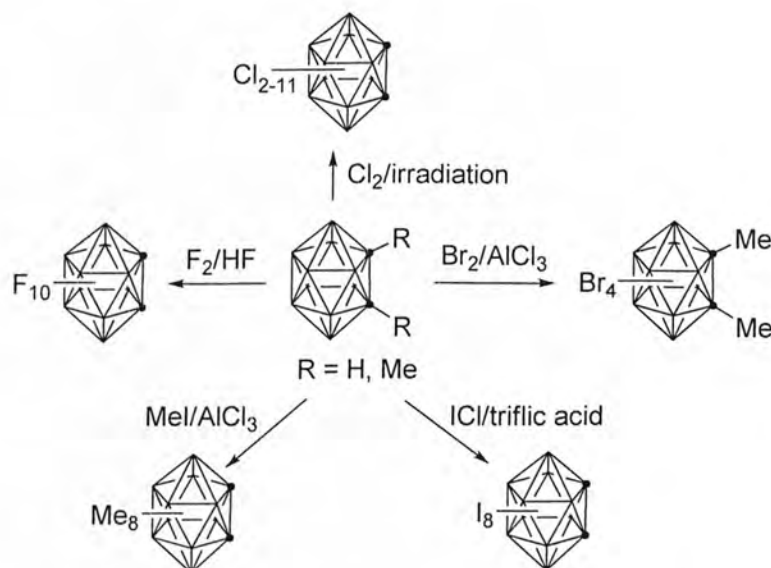
Scheme 1.4. Synthesis of mono-substituted *o*-carboranes.



It is generally accepted that icosahedral carboranes are aromatic¹⁸ and undergo electrophilic substitution reactions. The *o*-carborane contains four distinct types of

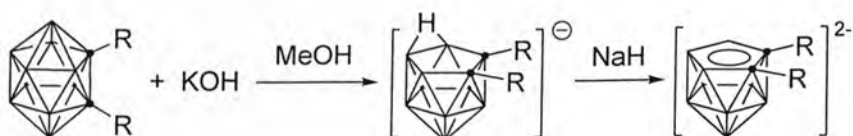
boron atoms that may be ordered according to their distance from the carbon atoms, with B(9,12) being the farthest away, followed by B(8,10), B(4,5,7,11), and B(3,6) which are adjacent to both carbon atoms. Those farthest from the carbon atoms are the more electron-rich and those closest are the more electron-poor. As a result, the full substitution is difficult to achieve except for the very strong electrophiles. For examples, the reaction of *o*-carborane with excess elemental fluorine in liquid hydrogen fluoride resulted in *o*-C₂B₁₀F₁₀H₂,¹⁹ and the chlorination resulted in the stepwise formation of a number of chlorocarboranes containing two to eleven chlorine atoms per molecule.²⁰ But perbromination has not been accomplished and only a maximum of four bromine atoms have been incorporated in carboranes to date.²¹ As the iodination of *o*-carborane with iodine in the presence of AlCl₃ can only give the diiodo-*o*-carborane,²² the reaction of ICl with *o*-carborane in triflic acid affords octaiodo-*o*-carborane.²³ Octamethyl-*o*-carborane has also been obtained by the direct methylation of *o*-carborane with MeI in the presence of AlCl₃ (Scheme 1.5).²⁴ It should be mentioned that the cage CH vertices are intact in these electrophilic reactions due to the higher electronegativity of carbon than that of boron.

Scheme 1.5. Electrophilic substitution reactions on *o*-carborane.

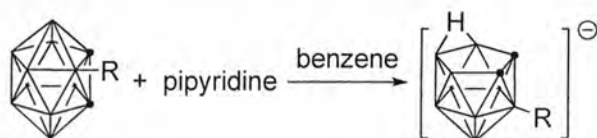


Although *o*-carborane cage exhibits a resistance to degradation that is extraordinary when compared to the binary boron hydrides and conventional organoboron structures, strong bases can remove the B(3) or B(6) vertex forming *nido*-C₂B₉H₁₂⁻ anion.²⁵ Deprotonation of this anion with strong base, such as NaH, ^{*n*}BuLi, gives the corresponding dianion *nido*-C₂B₉H₁₁²⁻ (Scheme 1.6).²⁶ The dicarbollide anion *nido*-C₂B₉H₁₁²⁻ is an isolobal analog of C₅H₅⁻ which makes it very useful for the preparation of metallocarborane and B(3) substituted carboranes. Pipyridine is a relatively mild deboration reagent when compared to KOH or MeOK, as the latter always results in C(cage)-C(organo-substituent) bond breaking and shows no selectivity for BH and BR moieties in the deboration process, whereas the former shows a good selectivity for both of them (Scheme 1.7).²⁷

Scheme 1.6. Deboration of *o*-carboranes.

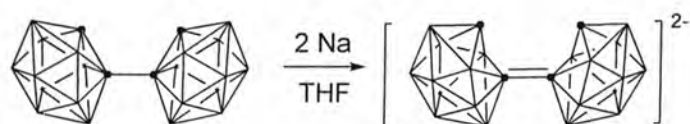


Scheme 1.7. Regioselective deboration of 3-substituted *o*-carboranes.

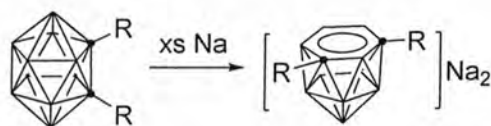


The electron-deficient carborane cage can accept electrons to form mono-, di-, or tetraanionic species with different types of geometries depending on the properties of the tethering groups of the carbon vertices. The only case of single-electron reduction of carborane was reported by Hawthorne. Partial reduction of C,C'-linked biscarborane with two equiv of sodium metal in THF affords a novel $\text{Na}_2[(\text{C}_2\text{B}_{10}\text{H}_{11})_2]$ salt, in which each carborane cage uptakes one electron leading to the cage C-C bond breaking and the formation of a multiple C(cage)-C'(cage) bond (Scheme 1.8).²⁸ Two-electron reduction is a popular phenomenon in the reduction of *o*- $\text{R}_2\text{C}_2\text{B}_{10}\text{H}_{10}$ ($\text{R} = \text{H}$, alkyl, aryl) with group 1 metals, which gives carbon-atom-apart dianionic species [*nido*-7,9- $\text{R}_2\text{C}_2\text{B}_{10}\text{H}_{10}$]²⁻ (Scheme 1.9).²⁹ These species hold an open six-membered C_2B_4 face with the carbon atoms in *meta* positions, which are isolobal analogy as benzene derivatives making them very useful for the preparation of metallocarboranes.

Scheme 1.8. Reduction of biscarborane.



Scheme 1.9. Synthesis of [*nido*-7,9- $\text{R}_2\text{C}_2\text{B}_{10}\text{H}_{10}$]²⁻ anions.



Our group developed an efficient method for the synthesis of different types of carborane anions.³⁰ By varying the bridge length of cage carbons-linked

o-carboranes, the two cage carbon atoms are locked in place during the reactions, leading to the controlled synthesis of *ortho*-, *meta*-, and *para*-isomer of *nido*-carborane dianions when *o*-carboranes are reduced by sodium or potassium metal.^{30c} Among these dianions, carbon-atom-adjacent *nido*-carborane dianions are more reactive than their carbons-apart counterparts and can be directly reduced by lithium metal to form the carbon-atom-adjacent *arachno*-carborane tetraanions.³⁰ These tetraanions can also be prepared by the direct interaction of the corresponding *o*-carboranes with excess lithium metal (Scheme 1.10). The *arachno*-carborane anions hold two open faces with one being a six-membered C₂B₄ face and the other being a five-membered C₂B₃ face. In the presence of transition metal ions, other two types of *arachno*-carborane tetraanions were also accessible. This will be discussed in the following part. Chart 1.1 lists the known geometries of C₂B₁₀ anions based on *o*-carboranes.

Scheme 1.10. Controlled synthesis of carborane anions.

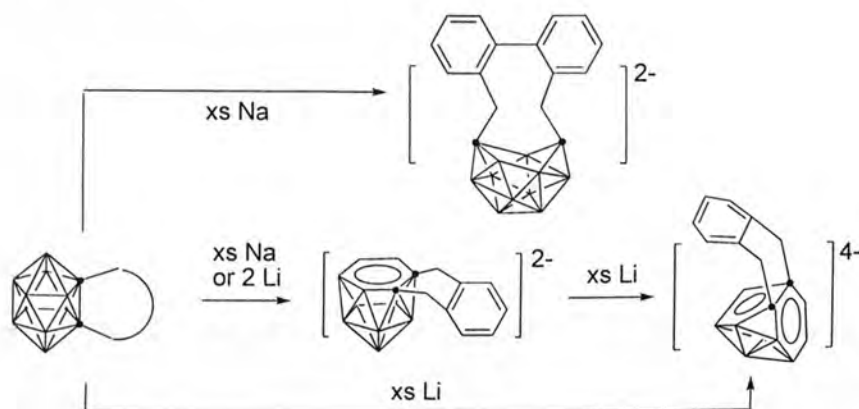
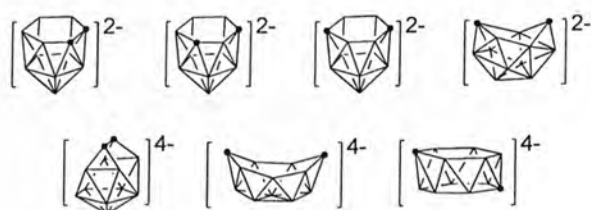
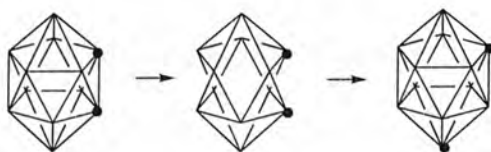


Chart 1.1. Reported carborane anions of the C₂B₁₀ system.



Another characteristic feature of *o*-carboranes and their derivatives is their thermal isomerization involving intramolecular rearrangement of the cage skeleton which makes the separation of the cage carbon atoms.³¹ The mechanism for the isomerization is still not clear which may involve several pathways. The “diamond-square-diamond” process³² originally proposed by Lipscomb plays a role in the rearrangement process of *o*-carborane to *m*-carborane as depicted in Scheme 1.11.

Scheme 1.11. Possible mechanism for isomerization of *o*-carborane to *m*-carborane.



1.2. C,C'-Linked 12-Vertex Carborane Anions

It is well established that the reduction of *o*-R₂C₂B₁₀H₁₀ by group 1 metals always results in the complete cleavage of the cage carbon-carbon bond, leading to the formation of “carbon-atom-apart” (CAp) *nido*-carborane dianions [7,9-*nido*-R₂C₂B₁₀H₁₀]²⁻ (*meta* in Chart 2.1).²⁹ They are very useful ligands for the production of numerous metallacarboranes of s, p, d, and f elements.^{33,34} Our group recently developed a method to control the relative positions of the cage carbon atoms during the reduction process by introducing a bridge between the two cage carbon atoms.³⁰ Thus the syntheses of “carbon-atom-adjacent” *nido*-carborane dianions (CAAd) [7,8-*nido*-R₂C₂B₁₀H₁₀]²⁻ (*ortho* in Chart 1.2) and CAp [7,10-*nido*-R₂C₂B₁₀H₁₀]²⁻ (*para* in Chart 1.2) were achieved.³⁰ The results showed that a short bridge can not only lock the cage carbon atoms in *ortho* positions, but

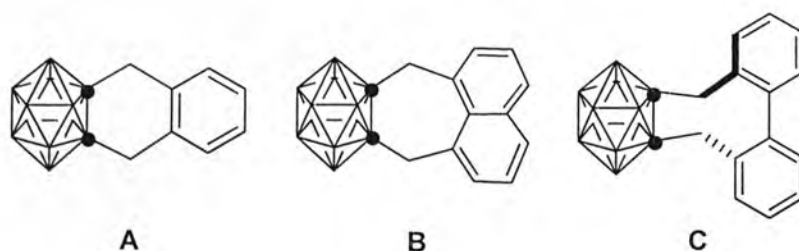
also lower the reducing power of the resulting dianions, leading to the formation of CAd [*arachno*-R₂C₂B₁₀H₁₀]⁴⁻ by further reduction with Li metal.³⁰

Chart 1.2. Isomers of *nido*-C₂B₁₀H₁₂²⁻.



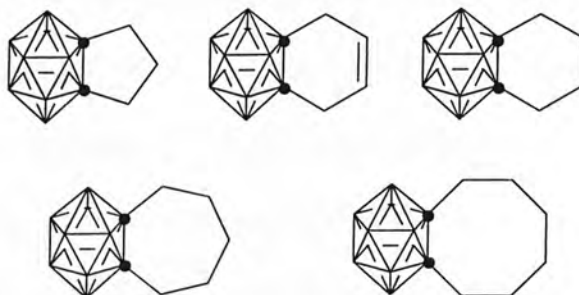
These CAd *nido*- and *arachno*-carborane anions are interesting ligands to transition metals.^{30c,35,36} Most importantly, they are finding applications in the preparation of 13-vertex carboranes. For example, the Welch's group reported the synthesis of a 13-vertex carborane 1,2-C₆H₄(CH₂)₂-3-Ph-1,2-C₂B₁₁H₁₀ using the CAd [*nido*-1,2-C₆H₄(CH₂)₂-1,2-C₂B₁₀H₁₀]²⁻ as the starting material.¹⁵

Chart 1.3. *o*-Carboranes with aromatic bridges.

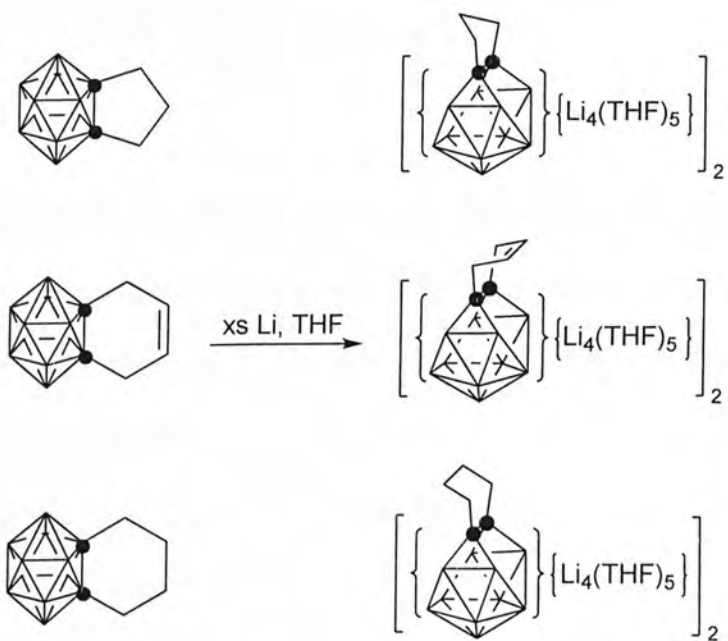


Our earlier study on the reactions of 1,2-Ar(CH₂)₂-1,2-C₂B₁₀H₁₀ (Chart 1.3) with group 1 metals showed that the aromatic bridges have significant effects on the formation of carborane anions.³⁰ However, the rigidity of these bridges made the conclusions ambiguous. Our group extended our research to include *o*-carboranes with aliphatic bridges, 1,2-(CH₂)_n-1,2-C₂B₁₀H₁₀ (n = 3 - 6) (Chart 1.4), and studied their reactions with group 1 metals.³⁷ Differences and similarities among carboranes with aromatic and aliphatic bridges in the reduction reactions are shown below.

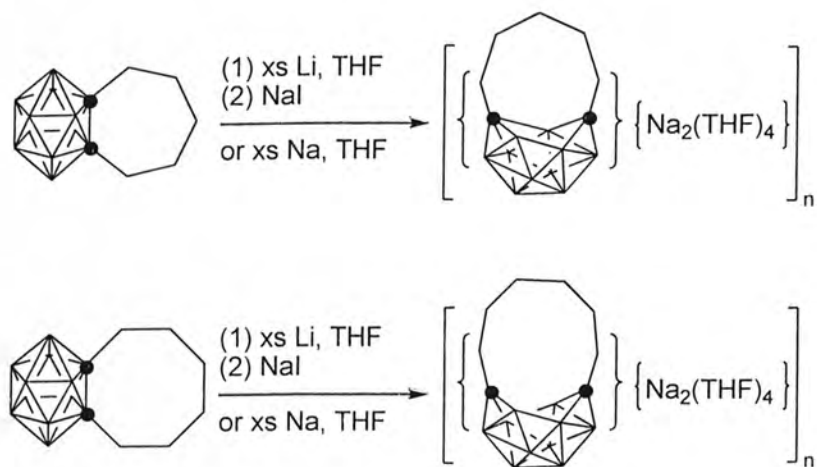
Chart 1.4. *o*-Carboranes with aliphatic bridges.



Scheme 1.12. Formation of CAd *arachno*-carborane tetraanions.



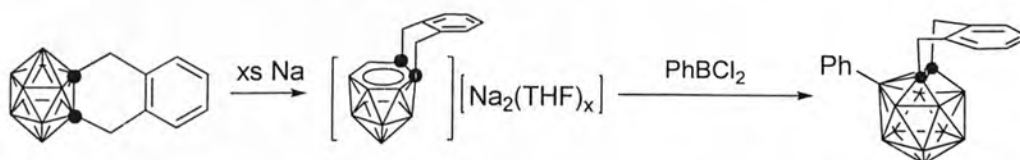
Scheme 1.13. Formation of CAP *nido*-carborane dianions.



1.3. 13-Vertex *closo*-Carboranes

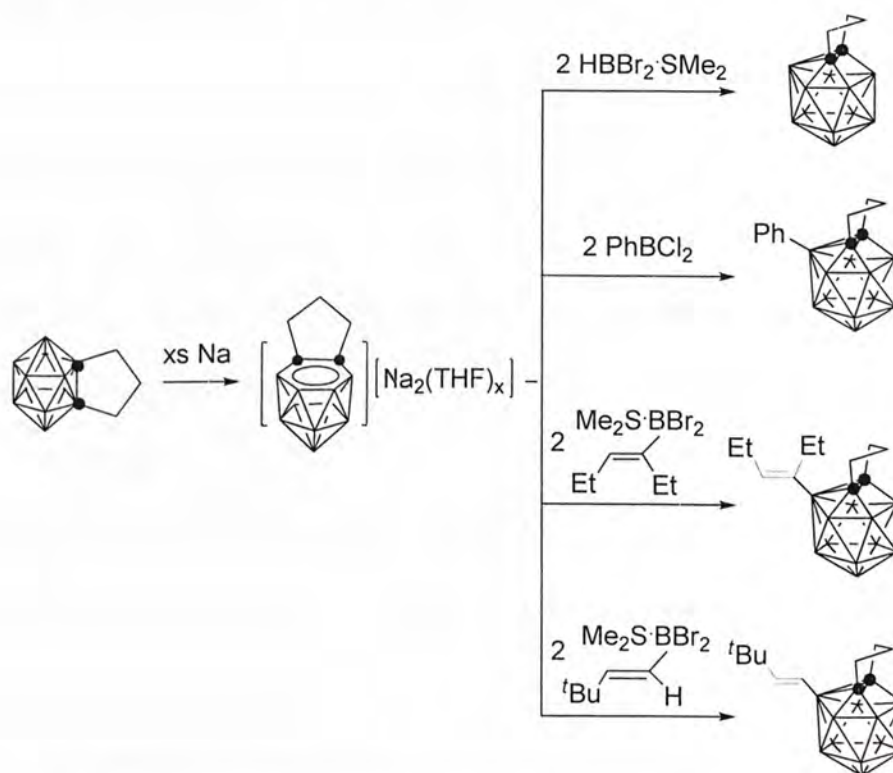
In 2003 the Welch's group reported the synthesis of the first 13-vertex carborane 3-Ph-1,2-C₆H₄(CH₂)₂-1,2-C₂B₁₁H₁₀ (Scheme 1.14).¹⁵ The very low yield of 6% adds some difficulties on the further exploration although the supra-icosahedral molecules might process a different property compared to the icosahedrons.

Scheme 1.14. Synthesis of 13-vertex carborane 3-Ph-1,2-C₆H₄(CH₂)₂-1,2-C₂B₁₁H₁₀.

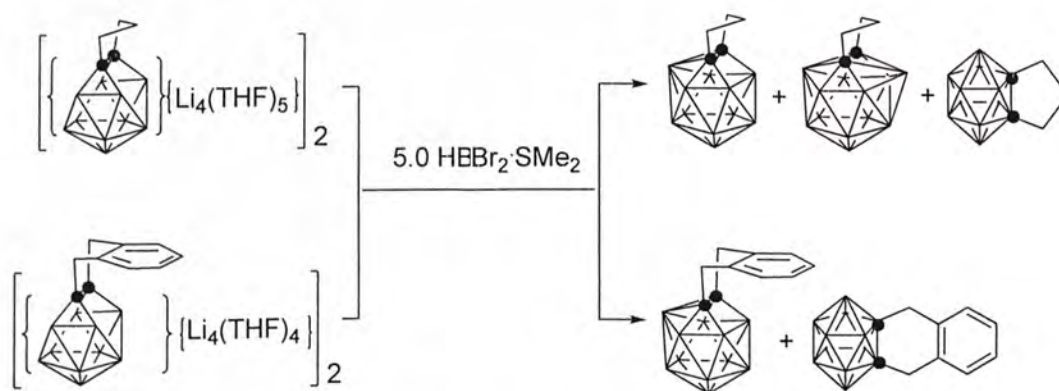


Our previous work showed that the linkages between the two cage carbon atoms of *o*-carboranes can control the relative positions of the cage carbon atoms during the reactions with group 1 metals.^{30,37} Recent results indicated that these bridges may also play a role in stabilizing supercarboranes.^{15,38} Considering the rigidity and relatively small size of the (CH₂)₃ unit, which may facilitate the capitation reaction with RBX₂, 1,2-(CH₂)₃-1,2-C₂B₁₀H₁₀³⁹ was chosen as the starting material for the preparation of supercarboranes (Scheme 1.15).⁴⁰

Scheme 1.15. Preparation of 13-vertex carboranes from *nido* species.



Scheme 1.16. Preparation of 13- and 14-vertex carboranes from *arachno* species.

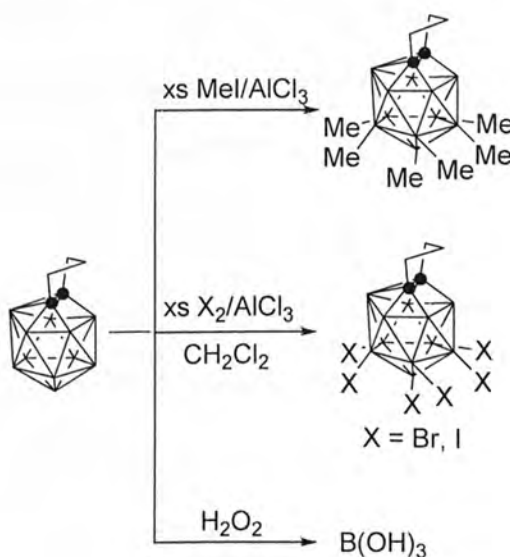


In view of the isolated yield of 20% for 1,2-(CH_2)₃-3-Ph-1,2- $\text{C}_2\text{B}_{11}\text{H}_{10}$ versus 6% for 1,2- $\text{C}_6\text{H}_4(\text{CH}_2)_2$ -3-Ph-1,2- $\text{C}_2\text{B}_{11}\text{H}_{10}$,¹⁵ it was suggested that 1,2-(CH_2)₃-1,2- $\text{C}_2\text{B}_{10}\text{H}_{10}$ was a much better starting material than 1,2- $\text{C}_6\text{H}_4(\text{CH}_2)_2$ -1,2- $\text{C}_2\text{B}_{10}\text{H}_{10}$.⁴⁰ Such differences could be ascribed to the presence of the more sterically demanding *o*-xylyl bridge. This assumption was supported by the experiments of Scheme 1.16. Reaction of the *arachno*-carborane salt

$[\{1,2-(\text{CH}_2)_3-1,2-\text{C}_2\text{B}_{10}\text{H}_{10}\}\{\text{Li}_4(\text{THF})_5\}]_2$ with 5.0 equiv of $\text{HBBr}_2\cdot\text{SMe}_2$ gave both the 13-vertex carborane $1,2-(\text{CH}_2)_3-1,2-\text{C}_2\text{B}_{11}\text{H}_{11}$ and a 14-vertex carborane $1,2-(\text{CH}_2)_3-1,2-\text{C}_2\text{B}_{12}\text{H}_{12}$ in 32% and 7% yields, respectively. However, treatment of the *arachno*-carborane salt $[\{1,2-\text{C}_6\text{H}_4(\text{CH}_2)_2-1,2-\text{C}_2\text{B}_{10}\text{H}_{10}\}\{\text{Li}_4(\text{THF})_6\}]_2^{30a}$ with 5.0 equiv of $\text{HBBr}_2\cdot\text{SMe}_2$ afforded only a 13-vertex carborane $1,2-\text{C}_6\text{H}_4(\text{CH}_2)_2-1,2-\text{C}_2\text{B}_{11}\text{H}_{11}$, and no 14-vertex species was detected (Scheme 1.16). These results suggested that the linkage played an important role in the preparation of supercarboranes.

It is also noted that methylation and halogenation of 13-vertex carboranes can be successfully done accord with properties found in the very rich electrophilic substitution reactions on icosahedral boranes⁴¹ and carboranes (Scheme 1.17).^{42,43}

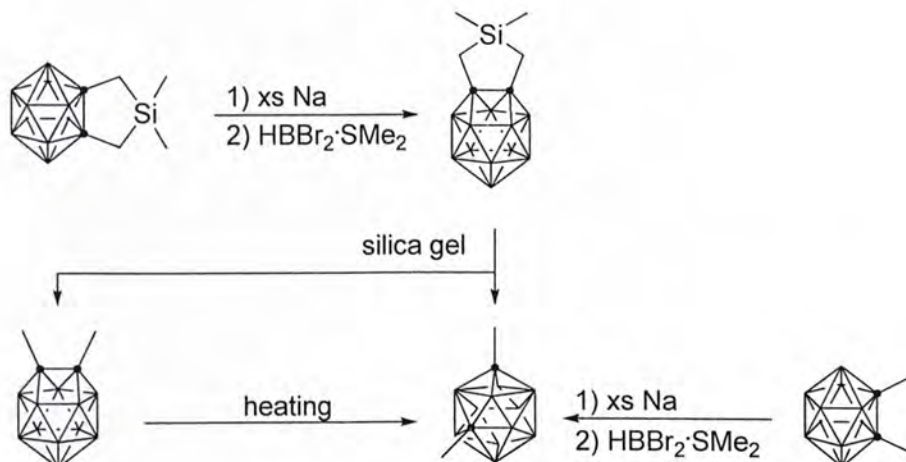
Scheme 1.17. Methylation/halogenation of 13-vertex carborane



The synthesis of both CAd and CAP 13-vertex carboranes without any C,C'-linkages has also been successful in our group. The results show that the C,C'-linkages do not have any obvious effect on the thermal and kinetic stability of 13-vertex carboranes, and the CAP isomer is thermodynamically more stable than the

CAd one. The role of the linkages is just to lower the reducing power of the *nido*-carborane dianions, facilitating the capitation reaction⁴⁴ (Scheme 1.18).

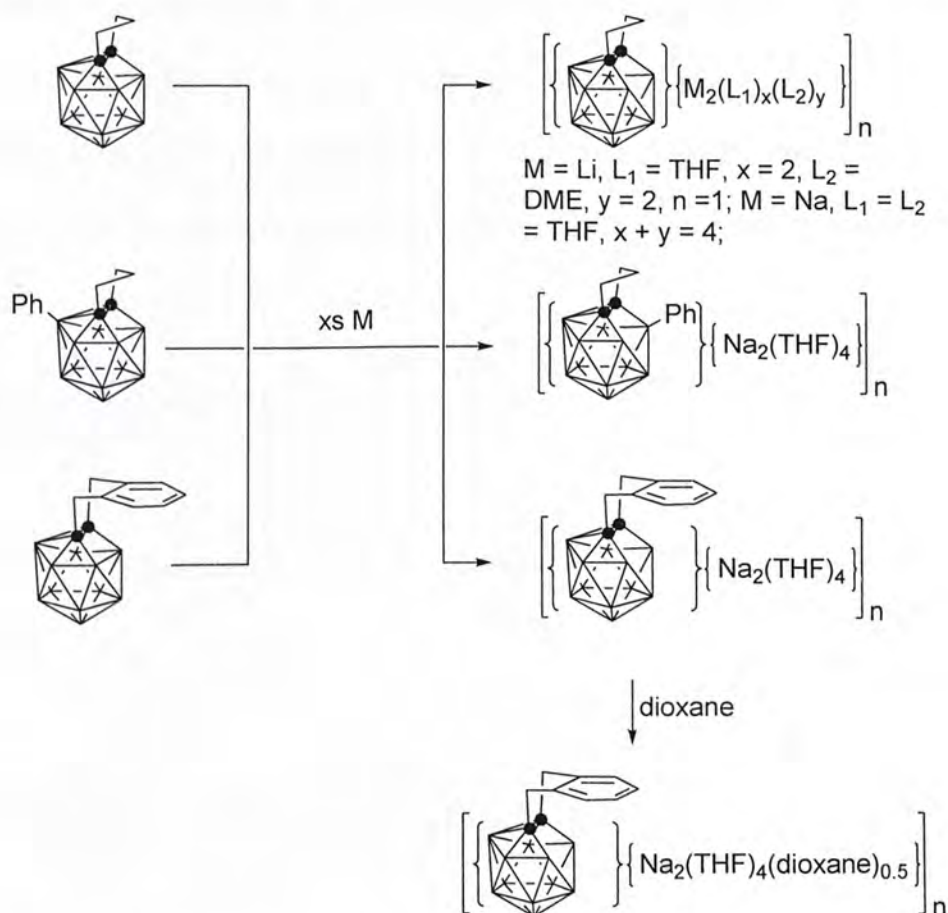
Scheme 1.18. The preparation of CAd and CAp 13-vertex carboranes.



1.4. 13-Vertex *nido*-Carborane Salts and 14-Vertex *closo*-Carboranes

It is well documented that $o\text{-R}_2\text{C}_2\text{B}_{10}\text{H}_{10}$ can be reduced by group 1 metals to form $[\text{nido-R}_2\text{C}_2\text{B}_{10}\text{H}_{10}]\text{M}_2$ or $[\text{arachno-R}_2\text{C}_2\text{B}_{10}\text{H}_{10}]\text{Li}_4$ (R_2 = linkages) salts.^{29,30} They are very useful synthons for the synthesis of metallacarboranes of p-, d-, and f-block elements and supercarborane.^{4c,15,34} Treatment of 13-vertex *closo*-carboranes with excess finely cut Na metal in THF at room temperature gave the corresponding 13-vertex *nido*-carborane salts (Scheme 1.19). It was noteworthy that these reactions proceeded much faster than those of icosahedral cages and naphthalene was not required, indicating that 13-vertex carboranes were more reactive than the 12-vertex ones.^{29,30} No *arachno* species was detected, indicating that the reducing power of the 13-vertex *nido*-carboranes is stronger than that of the 12-vertex ones.³⁰

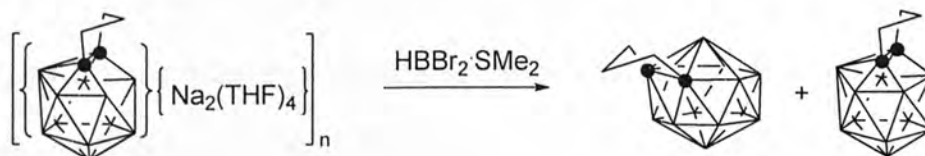
Scheme 1.19. Preparation of group 1 metal complexes of 13-vertex *nido*-carboranes.



The reaction of the *arachno*-carborane salt $[\{1,2-(\text{CH}_2)_3-1,2-\text{C}_2\text{B}_{10}\text{H}_{10}\}\{\text{Li}_4(\text{THF})_5\}]_2$ with 5.0 equiv of $\text{HBBr}_2 \cdot \text{SMe}_2$ gave both the 13-vertex carborane $1,2-(\text{CH}_2)_3-1,2-\text{C}_2\text{B}_{11}\text{H}_{11}$ and a 14-vertex carborane $2,3-(\text{CH}_2)_3-2,3-\text{C}_2\text{B}_{12}\text{H}_{12}$ in 32% and 7% yields, respectively.⁴⁰ This result clearly indicated that ‘carbon-atom-adjacent’ *arachno*-carborane tetraanions can react with $\text{HBBr}_2 \cdot \text{SMe}_2$ to afford 14-vertex carboranes.⁴⁰ Regarding the reaction mechanism, it is assumed that the addition of the first BH vertex to $[\{1,2-(\text{CH}_2)_3-1,2-\text{C}_2\text{B}_{10}\text{H}_{10}\}\{\text{Li}_4(\text{THF})_5\}]_2$ could result in the formation of *nido*-($\text{CH}_2)_3\text{C}_2\text{B}_{11}\text{H}_{11}^{2-}$ dianion which can either host the second BH vertex to form $1,2-(\text{CH}_2)_3-1,2-\text{C}_2\text{B}_{12}\text{H}_{12}$ or be oxidized by $\text{HBBr}_2 \cdot \text{SMe}_2$ to generate *closo*-carborane $1,2-(\text{CH}_2)_3-1,2-\text{C}_2\text{B}_{11}\text{H}_{11}$. The reaction of *nido*-carborane salt

$[\{1,2-(\text{CH}_2)_3-1,2-\text{C}_2\text{B}_{11}\text{H}_{11}\}\{\text{Na}_2(\text{THF})_4\}]_n$ with $\text{HBBr}_2\cdot\text{SMe}_2$ was examined sequentially. Treatment of $[\{1,2-(\text{CH}_2)_3-1,2-\text{C}_2\text{B}_{11}\text{H}_{11}\}\{\text{Na}_2(\text{THF})_4\}]_n$ with 1.5 equivalents of $\text{HBBr}_2\cdot\text{SMe}_2$ in toluene produced $1,2-(\text{CH}_2)_3-1,2-\text{C}_2\text{B}_{12}\text{H}_{12}$ and $1,2-(\text{CH}_2)_3-1,2-\text{C}_2\text{B}_{11}\text{H}_{11}$ in 30% and 12% yield, respectively (Scheme 1.20).⁴⁰

Scheme 1.20. Preparation of 14-vertex carborane from 13-vertex *nido*-carborane salt.



Scheme 1.21. Conversion between 2,3-isomer and 2,13-isomer of 14-vertex carborane.



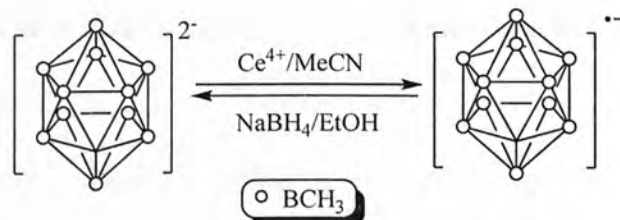
The strong reducing power of the 14-vertex *nido* salt made the further capitation reactions with $\text{HBBr}_2\cdot\text{SMe}_2$ infeasible. Thus the reactions of $[\{1,2-(\text{CH}_2)_3-1,2-\text{C}_2\text{B}_{12}\text{H}_{12}\}\{\text{Na}_2(\text{THF})_4\}]_n$ with $\text{HBBr}_2\cdot\text{SMe}_2$ in toluene afforded, after chromatographic separation, a redox reaction product $2,13-(\text{CH}_2)_3-2,13-\text{C}_2\text{B}_{12}\text{H}_{12}$. The formation of $2,13-(\text{CH}_2)_3-2,13-\text{C}_2\text{B}_{12}\text{H}_{12}$ indicates that $\text{HBBr}_2\cdot\text{SMe}_2$ functioned as an oxidant in this reaction. Hence, the reaction of $[\{1,2-(\text{CH}_2)_3-1,2-\text{C}_2\text{B}_{12}\text{H}_{12}\}\{\text{Na}_2(\text{THF})_4\}]_n$ with O_2 was also examined and gave the similar result. Complex $2,13-(\text{CH}_2)_3-2,13-\text{C}_2\text{B}_{12}\text{H}_{12}$ is isomeric with $1,2-(\text{CH}_2)_3-1,2-\text{C}_2\text{B}_{12}\text{H}_{12}$. Its reduction with excess sodium metal also gave the *nido* species $[\{1,2-(\text{CH}_2)_3-1,2-\text{C}_2\text{B}_{12}\text{H}_{12}\}\{\text{Na}_2(\text{THF})_4\}]_n$ (Scheme 1.21).⁴⁰

1.5. Carborane Radical Anions

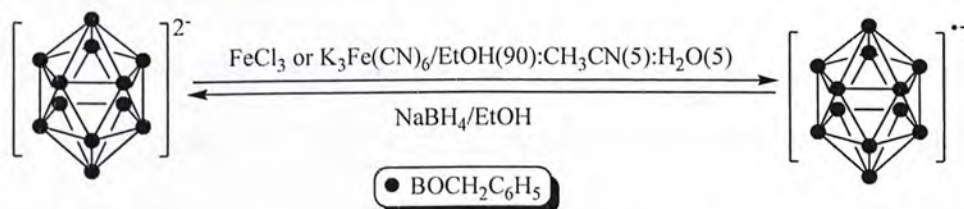
A wide variety of polyhedral boranes and carboranes are known, the precise shape of which can be inferred from Wade's electron-counting rules,⁴⁵ the rules for prediction of stable structures of polyhedral inorganic, organometallic, and organic compounds. If b stands for the skeletal electrons of polyhedral boranes and carboranes, n stands for the number of vertices, for deltahedral *closo* (closed) structures (characterized by triangle faces) with n vertices there exist $(n+1)$ bonding molecular orbitals which may be filled with not more than $2n+2$ skeletal electrons ($n = 4, 5 \dots$), for *nido* (nest-like) structures derived from the *closo*-forms through truncation of one apex there are $(n+2)$ bonding MOs which may be occupied with not more than $2n+4$ skeletal electrons and for *arachno* (web-like) structures derived from *nido*-forms through truncation of one apex, there are $(n+3)$ bonding MOs that may be occupied with not more than $2n+6$ skeletal electrons. Generally, closed clusters have $2n+2$ (*closo*) or $2n$ (*hyperclose*) skeletal electron counts, whereas open clusters have $2n+4$ (*nido*), $2n+6$ (*arachno*) or $2n+8$ (*hypho*) electron counts.⁴⁶ Polyhedral boron clusters with odd skeletal electron counts that do not accord with Wade's Rules are rare. A few examples of $2n+1$ clusters, lying between the $2n+2$ (*closo*) and $2n$ (*hyperclose*) structural types, have been reported, which include radical anions $B_nX_n^{\cdot-}$ ($X = \text{Cl, Br, I, } n = 6, 9$; $X = \text{Cl, } n = 8, 10$),⁴⁷ $B_{12}R_{12}^{\cdot-}$ ($R = \text{Me, OCH}_2\text{C}_6\text{H}_5$)⁴⁸ and neutral radical species $\cdot\text{CB}_{11}\text{Me}_{12}$ ⁴⁹ with the latter two being crystallographically characterized (Scheme 1.22, Scheme 1.23 and Scheme 1.24). Oxidation of the permethylated icosahedral borane $[\text{closo-B}_{12}(\text{CH}_3)_{12}]^{2-}$, by ceric(IV) ammonium nitrate in acetonitrile affords the blue, air-stable paramagnetic anion $\{[\text{closo-B}_{12}(\text{CH}_3)_{12}]^{\cdot-}\}^{\cdot-}$.^{48a} In $\{[\text{closo-B}_{12}(\text{CH}_3)_{12}]^{\cdot-}\}^{\cdot-}$, the unpaired electron is trapped within the hydrocarbon sheath of the permethylated borane cage, hence, this radical

anion is surprisingly stable with respect to reaction with oxygen.^{48a} The EPR spectrum of $\{[closo-B_{12}(CH_3)_{12}]^-\}^-$ exhibits a signal with $g = 2.0076$ and UV-Vis spectrum displays absorption in the visible region.^{48a} Cyclic voltammetry of $\{[closo-B_{12}(CH_3)_{12}]^-\}^-$ reveals a reversible wave with $E_{1/2} = 0.44$ V for the one-electron process $\{[closo-B_{12}(CH_3)_{12}]^-\}^- + e^- \rightarrow [closo-B_{12}(CH_3)_{12}]^{2-}$ and the X-ray crystal structure confirms that $\{[closo-B_{12}(CH_3)_{12}]^-\}^-$ is a permethylated monoanionic *closo*-borane.^{48a} Oxidation of $Cs^+CB_{11}Me_{12}^-$ either with PbO_2/CF_3COOH (74% yield) or electrochemically yields $CB_{11}Me_{12}^\bullet$ as shiny black tetrahedral crystals stable to air for a few days, sublimable under reduced pressure but destroyed by heating.⁴⁹ It dissolves in oxidation-resistant nonpolar solvents to gave deep blue solutions, and its pentane solution is stable to prolonged visible irradiation but unstable to air and extended UV irradiation.⁴⁹ The stability of $CB_{11}Me_{12}^\bullet$ is attributable to steric protection of the delocalized free valence carrying centers in the carborane icosahedrons by a sheath of methyl groups.⁴⁹ Solutions and low-temperature glasses containing $CB_{11}Me_{12}^\bullet$ exhibit a broad EPR signal, $g = 2.0037(3)$ and no NMR signals, and UV-visible absorption and magnetic circular dichroism of $CB_{11}Me_{12}^\bullet$ suggest the presence of a series of electronic transitions extending to exceptionally low energies and are compatible with excitation energies and oscillator strengths calculated by the INDO/S method.⁴⁹ The cathodic reduction potential of $CB_{11}Me_{12}^\bullet$ in acetonitrile is 1.27 V [Bu_4NPF_6 , $Ag/AgNO_3(MeCN)$; ferrocene, 0.09 V], equal to the anodic oxidation potential of $CB_{11}Me_{12}^-$ and no oxidation wave for $CB_{11}Me_{12}^\bullet$ was observed up to 2.6 V.⁴⁹

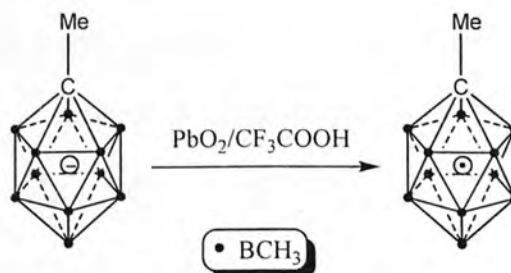
Scheme 1.22. Chemical interconversion of $\{[closo-B_{12}(CH_3)_{12}]^{\bullet-}\}^-$ and $[closo-B_{12}(CH_3)_{12}]^{2-}$.



Scheme 1.23. Chemical interconversion of $\{[closo-B_{12}(OCH_2C_6H_5)_{12}]^{\bullet-}\}^-$ and $[closo-B_{12}(OCH_2C_6H_5)_{12}]^{2-}$.



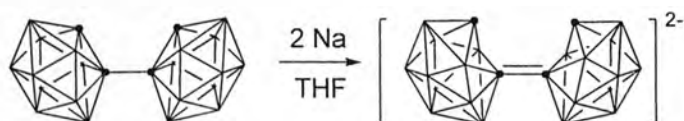
Scheme 1.24. Chemical interconversion of $[closo-CB_{11}(CH_3)_{12}]^-$ to $[closo-CB_{11}(CH_3)_{12}]^{\bullet}$.



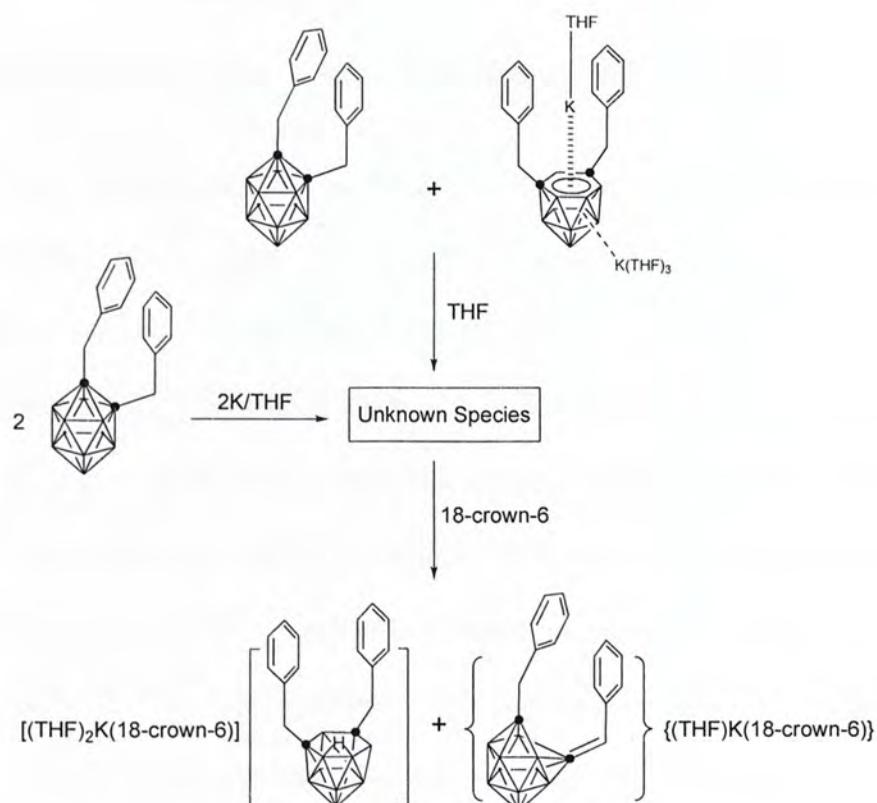
However, clusters with $2n+3$ framework electrons, which fall between the two well-established and abundant closed $2n+2$ (*closo*) and open $2n+4$ (*nido*) structural systems,⁵⁰ have never been isolated although they were detected by electrochemical techniques.⁵¹ For example, two sequential and reversible one-electron reduction waves were observed in the electrochemical studies of 1,2-Ph₂-1,2-C₂B₁₀H₁₀ in DMSO/0.1M NEt₄ClO₄ solution.⁵¹ IR, UV and EPR study of 1,2-Ph₂-1,2-C₂B₁₀H₁₀^{•-} which was electrochemically generated also indicate that radical anions with $2n+3$

framework electrons exists.^{51d} The electrochemical reduction of an MeCN-0.1M Bu₄NBF₄ solution of 1,2-Ph₂-1,2-C₂B₁₀H₁₀ to 1,2-Ph₂-1,2-C₂B₁₀H₁₀⁻ caused a shift in the three characteristic ν(BH) bands at 2650, 2600 and 2580 cm⁻¹ to a strong band centred at 2540 cm⁻¹ and further electrochemical reduction to the 1,2-Ph₂-1,2-C₂B₁₀H₁₀²⁻ caused a further shift in the ν(BH) band to 2450 cm⁻¹.^{51d} UV-Vis-NIR spectrum of 1,2-Ph₂-1,2-C₂B₁₀H₁₀ centred at 44000 cm⁻¹ and electrochemical reduction to 1,2-Ph₂-1,2-C₂B₁₀H₁₀⁻ resulted in a dramatic change with distance bands at 20100, 21700, 27500, 28600 and 31300 cm⁻¹ being observed.^{51d} The ESR spectrum of 1,2-Ph₂-1,2-C₂B₁₀H₁₀⁻, obtained following electrochemical generation, gave a broad simple signal confirming its paramagnetic character.^{51d} Treatment of biscarborane (C₂B₁₀H₁₁)₂ with 2 equiv of Na metal resulted in the isolation of [(C₂B₁₀H₁₁)₂]²⁻ with a C=C double bond between two carborane polyhedral (Scheme 1.25).²⁸ Reduction of 1,2-(PhCH₂)₂-1,2-C₂B₁₀H₁₀ with 1 equiv of K metal led to the deprotonated species [(C₆H₅CH₂)(C₆H₅CH)C₂B₁₀H₁₀]⁻ in which a C=C double bond is observed between the cage and benzylidene unit (Scheme 1.26).⁵² No radical anions R₂C₂B₁₀H₁₀^{·-} have been isolated thus far in spite of theoretical calculations suggesting that C₂B₁₀H₁₂^{·-} should have appreciable thermodynamic stability.^{51d,53}

Scheme 1.25. Reduction of biscarborane.



Scheme 1.26. Reduction of 1,2-(PhCH₂)₂-1,2-C₂B₁₀H₁₀.



1.6. Our Objectives

In view of the rich chemistry displayed by the icosahedral carboranes, we are interested in the virtually unknown chemistry of supra-icosahedral carboranes and carborane radical anions with $2n+3$ framework electrons. The objectives of this research are: (1) the exploration of a suitable synthetic method for supercarboranes, and (2) the synthesis, characterization and electrochemical studies of supercarborane radical anions. In this dissertation, we will describe the details of our work on the subjects mentioned above.

Chapter 2. 13-Vertex Carboranes

2.1. Synthesis and Characterization of 13-Vertex *closo*-Carboranes

It is well established that the reduction of $o\text{-R}_2\text{C}_2\text{B}_{10}\text{H}_{10}$ by group 1 metals always results in the complete cleavage of the cage carbon-carbon bond, leading to the formation of “carbon-atom-apart” (CAp) *nido*-carborane dianions $[7,9\text{-nido-R}_2\text{C}_2\text{B}_{10}\text{H}_{10}]^{2-}$ (*meta* in Chart 2.1).²⁹ They are very useful ligands for the production of numerous metallocarboranes of s, p, d, and f elements.^{33,34} Our group recently developed a method to control the relative positions of the cage carbon atoms during the reduction process by introducing a bridge between the two cage carbon atoms during the reduction process by introducing a bridge between the two cage carbon atoms.³⁰ Thus the syntheses of “carbon-atom-adjacent” *nido*-carborane dianions (CAAd) $[7,8\text{-nido-R}_2\text{C}_2\text{B}_{10}\text{H}_{10}]^{2-}$ (*ortho* in Chart 2.1) and CAp $[7,10\text{-nido-R}_2\text{C}_2\text{B}_{10}\text{H}_{10}]^{2-}$ (*para* in Chart 2.1) were achieved.³⁰ The results showed that a short bridge can not only lock the cage carbon atoms in *ortho* positions, but also lower the reducing power of the resulting dianions, leading to the formation of CAAd [*arachno*- $\text{R}_2\text{C}_2\text{B}_{10}\text{H}_{10}$]⁴⁻ by further reduction with Li metal.³⁰

Chart 2.1. Isomers of *nido*- $\text{C}_2\text{B}_{10}\text{H}_{12}^{2-}$.

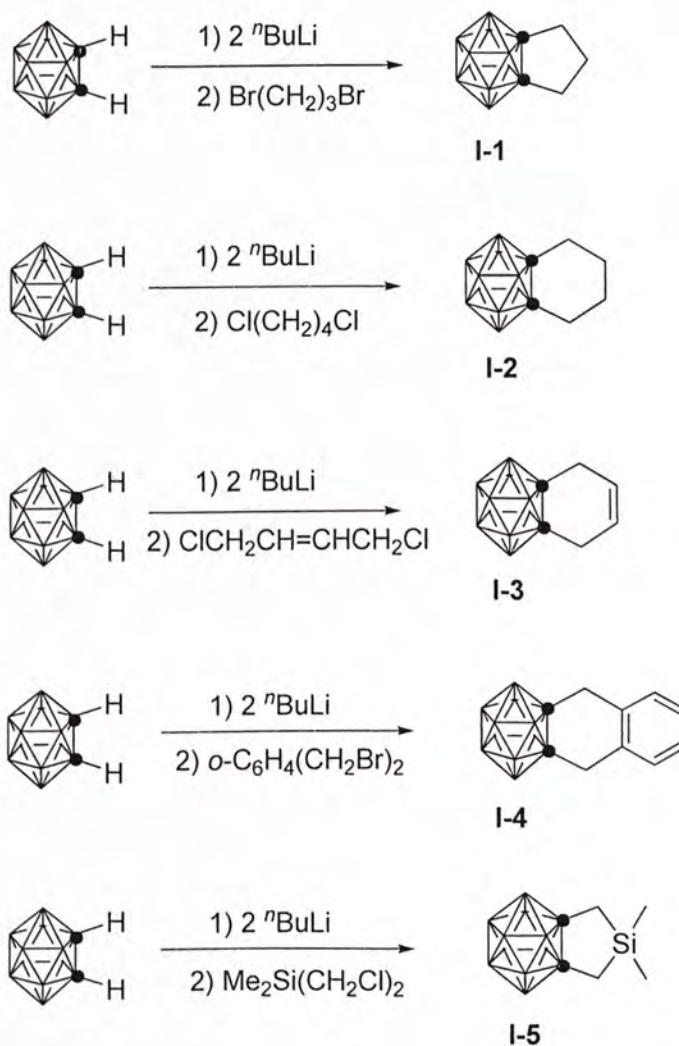


These CAAd *nido*- and *arachno*-carborane anions are interesting ligands to transition metals.^{30c,35,36} Most importantly, they are finding applications in the preparation of 13-vertex carboranes. For example, the Welch's group reported the synthesis of a 13-vertex carborane $1,2\text{-C}_6\text{H}_4(\text{CH}_2)_2\text{-3-Ph-1,2-C}_2\text{B}_{11}\text{H}_{10}$ using the CAAd

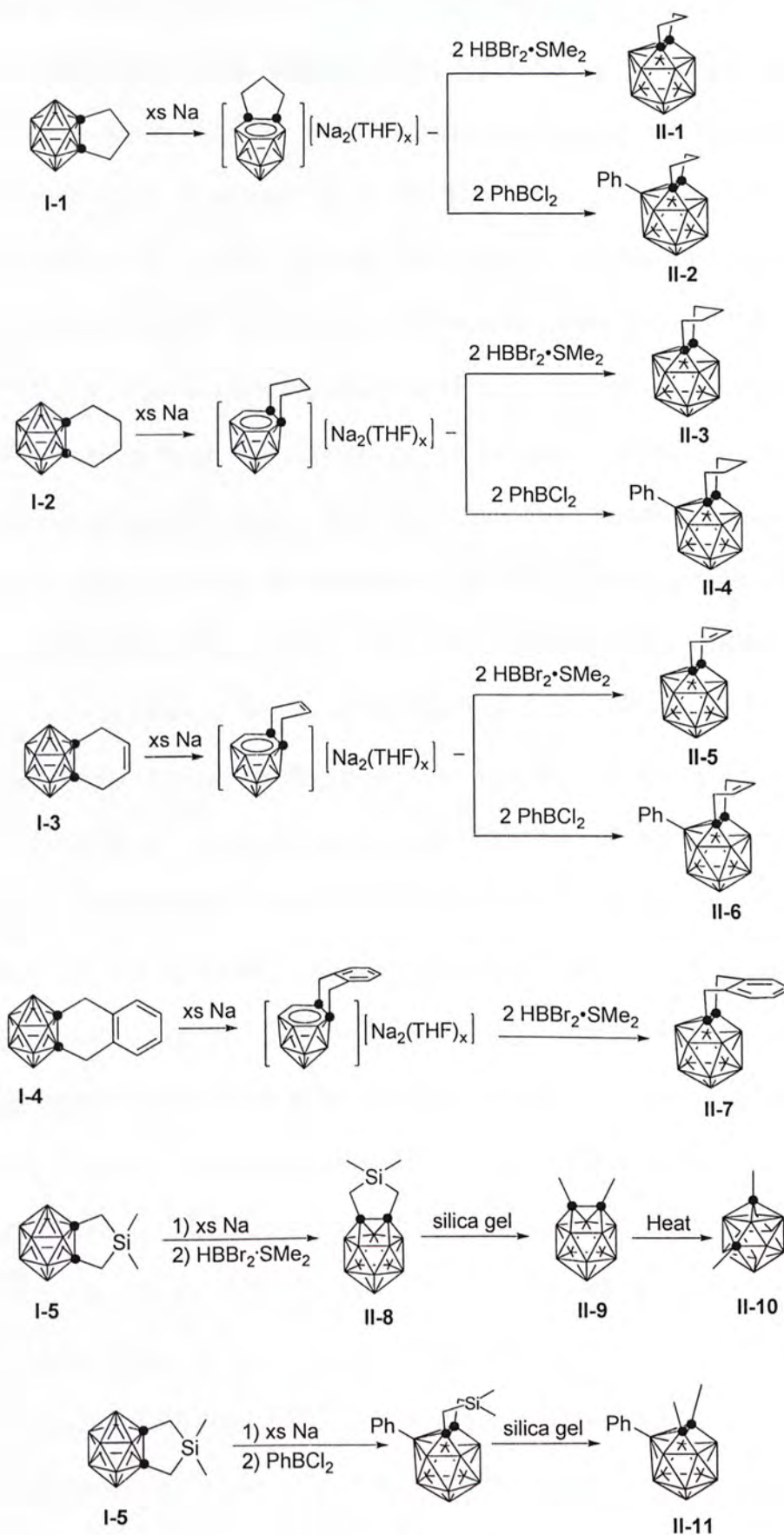
[*nido*-1,2- $\text{C}_6\text{H}_4(\text{CH}_2)_2$ -1,2- $\text{C}_2\text{B}_{10}\text{H}_{10}$] $^{2-}$ as the starting material.¹⁵ Our group prepared a series of 13-vertex carboranes using capitation reactions.⁴⁰

Our previous work showed that the linkage between the two cage carbon atoms of *o*-carboranes can control the relative positions of the cage carbons during the reactions with group 1 metals.³⁰ Compounds 1,2- $(\text{CH}_2)_3$ -1,2- $\text{C}_2\text{B}_{10}\text{H}_{10}$ (**I-1**),³⁹ 1,2- $(\text{CH}_2\text{CH}=\text{CHCH}_2)$ -1,2- $\text{C}_2\text{B}_{10}\text{H}_{10}$ (**I-3**),⁵⁴ 1,2- $(\text{CH}_2)_4$ -1,2- $\text{C}_2\text{B}_{10}\text{H}_{10}$ (**I-2**),³⁹ 1,2- $[o\text{-C}_6\text{H}_4(\text{CH}_2)_2]$ -1,2- $\text{C}_2\text{B}_{10}\text{H}_{10}$ (**I-4**),⁵⁵ 1,2- $\text{Me}_2\text{Si}(\text{CH}_2)_2$ -1,2- $\text{C}_2\text{B}_{10}\text{H}_{10}$ (**I-5**)⁵⁶ were prepared according to the reported methods. (Scheme 2.1)

Scheme 2.1. Preparation of 12-vertex closocarboranes.



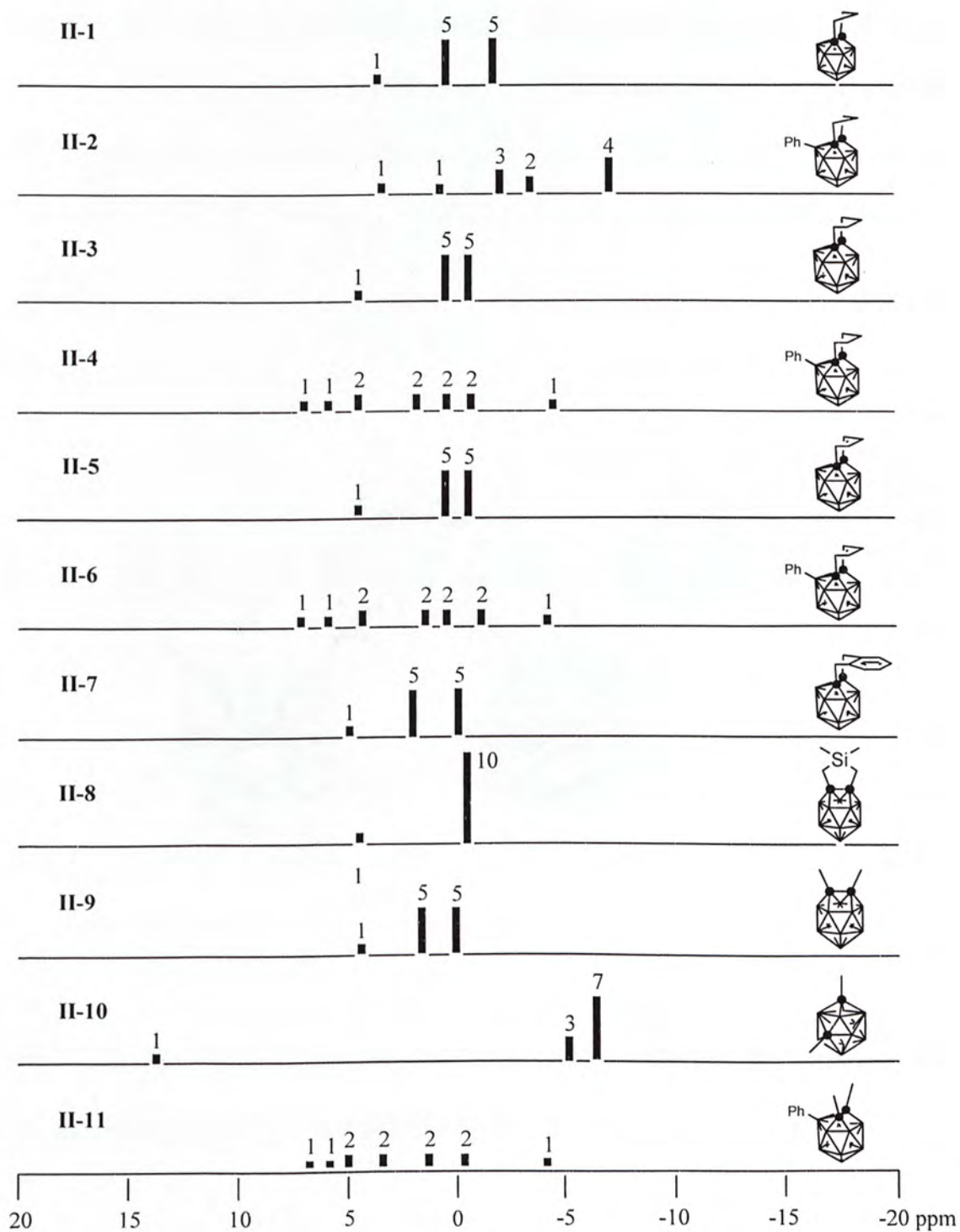
Scheme 2.2. Preparation of 13-vertex carboranes from *nido* species.



13-Vertex carboranes **II-1**, **II-2**, **II-7**, **II-8**, **II-9** and **II-10** were prepared according to literature methods.^{40a, 44} In a similar manner, **II-3**, **II-4**, **II-5**, **II-6** and **II-11** were also synthesized. Reduction of **I-1**, **I-2**, **I-3**, **I-4** or **I-5** with excess finely cut sodium metal in THF at room temperature gave the corresponding CAd *nido*-carborane salts. Treatment of these salts with 2 equiv of dihaloborane reagents in toluene from -78 to 25°C afforded, after column chromatographic separation, 13-vertex carboranes **II-1** ~**II-11** in 6 ~ 39% isolated yields (Scheme 2.2). A small amount of other boron-containing compounds were obtained in all cases. Many attempts to separate these boron-containing species failed. The control experiments indicated that the use of 2 equiv of dihaloborane reagents offered the highest isolated yield of 13-vertex carboranes. It was assumed that some boranes might be consumed by side reactions. More than 2 equiv of boranes were not necessary, which resulted in difficulty in separation. Donor solvents such as THF, DME, and Et₂O led to a much lower yield. In view of the isolated yield of 6% and 9% for **II-6** and **II-5** versus 37% for **II-1**,⁴⁰ it was suggested there might be side reactions between the double bond of the bridges and the dihaloborane reagents. These results implied that the nature of the linkages played an important role in the preparation of supercarboranes. Compounds **II-1** to **II-11** are quite stable in air and soluble in common organic solvents such as hexane, toluene, and THF. The ¹¹B NMR spectra of **II-1**, **II-3**, **II-5**, **II-7**, and **II-9** displayed a 1:5:5 pattern whereas those of **II-4**, **II-6**, and **II-11** showed a 1:1:2:2:2:2:1 pattern. The following ¹¹B NMR patterns were also observed: a 1:1:3:2:4 for **II-2**, 1:10 for **II-8** and 1:3:7 for **II-10** (Figure 2.1). The ¹H and ¹³C NMR spectra of **II-1**, **II-2**, **II-7**, **II-8**, **II-9** and **II-10** were identical with those reported in the literature.^{40a, 44} The new supercarboranes **II-3**, **II-4**, **II-5**, **II-6** and **II-11** were fully characterized by ¹H, ¹³C, and ¹¹B NMR spectroscopic

techniques as well as high-resolution mass spectrometry. The *BPh* vertex in compounds **II-2**, **II-4**, **II-6** and **II-11** can be easily identified using ^1H coupled ^{11}B NMR as the other boron atoms are all bonded with H atoms which will show doublets. The cage carbons of the newly synthesized compounds **II-3**, **II-4**, **II-6** and **II-11** were not observed while a relatively weak peak for the cage carbon atoms of compound **II-5** can be observed at δ 138.81 ppm in the ^{13}C NMR spectrum. The ^1H NMR of **II-11** shows only one singlet for its two methyl groups which reveals that the compound has a structure with a high symmetry. The bridging double bonds of **II-5** and **II-6** were observed both as triplets with $J = 2.1$ Hz at δ 6.01 ppm and 5.75 ppm, respectively.

Figure 2.1. Stick representation of the chemical shifts and relative intensities of the $^{11}\text{B}\{^1\text{H}\}$ spectra of compounds **II-1** to **II-11**.



2.2. Molecular Structures of II-4 and II-6

Single-crystal X-ray analyses revealed there are two crystallographically independent molecules in the unit cell of **II-4**. Figures 2.2 and 2.3 show the molecular structures of **II-4** and **II-6**, respectively. For easy comparison, the selected bond distances for 13-vertex carboranes are compiled in Table 2.1. There are no significant differences in the C-C, C-B and B-B distances among 13-vertex carboranes.

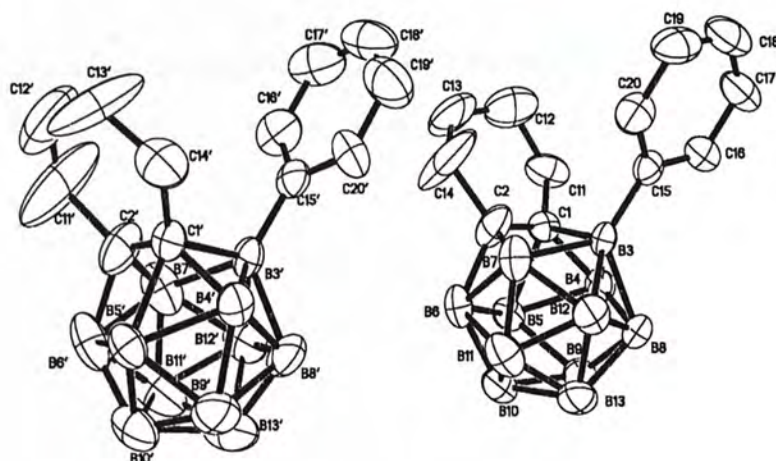


Figure 2.2. Molecular structure of 1,2-(CH₂)₄-3-Ph-1,2-C₂B₁₁H₁₀ (**II-4**), showing the two crystallographically independent molecules in the unit cell.

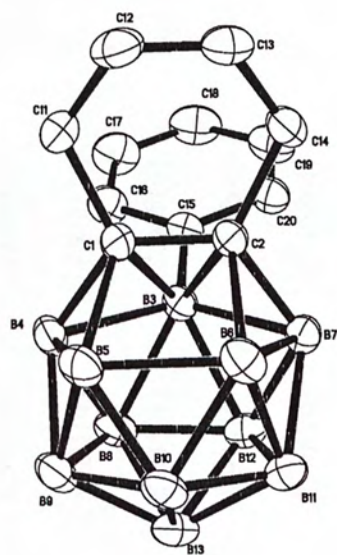


Figure 2.3. Molecular structure of 1,2-(CH₂CH=CHCH₂)-3-Ph-1,2-C₂B₁₁H₁₀ (**II-6**).

Table 2.1. Selected bond distances (Å) in 13-vertex carboranes.^a

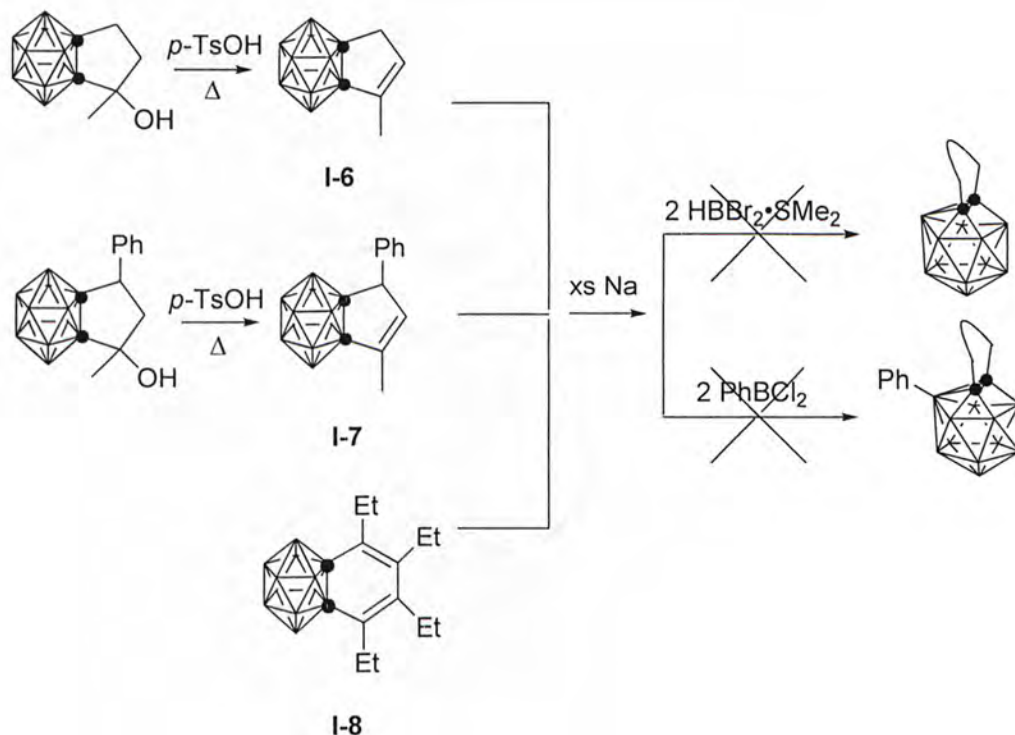
	II-2⁴⁰	II-7⁴⁰	II-4	II-6	II-8⁴⁴	II-9⁴⁴
C(1)-C(2)	1.443(2)	1.427(2)	1.379(6)	1.414(3)	1.439(3)	1.421(5)
C(1)-B(3)	2.086(3)	1.911(2)	1.908(5)	1.971(3)	1.854(4)	1.892(4)
C(1)-B(4)	1.607(3)	1.619(2)	1.571(6)	1.612(3)	1.579(4)	1.600(4)
C(1)-B(5)	1.699(3)	1.799(2)	1.832(5)	1.779(3)	1.821(4)	1.800(3)
C(1)-B(6)	2.239(3)	2.422(2)	2.610(7)	2.343(3)	2.535(4)	2.448(4)
C(2)-B(3)	1.952(3)	1.869(2)	2.194(7)	1.905(3)	1.904(4)	1.892(4)
C(2)-B(5)	2.550(3)	2.512(2)	2.099(7)	2.544(3)	2.400(4)	2.448(4)
C(2)-B(6)	1.776(3)	1.821(2)	1.675(7)	1.820(3)	1.795(4)	1.800(3)
C(2)-B(7)	1.531(3)	1.592(2)	1.688(7)	1.578(3)	1.607(4)	1.600(4)
Average B-B	1.797(4)	1.800(2)	1.785(7)	1.799(4)	1.800(5)	1.798(6)

^a For compounds **II-2**, **II-7** and **II-4**, only average values of crystallographically independent molecules are given.

2.3. Attempts to prepare 13-vertex carboranes with propenyl bridges

It was noted that the following attempts were unsuccessful to obtain the corresponding 13-vertex carboranes (Scheme 2.3).

Scheme 2.3. Unsuccessful preparation of 13-vertex carboranes with propenyl bridges.



Compounds **I-6** and **I-7** were prepared by the dehydration of their corresponding alcohols. 3-methyl-1,2-carboracyclopentane-3-ol⁵⁷ and 3-methyl-5-phenyl-1,2-carboracyclopentane-3-ol⁵⁷ were synthesized according to literature methods and fully characterized. Compounds 3-methyl-5-phenyl-1,2-carboracyclopentane-3-ol and *p*-TsOH were mixed in a glass tube in a molar ratio of 1:1. The tube was sealed and heated at 180 °C for 6 hours. The resulting black residue was dissolved in diethyl ether. Compound **I-7** was obtained after extraction and column chromatographic separation as a white solid in 81% yield. Compound **I-6** was prepared in 42% yield in the same manner as **I-7**. The

structure of compound **I-7** was shown in Figure 2.4. The ^1H NMR spectrum of **I-6** has a doublet at δ 5.53 ppm with $J = 2.1$ Hz for its olefin H, a triplet at δ 3.05 ppm with $J = 2.1$ Hz for its methylene group and a multiplet at δ 1.88 ppm for its methyl group. The ^1H NMR spectrum of **I-7** has a multiplet at δ 5.74 ppm for its olefin H. The ^{11}B NMR spectrum of **I-6** displayed a 3:1:2:2:2 pattern whereas that of **I-7** showed a 2:1:2:1:2:1:1 pattern. Compound **I-8** was prepared according to literature method and fully characterized.⁵⁸

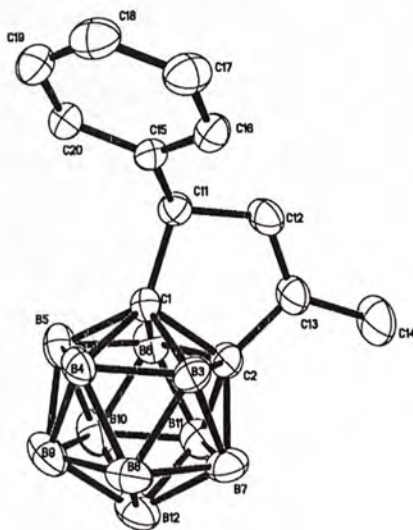


Figure 2.4. Molecular structure of 1, 2-[1-CH₃-3-Ph-(C=CHCH)]-1, 2-C₂B₁₀H₁₀ (**I-7**). Selected bond lengths [Å]: C1-C11 1.540(2), C11-C12 1.505(3), C12-C13 1.323(3), C13-C2 1.495(3), C2-C1 1.626(2).

Deep red solutions were obtained when compounds **I-6**, **I-7** and **I-8** were treated with 5 equiv of sodium metals in THF. Subsequent addition of dihaloborane reagents yielded suspensions in a lighter color. After quenching with water and column chromatographic separation, only 12-vertex **I-6**, **I-7**, **I-8** and some unknown highly

polar borane containing compounds were found according to ^{11}B NMR. It was thought that the intermediates formed when **I-6**, **I-7** and **I-8** were reduced by sodium might not be CAd *nido* salts, the bridges could be broken already.

2.4. Summary

New **II-3**, **II-4**, **II-5**, **II-6**, **II-11** and known **II-1**, **II-2**, **II-7**, **II-8**, **II-9**, **II-10** 13-vertex carboranes were prepared and fully characterized. The results show that the capitation reactions of CAd 12-vertex *nido*-carborane dianionic salts with dihaloboranes are generally a good method for the preparation of 13-vertex carboranes. The C, C'-linkages of the cages have a large effect on the formation of 13-vertex carboranes. Less sterically demanding linkages and dihaloboranes usually offer higher synthetic yields. These super-carboranes have more diverse structures than their icosahedral cousins.

Chapter 3. 13-Vertex Carborane Radical Anions

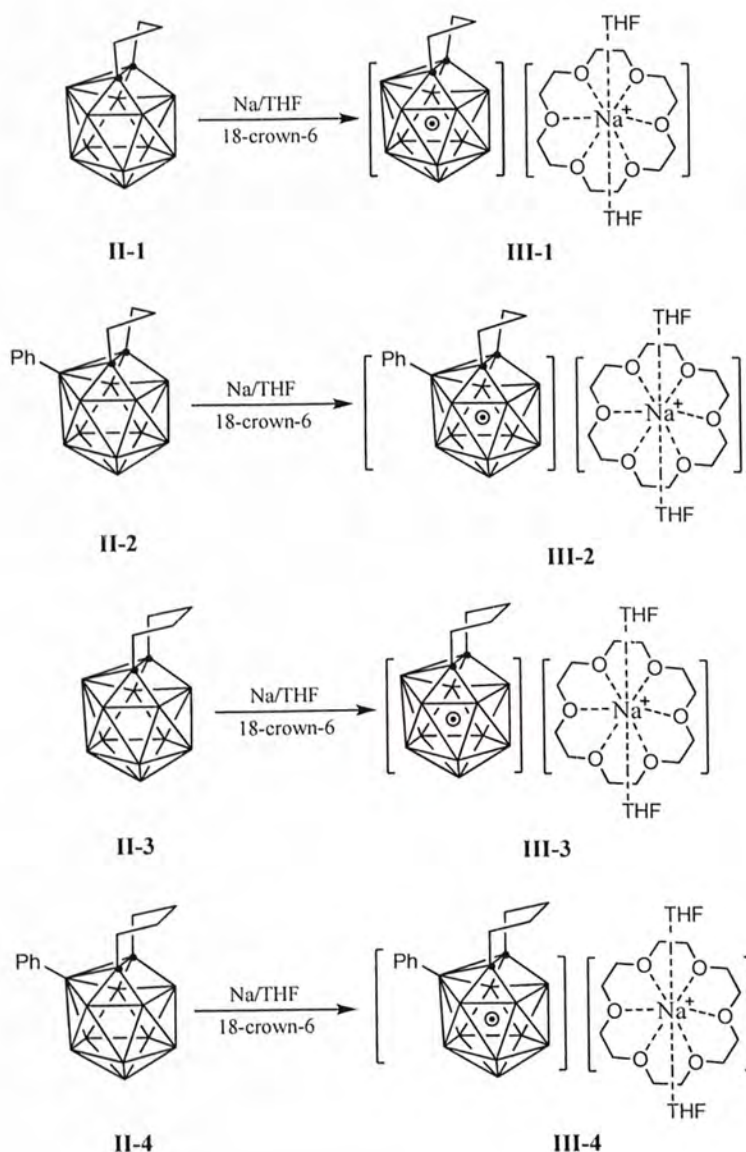
3.1. Synthesis

A series of 13-vertex carboranes provides new approaches to the long-sought $2n+3$ carborane radical anions. Is it possible to isolate the $2n+3$ carborane radical anions from the new supercarborane clusters? We discovered during the course of our studies on the reduction of supercarboranes that a dark-brown solution was generated when 13-vertex carborane 1,2-(CH₂)₃-1,2-C₂B₁₁H₁₁ was treated with an excess amount of Na metal in THF, which was slowly turned to a pale yellow solution within 12 h. The final product was [*nido*-(CH₂)₃C₂B₁₁H₁₁][Na₂(THF)₄] as colorless crystals. We wondered if the dark-brown solution contained the long-sought carborane radical anion with a $2n+3$ skeletal electron count. After many attempts, the first boron cluster with a $2n+3$ system [1,2-(CH₂)₃-1,2-C₂B₁₁H₁₁][Na(18-crown-6)(THF)₂] (**III-1**)⁶² was isolated and fully characterized.

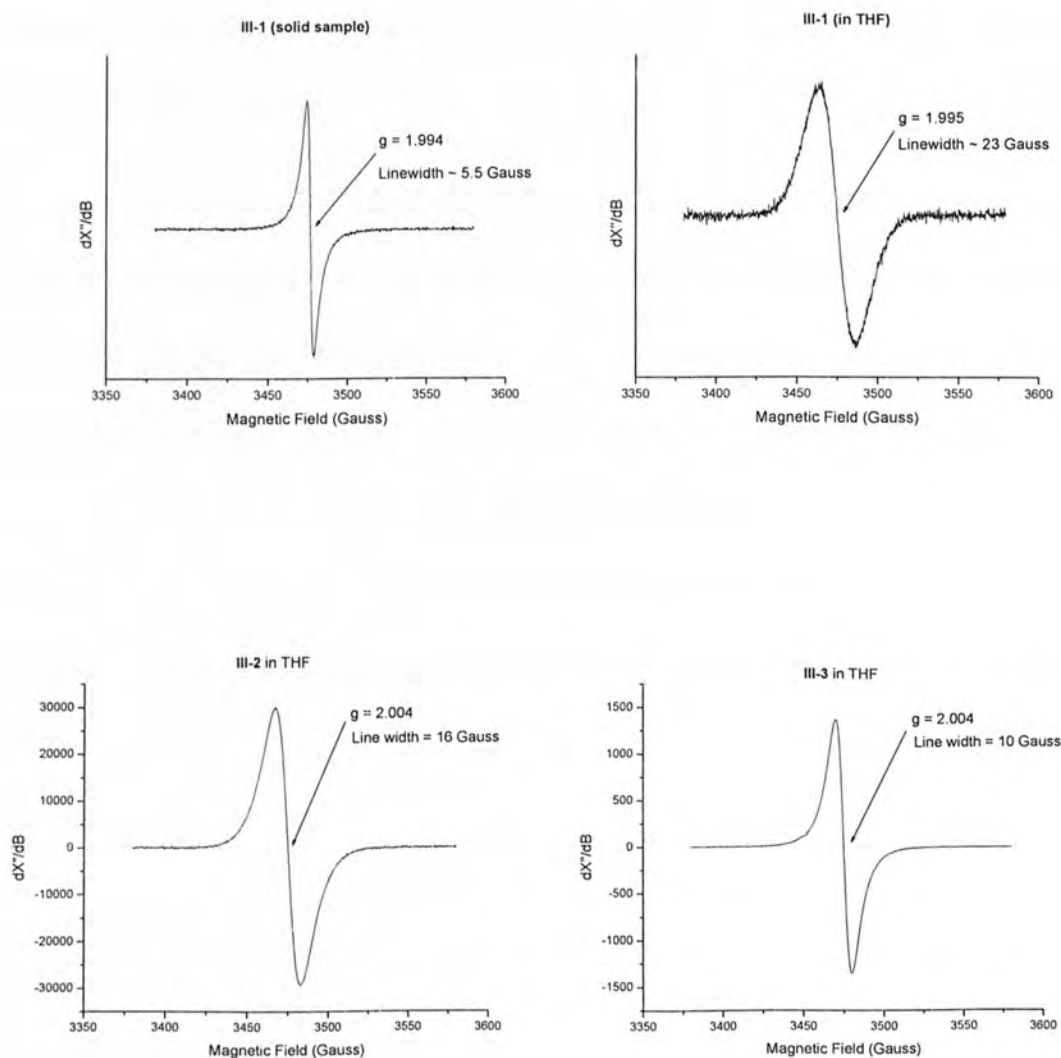
Treatment of 1,2-(CH₂)₃-1,2-C₂B₁₁H₁₁ (**II-1**)⁴⁰ with 1 equiv of finely cut sodium metal in THF at room temperature gave, after recrystallization from a mixed THF/hexane solution of 18-crown-6 ether, [1,2-(CH₂)₃-1,2-C₂B₁₁H₁₁][Na(18-crown-6)(THF)₂] (**III-1**) as brown crystals in 80% isolated yield (Scheme 3.1). In the same manner, treatment of 1,2-(CH₂)₃-3-Ph-1,2-C₂B₁₁H₁₁ (**II-2**)⁴⁰, 1,2-(CH₂)₄-1,2-C₂B₁₁H₁₁ (**II-3**), and 1,2-(CH₂)₄-3-Ph-1,2-C₂B₁₁H₁₁ (**II-4**) with 1 equiv of finely cut sodium metal in THF at room temperature gave, after recrystallization from a mixed THF/hexane solution of 18-crown-6 ether, [1,2-(CH₂)₃-3-Ph-1,2-C₂B₁₁H₁₁][Na(18-crown-6)(THF)₂] (**III-2**), [1,2-(CH₂)₄-1,2-C₂B₁₁H₁₁][Na(18-crown-6)(THF)₂] (**III-3**),

[1,2-(CH₂)₄-3-Ph-1,2-C₂B₁₁H₁₁][Na(18-crown-6)(THF)₂] (**III-4**) all as brown crystals in 80%, 75% and 90% isolated yield, respectively (Scheme 3.1). They are all very air- and moisture-sensitive but remain stable for months at room temperature under an inert atmosphere. Traces of air immediately convert the intensively colored radicals anions to pale yellow powder. They are soluble in THF and ether, insoluble in aromatic solvents and hexane.

Scheme 3.1. Preparation of 13-vertex Carborane Radical Anions **III-1**, **III-2**, **III-3** and **III-4**.



Both THF solution and solid samples of **III-1** exhibited an EPR signal as expected for radical anion with $g = 1.994$ (line width = 23 G in solution and 5.5 G in solid state) at room temperature (Figure 3.1) and no NMR signals, which is similar to those observed in $\cdot\text{CB}_{11}\text{Me}_{12}$ radical⁴⁹ and $\text{B}_{12}\text{Me}_{12}^{\cdot-}$ radical anion.⁴⁸ All THF solution of **III-2**, **III-3**, **III-4** exhibited EPR signals as expected for radical anions with g (**III-2**) = 2.004 (line width = 16 G), g (**III-3**) = 2.004 (line width = 10 G), g (**III-4**) = 2.004 (line width = 22 G) at room temperature (Figure 3.1) and no NMR signals, which is similar to those observed in **III-1**.



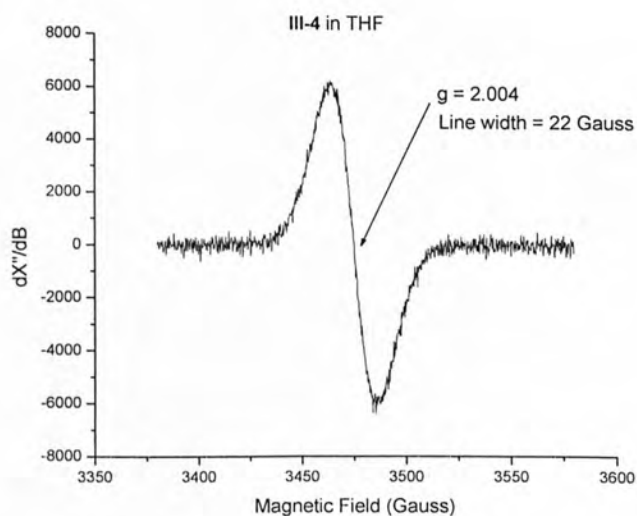


Figure 3.1 EPR spectra of **III-1** in solid state and THF solution and of **III-2**, **III-3** and **III-4** in THF solution.

The UV-Vis spectra of **III-1**, **III-2**, **III-3**, **III-4** and **II-2** in THF are shown in Figure 3.2. **III-1** and **III-3** in THF both displayed relatively intense absorption bands centered at 360 nm and 340 nm for the $n \rightarrow \sigma^*$ absorption of the radical electrons and 220 nm for the $\sigma \rightarrow \sigma^*$ absorption of the cages, while **III-2** and **III-4** both displayed absorption bands centered at 360 nm and 340 nm for the $n \rightarrow \sigma^*$ absorption of the radical electrons and broad absorption bands centred at 225 nm for the absorption of the phenyl rings and cages. Compound **III-3** showed another one absorption band centered at 260 nm.

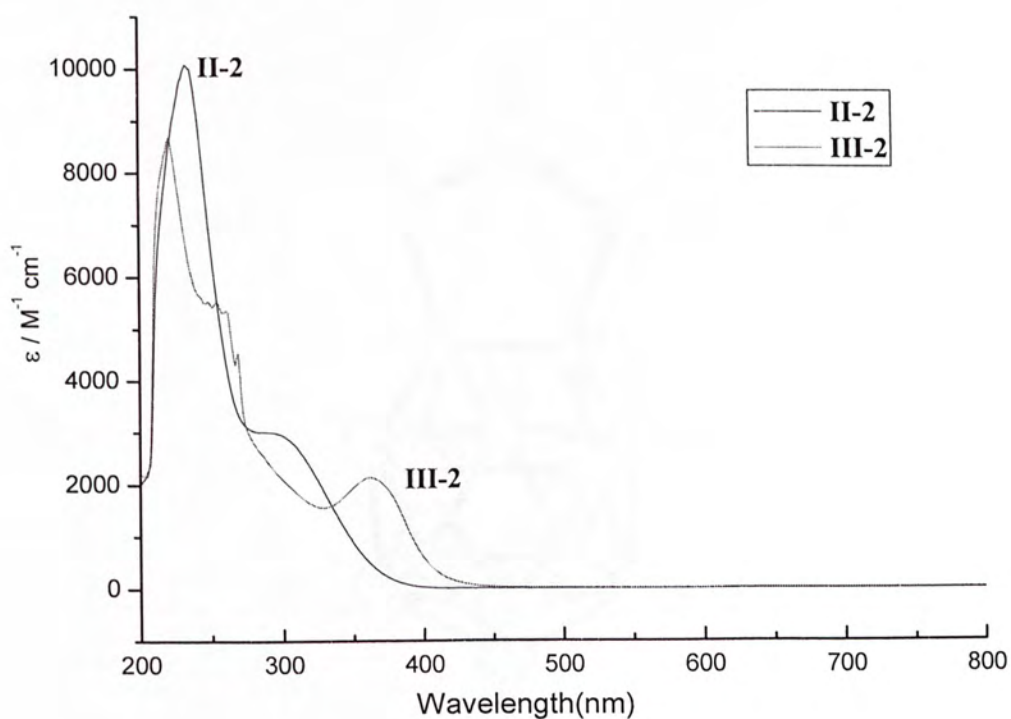
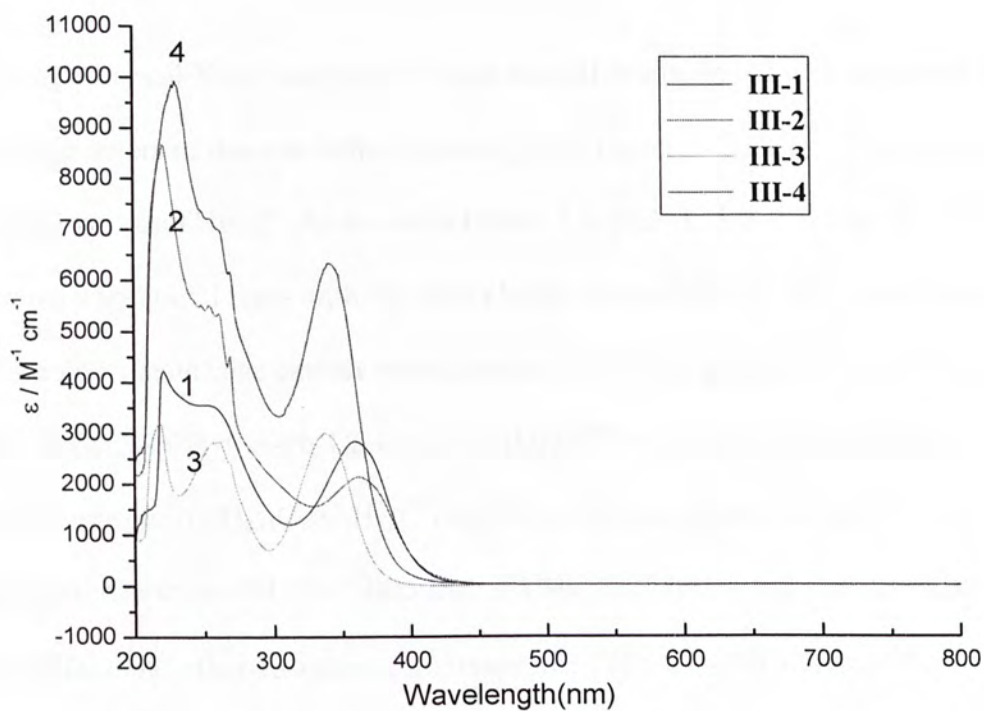


Figure 3.2. UV-Vis Spectra of **III-1**, **III-2**, **III-3**, **III-4** and **II-2**

3.2. Structures

Single-crystal X-ray analyses revealed that **III-1** consists of well-separated, alternating layers of discrete radical anions $[1,2-(\text{CH}_2)_3-1,2-\text{C}_2\text{B}_{11}\text{H}_{11}]^{\bullet-}$ and cations $[\text{Na}(\text{18-crown-6})(\text{THF})_2]^+$. As shown in Figure 3.3, $[1,2-(\text{CH}_2)_3-1,2-\text{C}_2\text{B}_{11}\text{H}_{11}]^{\bullet-}$ bears two trapezoidal faces with the others being triangulated, giving one five- and one four-coordinate cage carbon atoms, respectively. This geometry is similar to that observed in $1,2-(\text{CH}_2)_3-3\text{-Ph-}1,2-\text{C}_2\text{B}_{11}\text{H}_{10}$ (**II-2**),^{40a} but is significantly different from that of *nido*- $[(\text{CH}_2)_3\text{C}_2\text{B}_{11}\text{H}_{11}]^{2-}$ in $[(\text{CH}_2)_3\text{C}_2\text{B}_{11}\text{H}_{11}][\text{Na}_2(\text{THF})_4]$.^{40a,63} Although the average B-B/B-C distances of 1.80(1)/1.71(1) Å are close to those found in **II-2** and other 13-vertex carboranes, the C(1)⋯B(4)/B(3A) and C(1'A)⋯B(3)/B(2A) distances are much longer than the corresponding values observed in **II-2**.

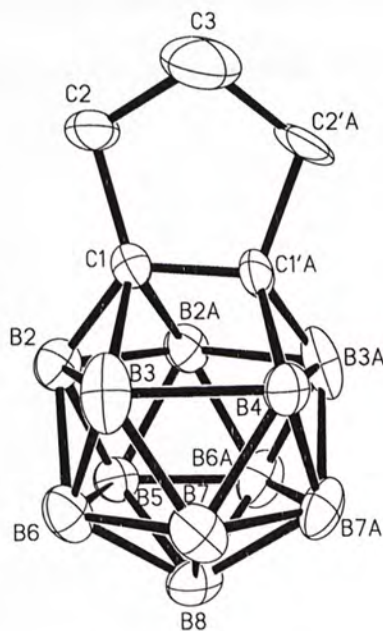


Figure 3.3. Molecular structure of $[(\text{CH}_2)_3\text{C}_2\text{B}_{11}\text{H}_{11}]^{\bullet-}$ in **III-1**, showing only one conformer. Selected bond lengths [Å]: C1-C1'A 1.45(1), C1-B2 1.49(1), C1-B3 1.91(1), C1-B2A 1.98(1), C1...B4 2.52 (1), C1...B3A 2.53 (1), C1'A...B3 2.37 (1), C1'A...B2A 2.17 (1), C1'A-B3A 1.49(1), C1'A-B4 1.67(1), C1-C2 1.56(1), C2-C3 1.52(1), C3-C2'A 1.47(1), C2'A-C1'A 1.51(1).

The single-crystal X-ray structures of **III-3** and **III-4** are shown in Figure 3.4 and Figure 3.5. Selected bond distances for radical anions **III-1**, **III-3** and **III-4** are listed in Table 3.1. The average B-B/B-C distances of 13-vertex carboranes and their radical anions are very close to each other (Table 3.2). The average B-B distances of 1.832(19) Å in **III-3** and 1.806(10) Å in **III-4** are longer than the average B-B distance of 1.785(7) Å in the neutral *closo* carborane **II-4** which implies the expansion of the cage after adding electron. The average B-C distances of 1.693(13) Å in **III-3** and 1.711(7) Å in **III-4** are shorter than the average B-C distance of 1.735(8) Å in the neutral *closo* carborane **II-4**. The $\text{C}_{\text{cage}}\text{-C}_{\text{cage}}$ distances of radical anions are found to be longer than the corresponding values observed in the neutral *closo* 13-vertex carboranes.

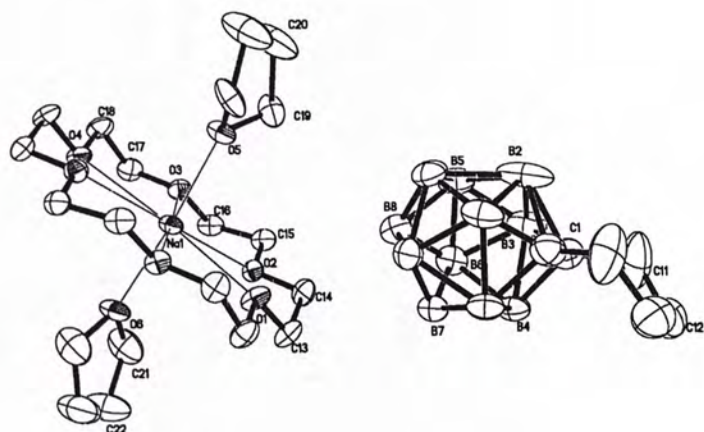


Figure 3.4. Molecular structure of
 $[1,2-(\text{CH}_2)_4-1,2-\text{C}_2\text{B}_{11}\text{H}_{11}][\text{Na}(18\text{-crown-6})(\text{THF})_2]$ (**III-3**).

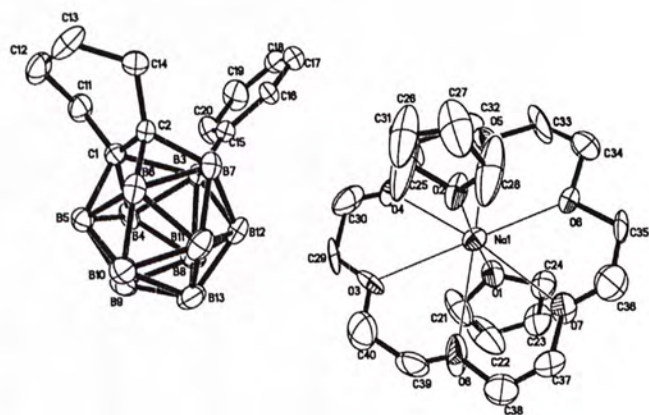


Figure 3.5. Molecular structure of
 $[1,2-(\text{CH}_2)_4-3\text{-Ph-}1,2-\text{C}_2\text{B}_{11}\text{H}_{11}][\text{Na}(18\text{-crown-6})(\text{THF})_2]$ (**III-4**).

Table 3.1. Selected bond distances (Å) in 13-vertex carborane radical anions.

	III-1	III-3	III-4
C(1)-C(2)	1.45(1)	1.51(1)	1.465(6)
C(1)-B(3)	1.98(1)	1.85(1)	1.913(6)
C(1)-B(4)	1.49(1)	1.55(1)	1.621(7)
C(1)-B(5)	1.91(1)	1.68(1)	1.720(7)
C(1)-B(6)	2.52(1)	2.44(1)	2.488(7)
C(2)-B(3)	2.17(1)	1.85(1)	2.099(7)
C(2)-B(5)	2.37(1)	2.44(1)	2.393(7)
C(2)-B(6)	1.67(1)	1.68(1)	1.668(7)
C(2)-B(7)	1.49(1)	1.55(1)	1.635(6)

Table 3.2. Average distances of C_{cage}-C_{cage}, C-B and B-B bonds in 13-vertex carboranes and their radical anions.

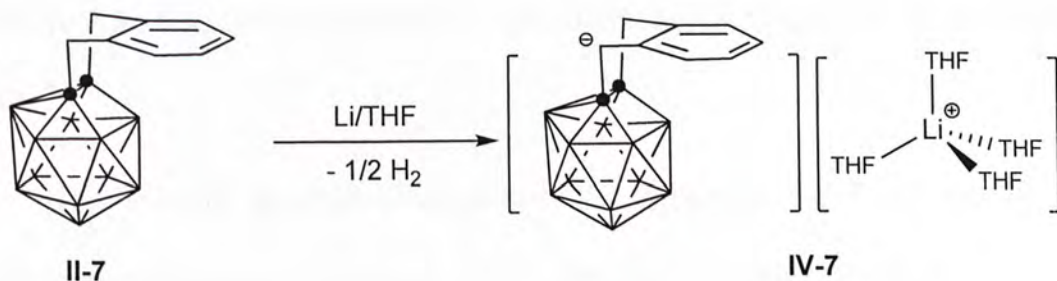
Average distances	II-2	II-7	II-4	II-6	II-8	II-9	III-1	III-3	III-4	IV-7
av. C _{cage} -C _{cage}	1.443(2)	1.43(2)	1.379(6)	1.414(3)	1.439(3)	1.421(5)	1.45(1)	1.51(1)	1.465(6)	1.456(3)
av. C-B bonds	1.726(3)	1.768(2)	1.735(8)	1.778(3)	1.760(4)	1.764(4)	1.71(1)	1.69(1)	1.711(7)	1.753(5)
av. B-B bonds	1.797(4)	1.80(2)	1.79(1)	1.799(4)	1.800(5)	1.798(6)	1.80(1)	1.83(2)	1.81(1)	1.774(7)

3.3. Synthesis and Structure of a monoanionic salt

[1,2- $\{o\text{-C}_6\text{H}_4(\text{CH}_2)(\text{CH})\}$ -1,2- $\text{C}_2\text{B}_{11}\text{H}_{11}$][Li(THF) $_4$] (IV-7)

Treatment of 1,2- $o\text{-C}_6\text{H}_4(\text{CH}_2)_2$ -1,2- $\text{C}_2\text{B}_{11}\text{H}_{11}$ (**II-7**) with 1 equiv of finely cut lithium metal in THF at room temperature gave, after recrystallization from THF, [1,2- $\{o\text{-C}_6\text{H}_4(\text{CH}_2)(\text{CH})\}$ -1,2- $\text{C}_2\text{B}_{11}\text{H}_{11}$][Li(THF) $_4$] (**IV-7**) as yellow crystals in 90% isolated yield (Scheme 3.2). It is air- and moisture-sensitive but remains stable for months at room temperature under an inert atmosphere. It is soluble in THF and ether, insoluble in aromatic solvents and hexane.

Scheme 3.2. Preparation of [1,2- $\{o\text{-C}_6\text{H}_4(\text{CH}_2)(\text{CH})\}$ -1,2- $\text{C}_2\text{B}_{11}\text{H}_{11}$][Li(THF) $_4$] (**IV-7**)



The methylene protons may be very acidic due to the joint effect of the aromatic ring and the cage, which can react with lithium metal in THF to generate monoanion [1,2- $\{o\text{-C}_6\text{H}_4(\text{CH}_2)(\text{CH})\}$ -1,2- $\text{C}_2\text{B}_{11}\text{H}_{11}$] $^-$ and release H₂.

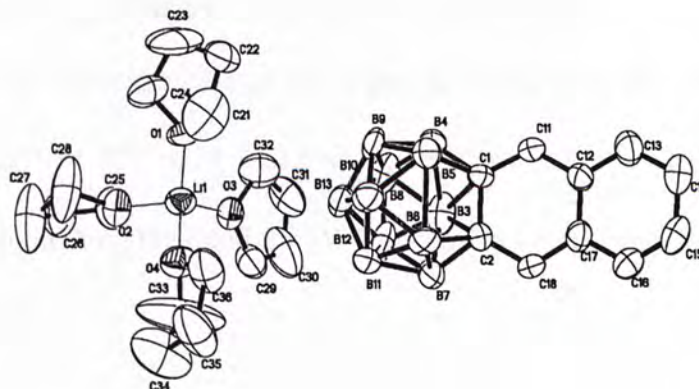


Figure 3.6 Molecular structure of [1,2- $\{o\text{-C}_6\text{H}_4(\text{CH}_2)(\text{CH})\}$ -1,2- $\text{C}_2\text{B}_{11}\text{H}_{11}$][Li(THF) $_4$] (**IV-7**).

The ^1H NMR spectrum of compound **IV-7** has a singlet at δ 6.04 ppm for the CH group and another singlet at δ 3.47 ppm for the methylene group, while the compound **II-7**^{40a} has a singlet at δ 4.35 ppm for the methylene groups, suggesting the elimination of H atom in compound **IV-7**. Similar comparison in the ^{13}C NMR spectra also shows the deprotonation process of compound **II-7**^{40a} to form compound **IV-7**, as δ 122.4 (CH), 46.41 (CH_2) ppm in **IV-7** and δ 50.81 (CH_2) ppm in **II-7**.^{40a} The ^{11}B NMR spectra of **IV-7** and **II-7** display the same pattern of 1:5:5 with different chemical shifts, which suggests that the cage is not affected after the deprotonation. The NMR data indicate that **IV-7** is not a radical rather a diamagnetic species.

The molecular structure of **IV-7** has been confirmed and shown in Figure 3.6. For easy comparison, the selected bond distances and angles for **II-7**^{40a} and **IV-7** are

compiled in Table 3.3. No significant differences are observed in the B-B and C-B distances. However, C_{cage}-C_{cage} bond in **IV-7** was somewhat elongated than that in **II-7**, and C_{cage}-C_{bridge} distances were significantly shortened in **IV-7**, which might be the results of the delocalization of the negative charge over the ring of the bridge. The bond angles of C1—C11—C12 and C2—C18—C17 in **IV-7** are larger than those in **II-7**, indicating the trend for **IV-7** to adopt a more planar geometry of C(11) and C(18) atoms.

Table 3.3. Selected bond distances (Å) and angels (deg) in **IV-7** and **II-7**.^a

	II-7	IV-7	II-7	IV-7
C(1)-B(3)	1.911(2)	2.010(5)	C(1)-C(2)	1.43(2)
C(1)-B(4)	1.619(2)	1.602(5)	C(1)-C(11)	1.51(2)
C(1)-B(5)	1.799(2)	1.786(5)	C(2)-C(18)	1.52(2)
C(1)-B(6)	2.422(2)	2.446(5)	C(11)-C(12)	1.51(2)
C(2)-B(3)	1.869(2)	1.944(5)	C(18)-C(17)	1.50(2)
C(2)-B(5)	2.512(2)	2.548(5)	C1---C11---C12	112.0(1)
C(2)-B(6)	1.821(2)	1.803(4)	C2---C18---C17	112.0(1)
C(2)-B(7)	1.592(2)	1.631(5)		
				118.64(2)
				118.62(3)

^a For compound **II-7**, only average values of two crystallographically independent molecules are given.

3.4. Summary

The carborane radical anions with $2n+3$ framework electrons have been isolated and structurally characterized for the first time. They are intermediates between the two well-established and abundant $2n+2$ (*closo*) and $2n+4$ (*nido*) systems. This result may imply that larger cages would enhance the thermodynamical stability of clusters with $2n+3$ systems. The role of the linkage between the two cage carbons is not clear yet at this stage.

Chapter 4 Electrochemical Study of 12- and 13-Vertex

closo-Carboranes

4.1 Electrochemical Study of 12-Vertex Carboranes

The cyclic voltammogram of 12-vertex carborane **I-1** shows one pair of reversible peaks and one possible irreversible reduction wave. The first pair could be ascribed to the one-electron process from **I-1** + e⁻ → **I-1**^{•-}. The second one may be corresponding to the one-electron process of **I-1**^{•-} + e⁻ → *nido*-[1,2-(CH₂)₃-1,2-C₂B₁₀H₁₀]²⁻. It is noted that treatment of **I-1** with 1 equivalent of sodium or lithium in THF, gave only *nido*-[1,2-(CH₂)₃-1,2-C₂B₁₀H₁₀]²⁻. No deep red solution was formed and no radical anion was observed.

I-2, **I-3** and **I-4** have similar structures and it would be easy to explain why they have similar CV graphs as shown in Figures 4.2, 4.3 and 4.4. All these three have one reduction peak with $E = -1.77$ V for **I-2**, -1.72 V for **I-3** and -1.64 V for **I-4**, and one oxidation peak with $E = -0.78$ V for **I-2**, -0.88 V for **I-3** and -0.86 V for **I-4**. However, these reduction and oxidation peaks do not seem to be pairs according to the peak intervals, and the reduction peaks may represent the *closo* to *nido* process while the oxidation peaks may stand for processes from radical anions to *closo* species.

The CV graph of **I-6** as shown in Figure 4.5 has only one irreversible reduction peak for the process probably from *closo* to *nido* species with $E = -1.87$ V. The cyclic voltammogram of compound **I-7** (Figure 4.6) displays one pair of reversible peaks at low potential with $E_{1/2} = -1.23$ V referring to the radical anion formation, and another irreversible reduction peak at higher potential with $E = -2.77$ V represents

the formation of corresponding *nido* species. It is not clear why **I-6** and **I-7** have a different type of CV graphs while they have similar structures.

The electrochemical process of **I-8** (Figure 4.7) exhibits one pair of reversible peaks with $E_{1/2} = -0.98$ V which might represent the process of radical anion formation. The radical anion might be stabilized by the butadiene bridge, and corresponding *nido* species would not be formed.

The CV graph of **I-9** (Figure 4.8) is quite strange and difficult to explain. The cyclic voltammogram of **I-10** as shown in Figure 4.9 has one irreversible reduction peak with $E = -1.92$ V representing the formation of corresponding *nido* species.

Generally speaking, 12-vertex carboranes are reduced stepwise with two one-electron processes.⁶⁴ It could be observed two sequential reversible peaks for 1,2-(C₆H₅CH₂)₂-1,2-C₂B₁₀H₁₀ in cyclic voltammogram.^{51d} However, the corresponding radical anions for 12-vertex *closo* carboranes may not be stable, and they are converted to corresponding *nido* species immediately once formed, which may explain that only one reduction peak could be observed normally in cyclic voltammogram for 12-vertex *closo* carboranes. No 12-vertex carborane radical anion has ever been isolated yet.^{29d, 51d}

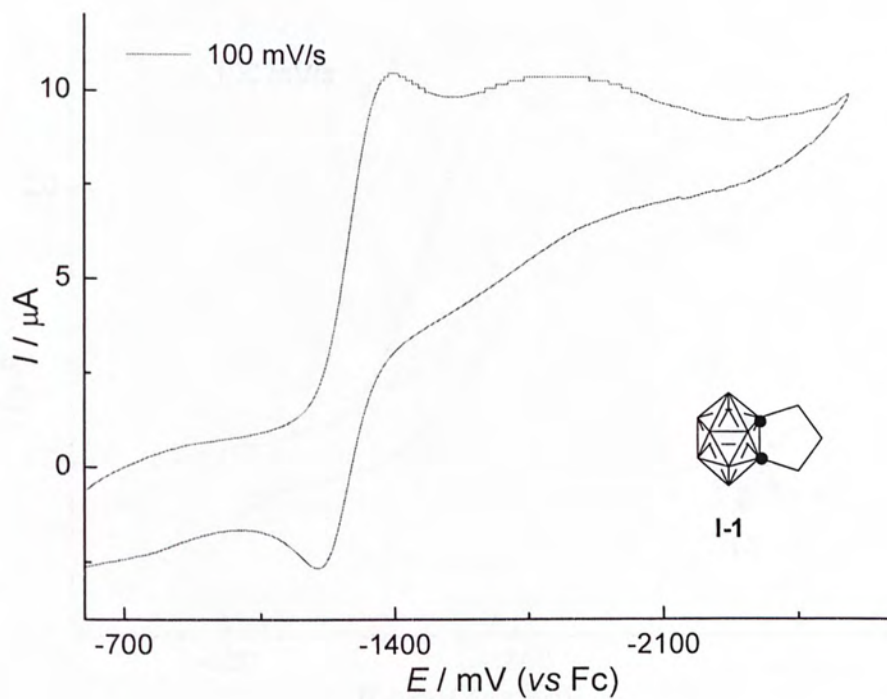


Figure 4.1.

Figure 4.1. Cyclic voltammogram of **I-1** in MeCN/0.1M Bu₄NPF₆ recorded at 100 mV/s. Cyclic voltammetry of **I-1** in MeCN/0.1M Bu₄NPF₆ showed one reversible waves with $E_{1/2} = -1.30$ V, and one possible irreversible reduction peak with $E = -1.83$ V (vs ferrocene (Fc)).

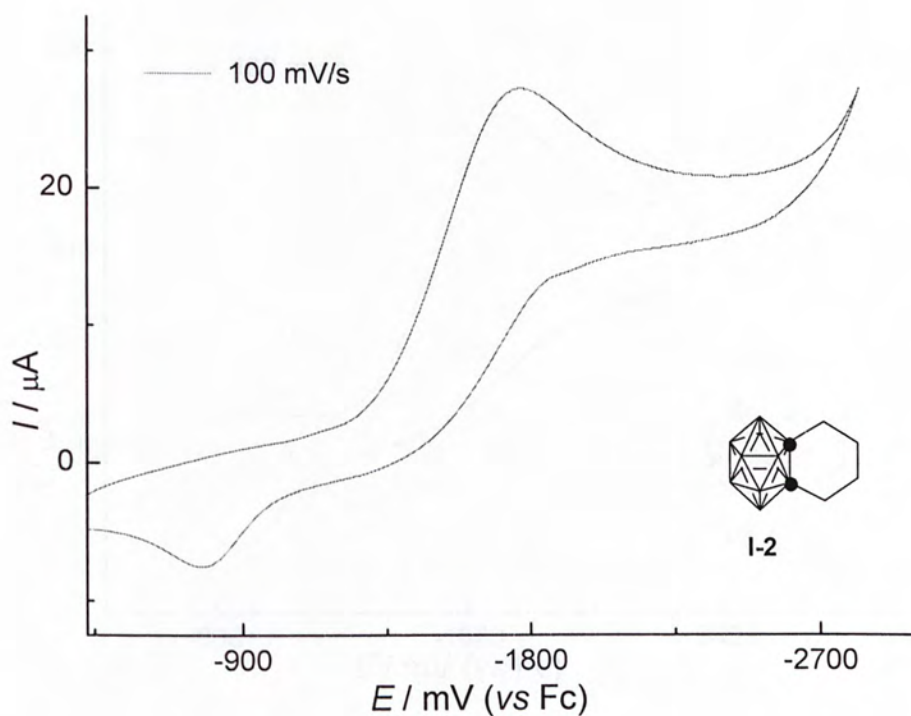


Figure 4.2.

Figure 4.2. Cyclic voltammogram of **I-2** in MeCN/0.1M Bu₄NPF₆ recorded at 100 mV/s. Cyclic voltammetry of **I-2** in MeCN/0.1M Bu₄NPF₆ showed one irreversible reduction wave with $E = -1.77$ V, and one irreversible oxidation peak with $E = -0.78$ V (vs ferrocene (Fc)).

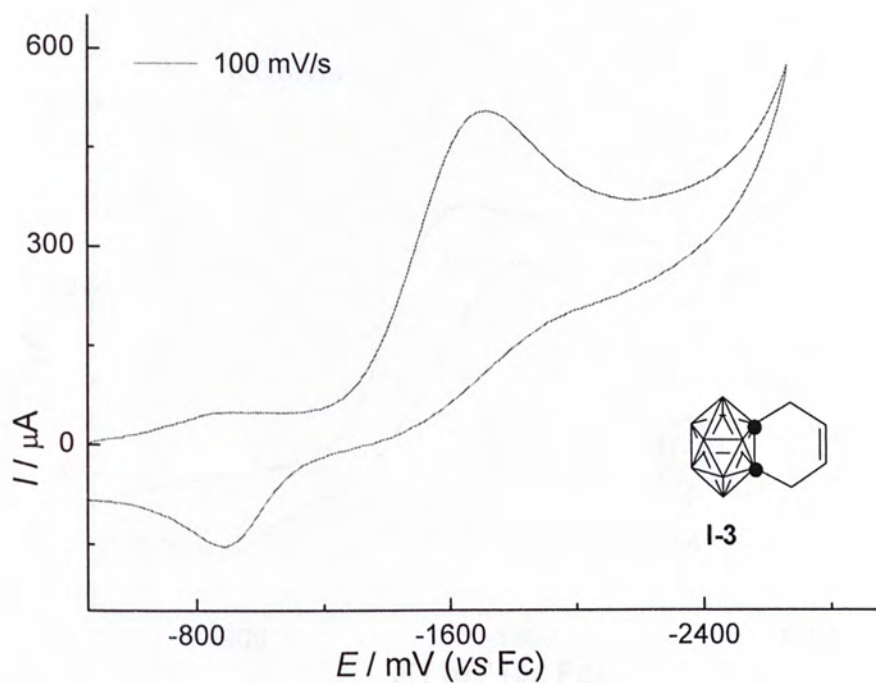


Figure 4.3.

Figure 4.3. Cyclic voltammogram of **I-3** in MeCN/0.1M Bu₄NPF₆ recorded at 100 mV/s. Cyclic voltammetry of **I-3** in MeCN/0.1M Bu₄NPF₆ showed one irreversible reduction wave with $E = -1.72$ V, and one irreversible oxidation peak with $E = -0.88$ V (vs ferrocene (Fc)).

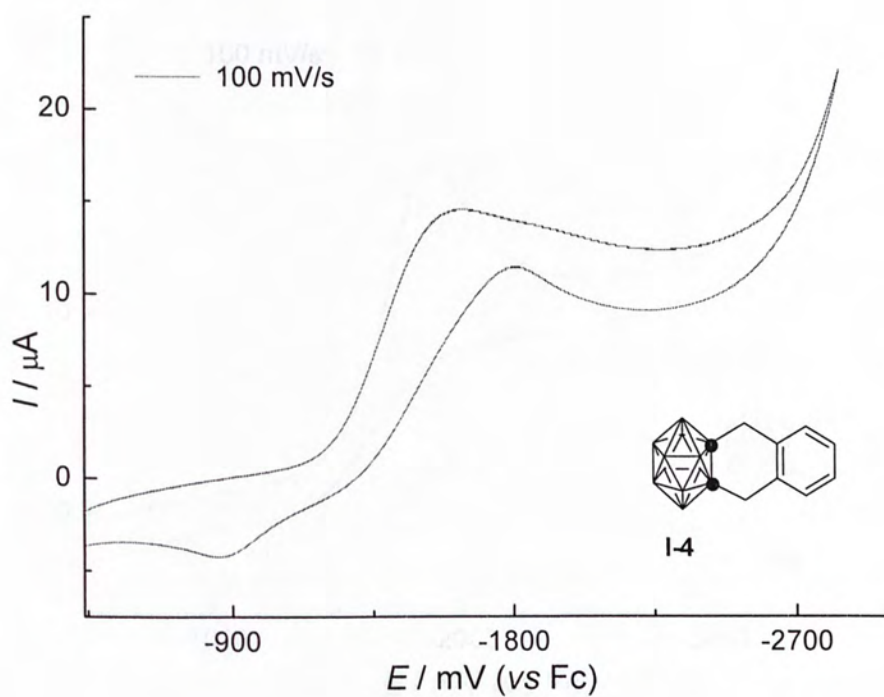


Figure 4.4.

Figure 4.4. Cyclic voltammogram of **I-4** in MeCN/0.1M Bu₄NPF₆ recorded at 100 mV/s. Cyclic voltammetry of **I-4** in MeCN/0.1M Bu₄NPF₆ showed one irreversible reduction wave with $E = -1.64$ V, and one irreversible oxidation peak with $E = -0.86$ V (vs ferrocene (Fc)).

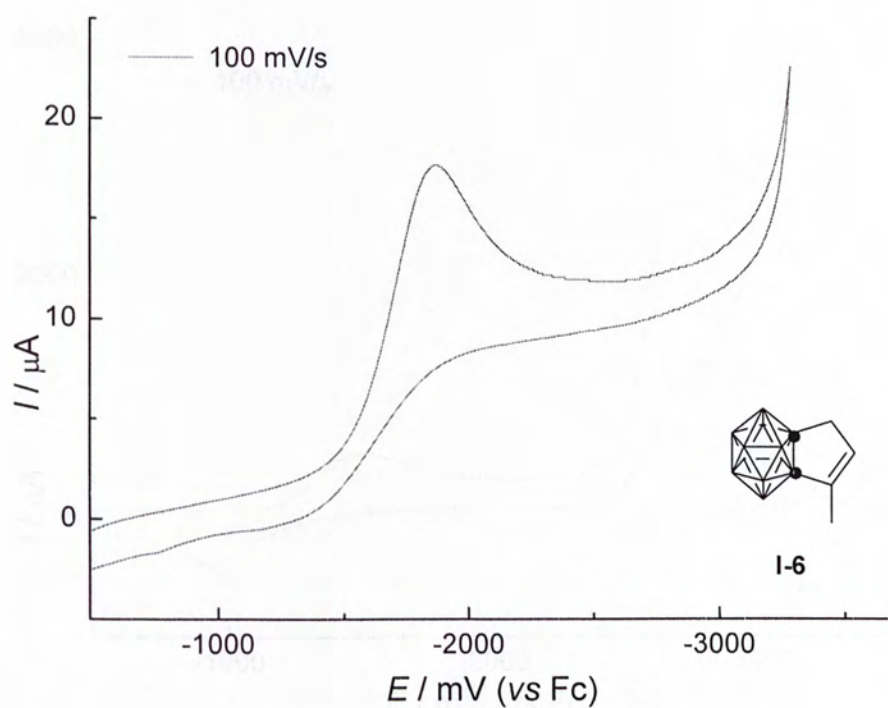


Figure 4.5.

Figure 4.5. Cyclic voltammogram of **I-6** in MeCN/0.1M Bu₄NPF₆ recorded at 100 mV/s. Cyclic voltammetry of **I-6** in MeCN/0.1M Bu₄NPF₆ showed one irreversible reduction wave with $E = -1.87$ V (vs ferrocene (Fc)).

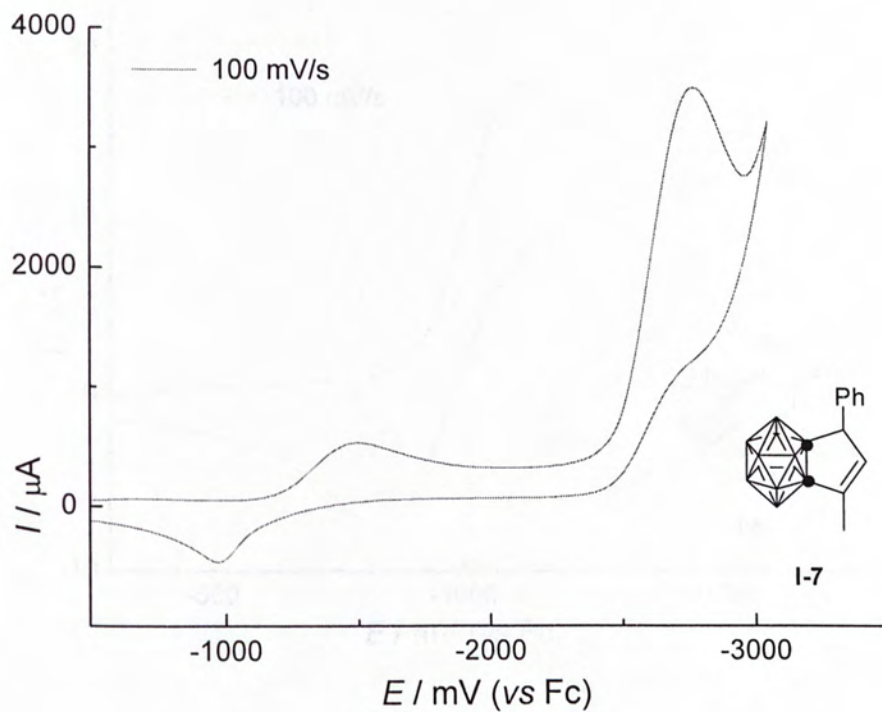


Figure 4.6.

Figure 4.6. Cyclic voltammogram of **I-7** in MeCN/0.1M Bu₄NPF₆ recorded at 100 mV/s. Cyclic voltammetry of **I-7** in MeCN/0.1M Bu₄NPF₆ showed one reversible waves with $E_{1/2} = -1.23$ V, and one irreversible reduction peak with $E = -2.77$ V (vs ferrocene (Fc)).

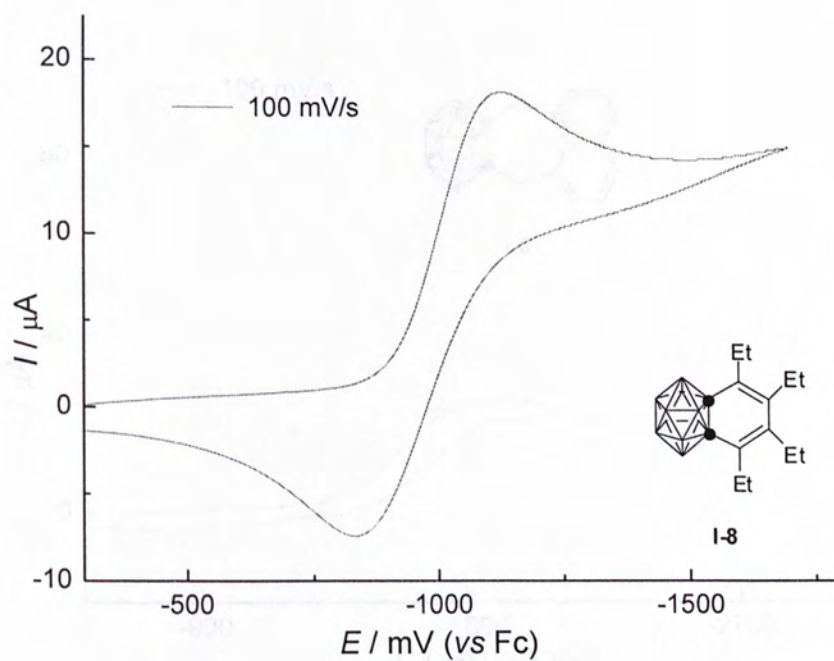


Figure 4.7.

Figure 4.7. Cyclic voltammogram of **I-8** in MeCN/0.1M Bu₄NPF₆ recorded at 100 mV/s. Cyclic voltammetry of **I-8** in MeCN/0.1M Bu₄NPF₆ showed one reversible waves with $E_{1/2} = -0.98$ V (vs ferrocene (Fc)).

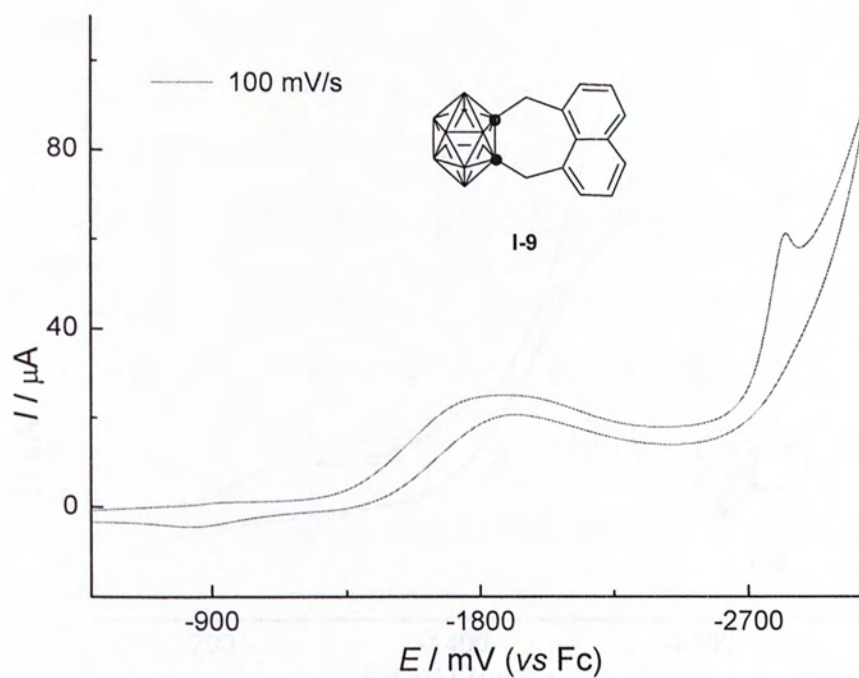


Figure 4.8.

Figure 4.8. Cyclic voltammogram of **I-9** in MeCN/0.1M Bu₄NPF₆ recorded at 100 mV/s. Cyclic voltammetry of **I-9** in MeCN/0.1M Bu₄NPF₆ showed one irreversible reduction wave with $E = -2.83$ V (vs ferrocene (Fc)).

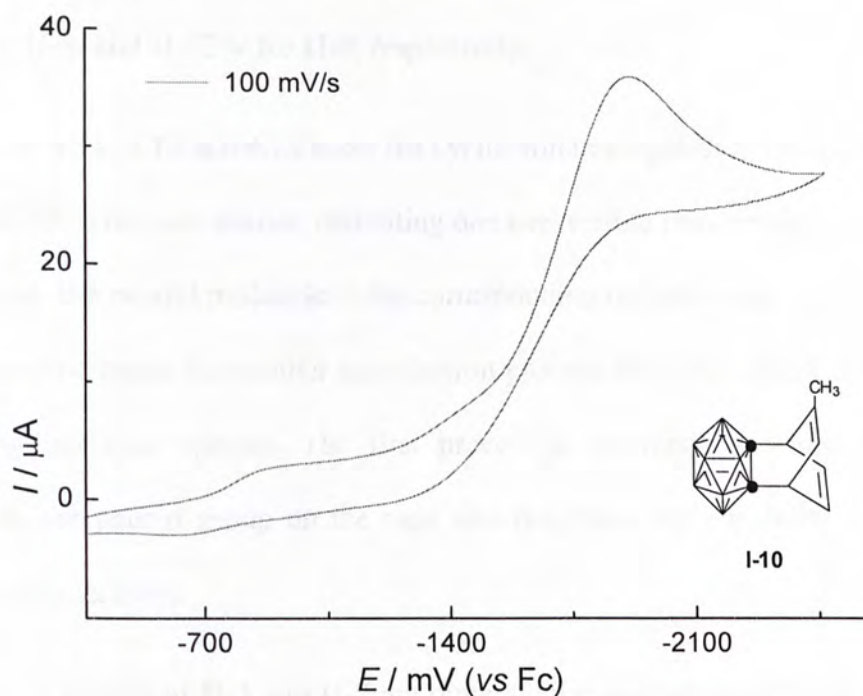


Figure 4.9.

Figure 4.9. Cyclic voltammogram of **I-10** in MeCN/0.1M Bu₄NPF₆ recorded at 100 mV/s. Cyclic voltammetry of **I-10** in MeCN/0.1M Bu₄NPF₆ showed one irreversible reduction wave with $E = -1.92$ V (vs ferrocene (Fc)).

4.2 Electrochemical Study of 13-Vertex Supercarboranes

As shown in Figures 4.10, 4.17 and 4.18, the cyclic voltammograms of compounds **II-1**, **II-8** and **II-9** are similar to each other displaying one reversible pair of peaks and one quasi-reversible pair of waves. The first pair is the one electron process from the neutral compound to the corresponding radical anion with $E_{1/2} = -1.28$ V for **II-1**, -1.23 V for **II-8**, and -0.90 V for **II-9**, and the second pair is from

the radical anion to the corresponding *nido* species with $E_{1/2} = -1.85$ V for **II-1**, -1.94V for **II-8**, and -1.72 V for **II-9**, respectively.

Figures 4.11, 4.13 and 4.20 show the cyclic voltammograms of compounds **II-2**, **II-4** and **II-11**. They are similar, exhibiting one irreversible peak for the one electron process from the neutral molecule to the corresponding radical anion, and one pair of quasi-reversible peaks for another one electron process from the radical anion to the corresponding *nido* species. The first process is irreversible, which might be ascribed to the phenyl group on the cage that may have the capability to store or influence the electrons.

The CV graphs of **II-3** and **II-7** are quite similar as shown in Figures 4.12 and 4.16, but they may undergo different electrochemical processes. When 1 equivalent of sodium metal and 1 equivalent of 18-crown-6 ether were added to **II-3** in THF, a deep red solution was generated, from which the radical anion **III-3** was isolated. On the other hand, if 1 equivalent of sodium or lithium metal was added to **II-7** in the same manner, a bright yellow solution was produced, from which a monoanionic salt **IV-7** was obtained. For **II-7**, the first process is the deprotonation, and the second process is probably the reduction to form *nido*-[1,2-{*o*-C₆H₄(CH₂)₂}-1,2-C₂B₁₁H₁₁]²⁻.^{40a} For **II-3**, the first process refers to the radical anion formation, and the second one represents the formation of corresponding *nido* species. It is not clear why **II-1** and **II-3** have a different type of CV graphs.

The cyclic voltammograms of compounds **II-5** and **II-6** are similar to each other (Figures 4.14 and 4.15). The first irreversible peak and the second quasi-reversible waves may stand for the similar electrochemical processes to those observed in **II-2**,

II-4 and **II-11**. The 3rd pair of quasi-reversible peaks might be attributable to the electrochemical reaction of the double bond of the bridges.

The 13-vertex carborane **II-10** shows a unique cyclic voltammogram (Figure 4.19). It is noted that **II-10** is a C_{Ap} supercarborane and the electrochemical process may be coupled with the rearrangement of the cage atoms, which results in the irreversible process.

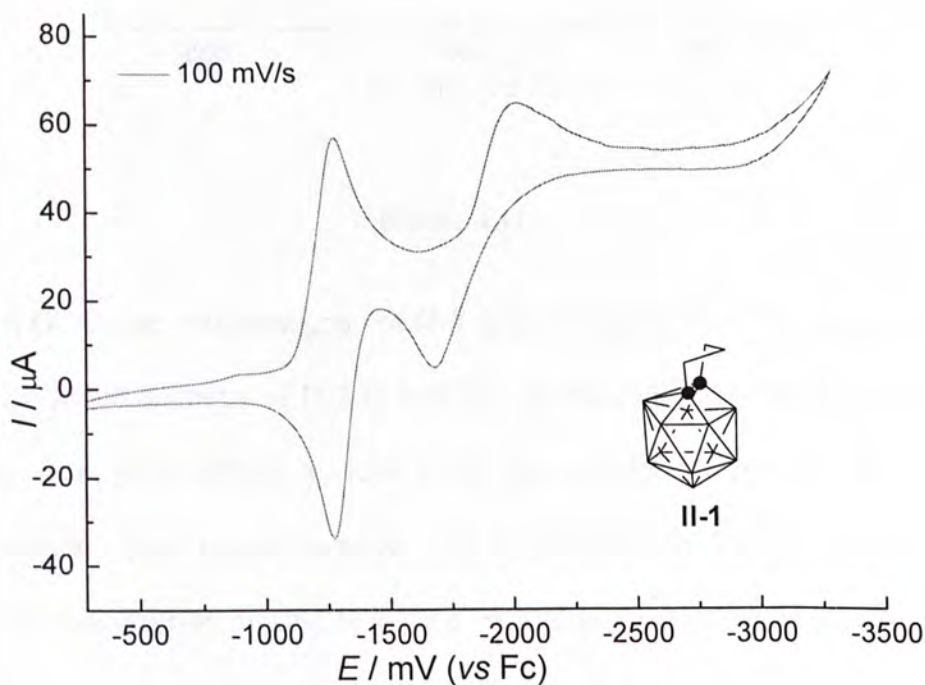


Figure 4.10.

Figure 4.10. Cyclic voltammogram of **II-1** in MeCN/0.1M Bu₄NPF₆ recorded at 100 mV/s. Cyclic voltammetry of **II-1** in MeCN/0.1M Bu₄NPF₆ showed one reversible waves with $E_{1/2}(0/-1) = -1.28$ V for the one-electron process $\text{II-1} + e^- \rightarrow \text{II-1}^{\bullet-}$, and one quasi-reversible peaks with $E_{1/2}(-1/-2) = -1.85$ V (vs ferrocene (Fc)) for another one-electron process $\text{II-1}^{\bullet-} + e^- \rightarrow [(\text{CH}_2)_3\text{C}_2\text{B}_{11}\text{H}_{11}]^{2-}$.

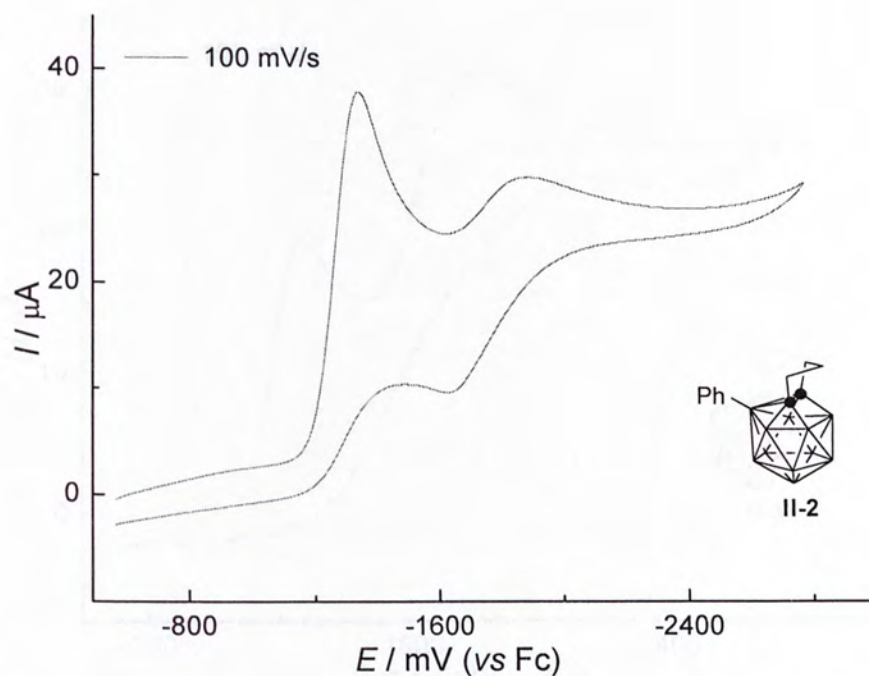


Figure 4.11.

Figure 4.11. Cyclic voltammogram of **II-2** in MeCN/0.1M Bu₄NPF₆ recorded at 100 mV/s. Cyclic voltammetry of **II-2** in MeCN/0.1M Bu₄NPF₆ showed one irreversible reduction peak with $E(0/-1) = -1.34$ V for the one-electron process $\text{II-2} + e^- \rightarrow \text{II-2}^{\cdot-}$, and one quasi-reversible peaks with $E_{1/2}(-1/-2) = -1.76$ V (vs ferrocene (Fc)) for another one-electron process $\text{II-2}^{\cdot-} + e^- \rightarrow [1,2-(\text{CH}_2)_3-3\text{-Ph-1,2-C}_2\text{B}_{11}\text{H}_{11}]^{2-}$.

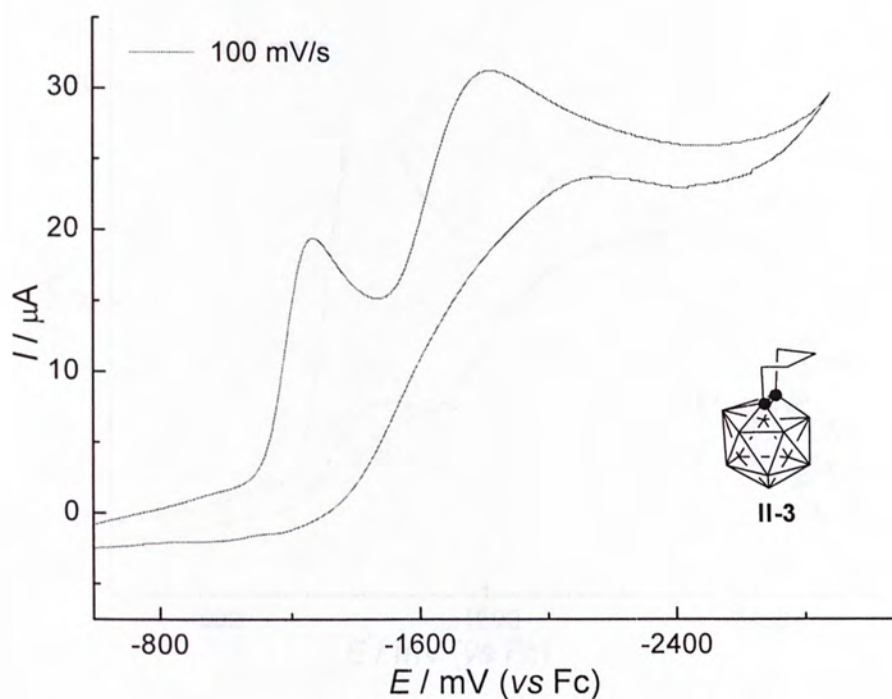


Figure 4.12.

Figure 4.12. Cyclic voltammogram of **II-3** in MeCN/0.1M Bu₄NPF₆ recorded at 100 mV/s. Cyclic voltammetry of **II-3** in MeCN/0.1M Bu₄NPF₆ showed one irreversible reduction peak with $E(0/-1) = -1.27$ V for the one-electron process $\text{II-3} + e^- \rightarrow \text{II-3}^{\bullet-}$, and one irreversible reduction peak with $E(-1/-2) = -1.83$ V (vs ferrocene (Fc)) for another one-electron process $\text{II-3}^{\bullet-} + e^- \rightarrow [(\text{CH}_2)_4\text{C}_2\text{B}_{11}\text{H}_{11}]^{2-}$.

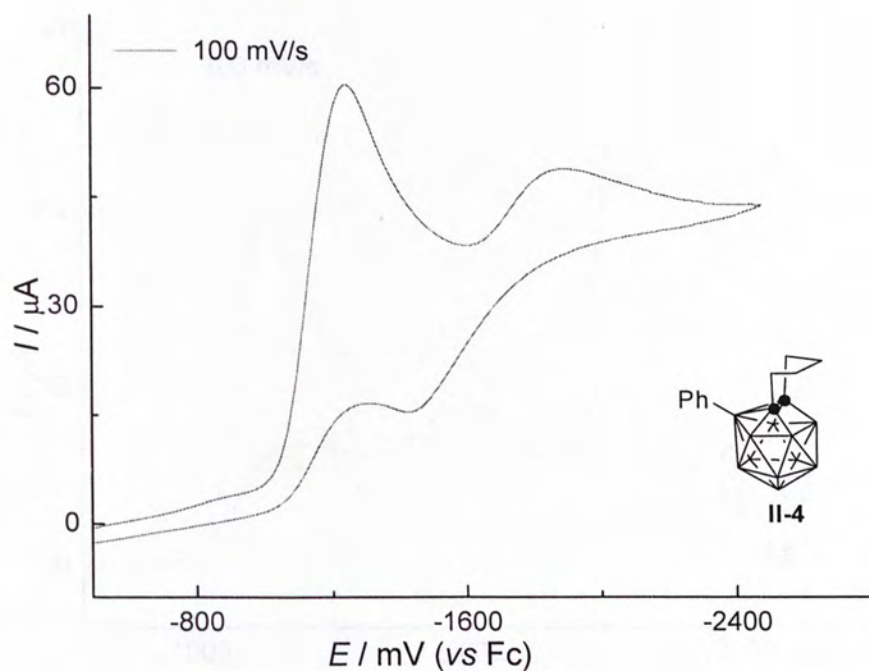


Figure 4.13.

Figure 4.13. Cyclic voltammogram of **II-4** in MeCN/0.1M Bu₄NPF₆ recorded at 100 mV/s. Cyclic voltammetry of **II-4** in MeCN/0.1M Bu₄NPF₆ showed one irreversible reduction peak with $E(0/-1) = -1.24$ V for the one-electron process $\text{II-4} + e^- \rightarrow \text{II-4}^{\bullet-}$, and one quasi-reversible peaks with $E_{1/2}(-1/-2) = -1.66$ V (vs ferrocene (Fc)) for another one-electron process $\text{II-4}^{\bullet-} + e^- \rightarrow [1,2-(\text{CH}_2)_4-3\text{-Ph-C}_2\text{B}_{11}\text{H}_{11}]^{2-}$.

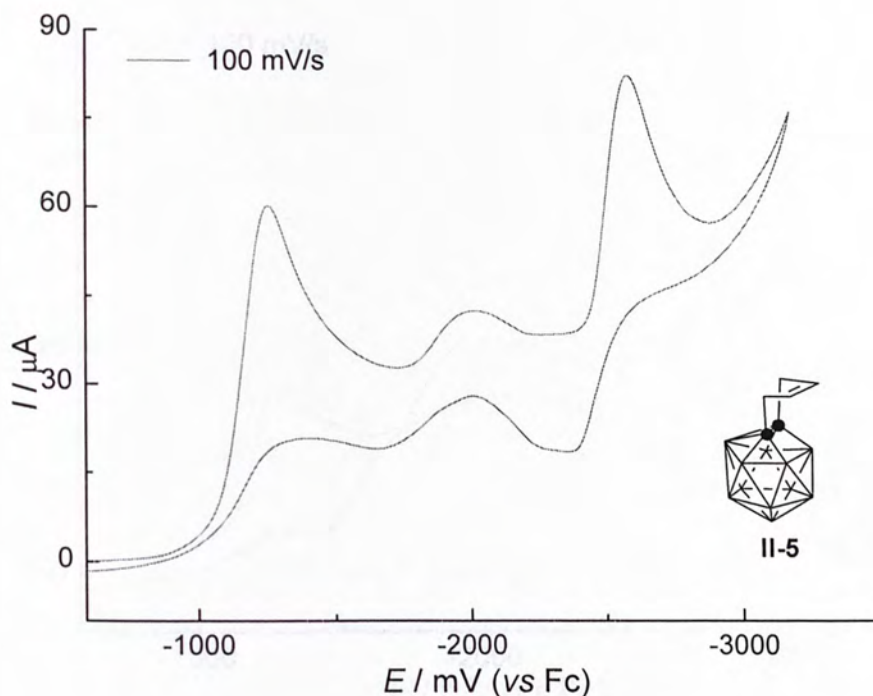


Figure 4.14.

Figure 4.14. Cyclic voltammogram of **II-5** in MeCN/0.1M Bu₄NPF₆ recorded at 100 mV/s. Cyclic voltammetry of **II-5** in MeCN/0.1M Bu₄NPF₆ showed one irreversible reduction wave with $E(0/-1) = -1.25$ V for the one electron process $\text{II-5} + e^- \rightarrow \text{II-5}^{\bullet-}$, one quasi-reversible peaks with $E_{1/2}(-1/-2) = -1.83$ V for the one electron process $\text{II-5}^{\bullet-} + e^- \rightarrow [1,2-(\text{CH}_2\text{CH}=\text{CHCH}_2)\text{-}1,2\text{-C}_2\text{B}_{11}\text{H}_{11}]^{2-}$ and one quasi-reversible waves with $E_{1/2} = -2.47$ V (vs ferrocene (Fc)) which may be corresponding to the reaction of double bond.

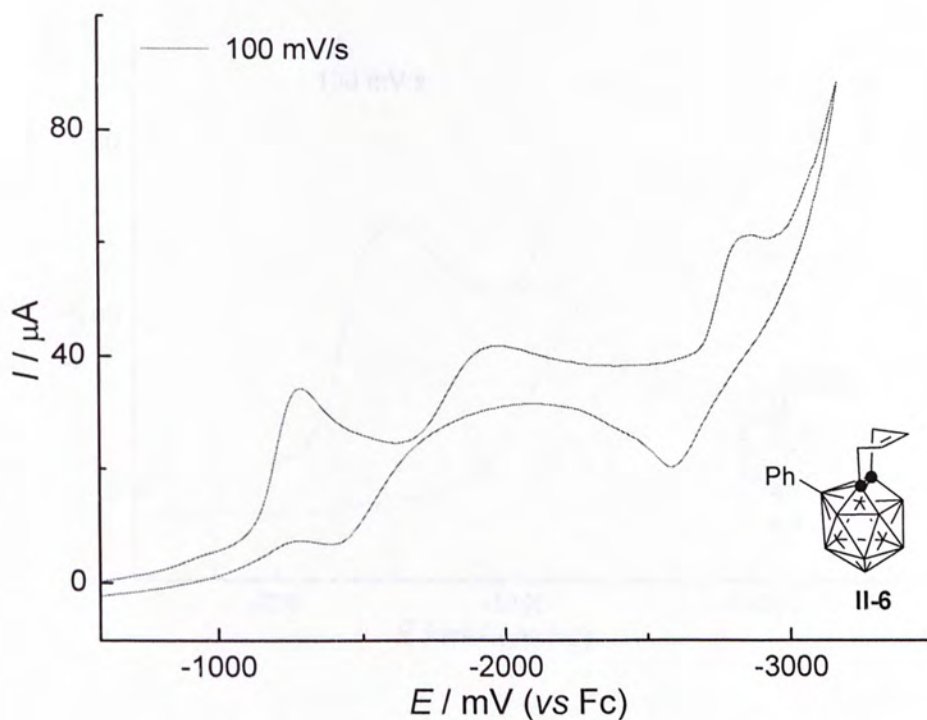


Figure 4.15.

Figure 4.15. Cyclic voltammogram of **II-6** in MeCN/0.1M Bu₄NPF₆ recorded at 100 mV/s. Cyclic voltammetry of **II-6** in MeCN/0.1M Bu₄NPF₆ showed one irreversible reduction wave with $E(0/-1) = -1.29$ V for the one electron process $\text{II-6} + e^- \rightarrow \text{II-6}^{\cdot-}$, one quasi-reversible peaks with $E_{1/2}(-1/-2) = -1.69$ V for the one electron process $\text{II-6}^{\cdot-} + e^- \rightarrow [1,2-(\text{CH}_2\text{CH}=\text{CHCH}_2)\text{-3-Ph-1,2-C}_2\text{B}_{11}\text{H}_{11}]^{2-}$ and one quasi-reversible waves with $E_{1/2} = -2.73$ V (vs ferrocene (Fc)) which may be corresponding to the reaction of double bond.

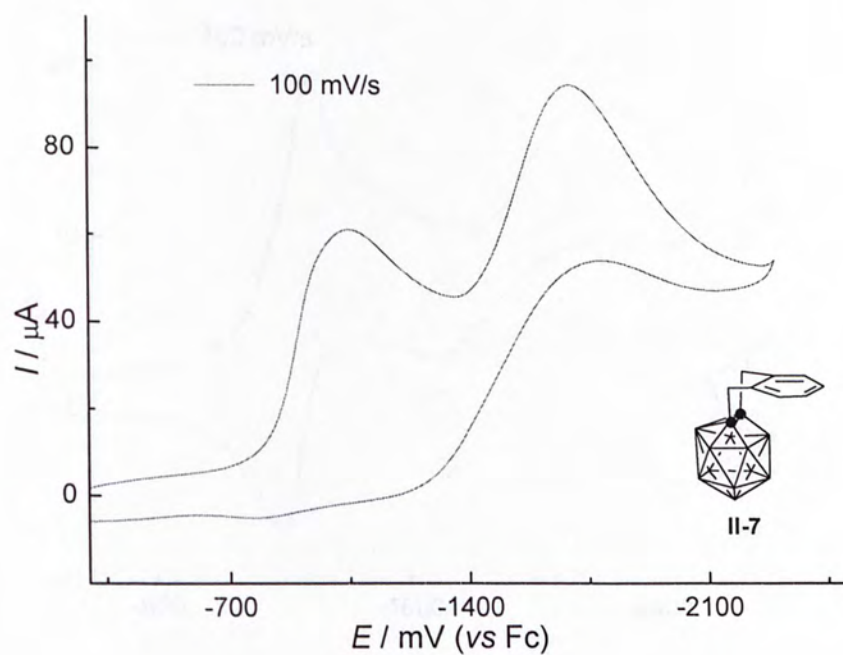


Figure 4.16.

Figure 4.16. Cyclic voltammogram of **II-7** in MeCN/0.1M Bu₄NPF₆ recorded at 100 mV/s. Cyclic voltammetry of **II-7** in MeCN/0.1M Bu₄NPF₆ showed one irreversible reduction wave with $E(0/-1) = -1.05$ V for the one-electron process $\text{II-7} + e^- \rightarrow [1,2-\{o\text{-C}_6\text{H}_4(\text{CH}_2)(\text{CH})\}\text{-1,2-C}_2\text{B}_{11}\text{H}_{11}]^-$, and one irreversible reduction peak with $E = -1.70$ V (vs ferrocene (Fc)) for the two-electron process $[1,2-\{o\text{-C}_6\text{H}_4(\text{CH}_2)(\text{CH})\}\text{-1,2-C}_2\text{B}_{11}\text{H}_{11}]^- + 2e^- \rightarrow [1,2-\{o\text{-C}_6\text{H}_4(\text{CH}_2)(\text{CH})\}\text{-1,2-C}_2\text{B}_{11}\text{H}_{11}]^{3-} (\text{nido})$.

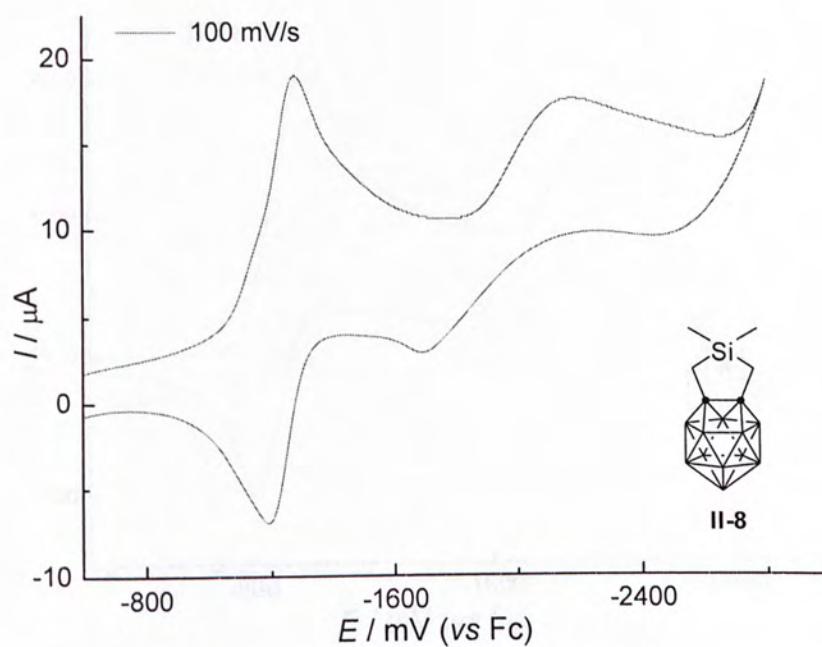


Figure 4.17.

Figure 4.17. Cyclic voltammogram of **II-8** in MeCN/0.1M Bu₄NPF₆ recorded at 100 mV/s. Cyclic voltammetry of **II-8** in MeCN/0.1M Bu₄NPF₆ showed one reversible waves with $E_{1/2}(0/-1) = -1.23$ V for the one-electron process $\text{II-8} + e^- \rightarrow \text{II-8}^{\bullet-}$, and one quasi-reversible peaks with $E_{1/2}(-1/-2) = -1.94$ V (vs ferrocene (Fc)) for another one-electron process $\text{II-8}^{\bullet-} + e^- \rightarrow [1,2\text{-Me}_2\text{Si}(\text{CH}_2)_2\text{-1,2-C}_2\text{B}_{11}\text{H}_{11}]^{2-}$.

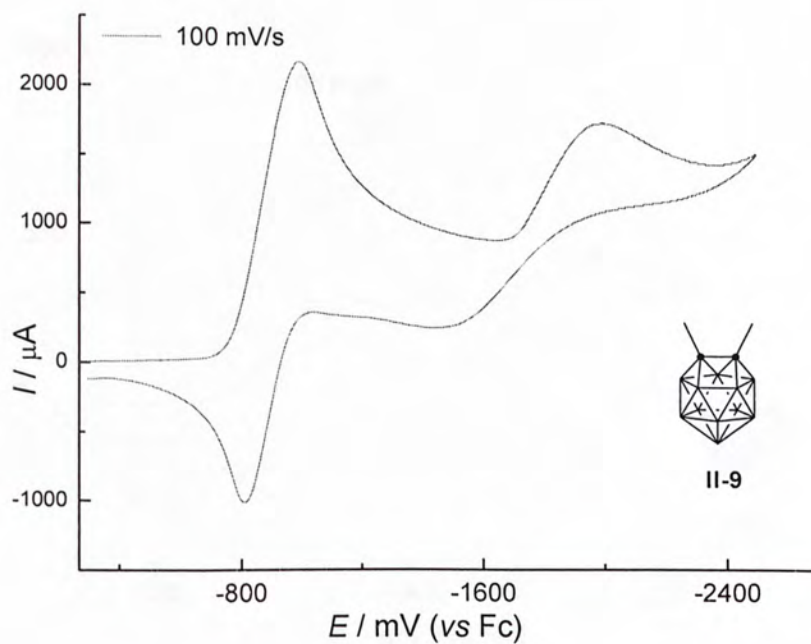


Figure 4.18.

Figure 4.18. Cyclic voltammogram of **II-9** in MeCN/0.1M Bu₄NPF₆ recorded at 100 mV/s. Cyclic voltammetry of **II-9** in MeCN/0.1M Bu₄NPF₆ showed one reversible waves with $E_{1/2}(0/-1) = -0.90$ V for the one-electron process $\text{II-9} + e^- \rightarrow \text{II-9}^{\bullet-}$, and one quasi-reversible peaks with $E_{1/2}(-1/-2) = -1.72$ V (vs ferrocene (Fc)) for another one-electron process $\text{II-9}^{\bullet-} + e^- \rightarrow [(\text{CH}_3)_2\text{C}_2\text{B}_{11}\text{H}_{11}]^{2-}$.

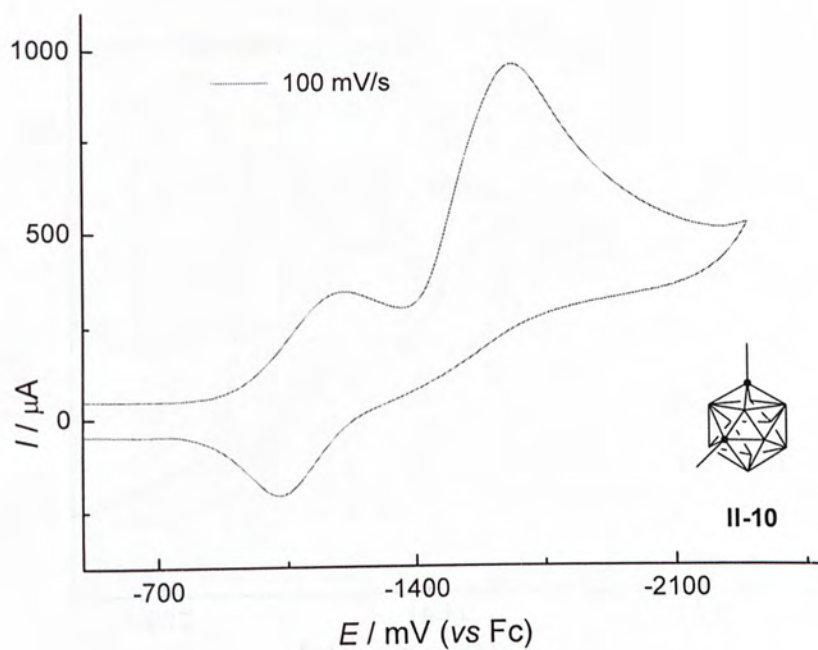


Figure 4.19.

Figure 4.19. Cyclic voltammogram of **II-10** in MeCN/0.1M Bu₄NPF₆ recorded at 100 mV/s. Cyclic voltammetry of **II-10** in MeCN/0.1M Bu₄NPF₆ showed one reversible waves with $E_{1/2}(0/-1) = -1.12$ V for the one-electron process **II-10** + e⁻ → **II-10**^{•-}, and one irreversible reduction peak with $E = -1.67$ V (vs ferrocene (Fc)) for another one-electron process **II-10**^{•-} + e⁻ → [(CH₃)₂C₂B₁₁H₁₁]²⁻.

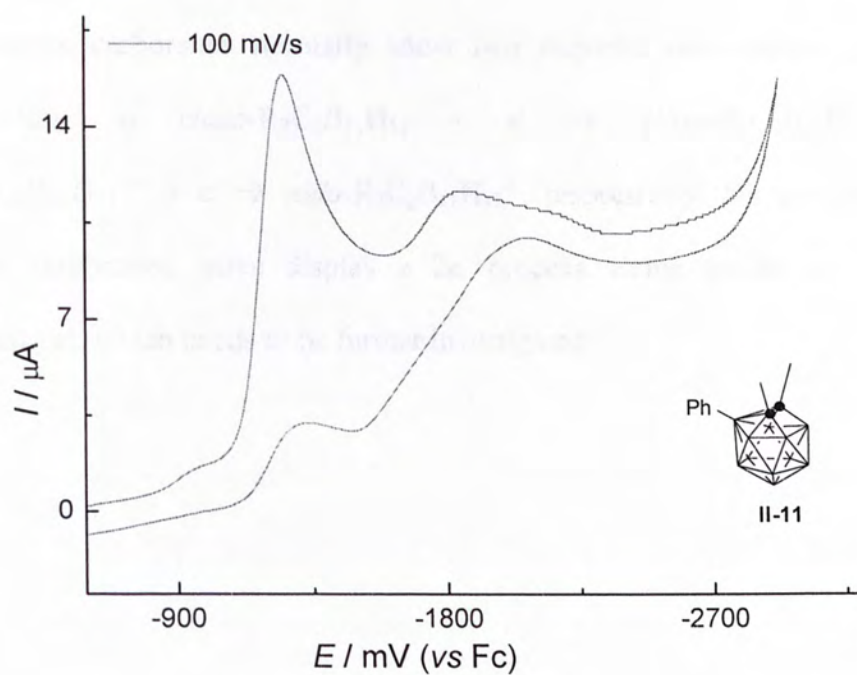


Figure 4.20.

Figure 4.20. Cyclic voltammogram of **II-11** in MeCN/0.1M Bu₄NPF₆ recorded at 100 mV/s. Cyclic voltammetry of **II-11** in MeCN/0.1M Bu₄NPF₆ showed one irreversible reduction wave with $E(0/-1) = -1.25$ V for the one-electron process **II-11** + e⁻ → **II-11**^{•-}, and one quasi-reversible peaks with $E_{1/2}(-1/-2) = -1.67$ V (vs ferrocene (Fc)) for another one-electron process **II-11**^{•-} + e⁻ → [1,2-Me₂-3-Ph-1,2-C₂B₁₁H₁₀]²⁻.

4.3. Summary

13-vertex carboranes normally show two stepwise one electron processes, corresponding to $closo-R_2C_2B_{11}H_{11} + e^- \rightarrow closo-R_2C_2B_{11}H_{11}^{\bullet-}$ and $closo-R_2C_2B_{11}H_{11}^{\bullet-} + e^- \rightarrow nido-R_2C_2B_{11}H_{11}^{2-}$, respectively. On the other hand, 12-vertex carboranes, often display a $2e^-$ process. Some results are not fully understood yet, which needs to be further investigated.

Chapter 5. Conclusion

In this thesis, we described our efforts on developing the chemistry of carboranes in following aspects: (1) exploration on the chemistry of supercarboranes, (2) development of the chemistry of 13-vertex carborane radical anions with $2n+3$ framework electrons, and (3) electrochemical study of carboranes.

From the capitation reaction of 12-vertex CAd *nido*-carborane dianions with dihaloboranes, we learn that the chain length of the linkages has a significant effect on the formation of carborane anions and the subsequent capitation reactions. Reduction of tri- or tetramethylene-linked carboranes affords CAd carborane dianions, which can function as good starting materials for the preparation of supercarboranes. The capitation reactions of 12-vertex CAd *nido* carboranes with various RBX_2 reagents give a class of 13-vertex carboranes. Single-crystal X-ray analyses reveal that these 13-vertex species adopt a heneicosahedral geometry.

Reaction of 13-vertex carboranes with 1 equiv of Na in THF generates the 13-vertex carborane radical anions with $2n+3$ framework electrons. They have very similar molecular structure to their parent 13-vertex carboranes with slightly longer bond distances. It is an intermediate between the two well-established and abundant $2n+2$ (*closo*) and $2n+4$ (*nido*) systems, which may imply that larger cages would enhance the thermodynamical stability of clusters with $2n+3$ systems.

The electrochemical process of 13-vertex supercarboranes, shows normally two stepwise one electron processes, $\text{closo-R}_2\text{C}_2\text{B}_{11}\text{H}_{11} + \text{e}^- \rightarrow \text{closo-R}_2\text{C}_2\text{B}_{11}\text{H}_{11}^{\cdot-}$ and $\text{closo-R}_2\text{C}_2\text{B}_{11}\text{H}_{11}^{\cdot-} + \text{e}^- \rightarrow \text{nido-R}_2\text{C}_2\text{B}_{11}\text{H}_{11}^{2-}$. On the other hand, 12-vertex carboranes, usually exhibit a two electron process $\text{closo-R}_2\text{C}_2\text{B}_{10}\text{H}_{10} + 2\text{e}^- \rightarrow$

Chapter 6. Experimental Section

General Procedures. All experiments were performed under an atmosphere of dry dinitrogen with the rigid exclusion of air and moisture using standard Schlenk or cannula techniques, or in a glovebox. All organic solvents (except CH_2Cl_2) were refluxed over sodium benzophenone ketyl for several days and freshly distilled prior to use. CH_2Cl_2 was refluxed over CaH_2 for several days and distilled immediately prior to use. All chemicals were purchased from either Aldrich or Acros Chemical Co. and used as received unless otherwise noted. 1,2- $(\text{CH}_2)_3$ -1,2- $\text{C}_2\text{B}_{10}\text{H}_{10}$ (**I-1**),³⁹ 1,2- $(\text{CH}_2\text{CH}=\text{CHCH}_2)$ -1,2- $\text{C}_2\text{B}_{10}\text{H}_{10}$ (**I-3**),⁵⁴ 1,2- $(\text{CH}_2)_4$ -1,2- $\text{C}_2\text{B}_{10}\text{H}_{10}$ (**I-2**),³⁹ 1,2- $\text{Me}_2\text{Si}(\text{CH}_2)_2$ -1,2- $\text{C}_2\text{B}_{10}\text{H}_{10}$ (**I-5**)⁵⁶ were prepared according to literature methods. Infrared spectra were obtained from KBr pellets prepared in the glovebox on a Perkin-Elmer 1600 Fourier transform spectrometer. UV-Visible absorption spectra were recorded on a Varian Cary5G UV-Vis-NIR spectrophotometer (in the range of 200-800 nm) using 1 cm quartz cells under N_2 . Cyclic voltammetric measurements were carried out at 25 °C under N_2 using a BAS CV-50W voltammetric analyzer. EPR spectra were recorded on a Bruker EMX-10/12 spectrometer at 25 °C. The ^1H and ^{13}C NMR spectra were recorded on a Bruker DPX 300 spectrometer at 300.1 and 75.5 MHz, respectively. The ^{11}B NMR spectra were recorded on a Varian Inova 400 spectrometer at 128.3 MHz. All chemical shifts were reported in δ units with references to the residual protons of the deuterated solvents for proton chemical shifts, to the carbons of the deuterated solvents for carbon chemical shifts, and to

external $\text{BF}_3 \cdot \text{OEt}_2$ (0.00 ppm) for boron chemical shifts. Mass spectra were recorded on Thermo Finnigan MAT 95 XL spectrometry. Elemental analyses were performed by MEDAC Ltd., Brunel University, Middlesex, U.K. or Shanghai Institute of Organic Chemistry, CAS, China.

Preparation of 1,2-[*o*-C₆H₄(CH₂)₂]-1,2-C₂B₁₀H₁₀ (I-4). This compound was prepared using a modified literature method.⁵⁵ To a solution of *o*-C₂B₁₀H₁₂ (7.20 g, 50.0 mmol) in a dry toluene/Et₂O (2:1, 50 mL) was added a 1.60 M solution of BuⁿLi in *n*-hexane (62.5 mL, 100.0 mmol) dropwise with stirring at 0°C. The mixture was allowed to warm to room temperature and stirred for 30 min. The solution was then cooled to 0°C, and a solution of *o*-C₆H₄(CH₂Br)₂ (13.2 g, 50.0 mmol) in toluene/Et₂O (2:1, 30 mL) was slowly added with stirring. The reaction mixture was refluxed overnight and then quenched with 50 mL of water. The organic layer was separated, and the aqueous layer was extracted with Et₂O (50 mL x 3). The combined organic portions were dried over anhydrous Na₂SO₄. Removal of the solvents gave a white solid that was washed with *n*-hexane (15 mL x 3) and dried under vacuum to afford **I-4** as a white powder (11.7 g, 95%). ¹H NMR (CDCl₃): δ 7.28 (m, 2H, aryl *H*), 7.12 (m, 2H, aryl *H*), 3.75 (s, 4H, C₆H₄(CH₂)₂). ¹¹B{¹H} NMR (CDCl₃): δ -5.40 (2B), -9.61 (8B).

Preparation of 3-methyl-5-phenyl-1,2-carboracyclopentan-3-ol. This compound was prepared according to a literature method.⁵⁷ To a THF solution (20.0 mL) of *o*-C₂B₁₀H₁₂ (1.44 g, 10.0 mmol) and 4-phenylbut-3-en-2-one (1.46 g, 10.0 mmol) was added ⁿBu₄NF (1.0 M in THF, 30.0 mL) under N₂ atmosphere, and the

mixture was stirred at room temperature for 10 min. The reaction was quenched by a saturated aqueous NH_4Cl , and the mixture was extracted with ether, washed with saturated aqueous NaCl , dried over anhydrous MgSO_4 , and then concentrated. Purification by silica gel column chromatography (hexane:ethyl acetate = 4:1) gave the annulated product as a white solid in 72% yield (2.08 g, 7.2 mmol). ^1H NMR (CDCl_3) anti isomer: δ 7.24-7.41 (m, 5H, C_6H_5), 4.21 (dd, J = 10.5, 8.0 Hz, 1H, PhCH), 2.75 (dd, J = 14.0, 10.5 Hz, 1H, CH_2), 2.67 (dd, J = 14.0, 8.0 Hz, 1H, CH_2), 2.13 (s, 1H, OH), 1.69 (s, 3H, CH_3), syn isomer: δ 7.24-7.41 (m, 5H, C_6H_5), 4.04 (t, J = 8.0 Hz, 1H, PhCH), 2.77 (m, 2H, CH_2), 2.17 (s, 1H, OH), 1.74 (s, 3H, CH_3). $^{11}\text{B}\{^1\text{H}\}$ NMR (CDCl_3): δ -4.89 (1B), -6.34 (3B), -10.1 (3B), -13.2 (2B), -14.2 (1B).

Preparation of 3-methyl-1,2-carboracyclopentan-3-ol. This compound was prepared according to a literature method.⁵⁷ To a THF solution (20 mL) of $o\text{-C}_2\text{B}_{10}\text{H}_{12}$ (1.44 g, 10.0 mmol) and but-3-en-2-one (0.70 g, 10.0 mmol) was added $n\text{Bu}_4\text{NF}$ (1.0 M in THF, 30.0 mL) under N_2 atmosphere, and the mixture was stirred at room temperature for 10 min. The reaction was quenched by a saturated aqueous NH_4Cl , and the mixture was extracted with ether, washed with saturated aqueous NaCl , dried over anhydrous MgSO_4 , and then concentrated. Purification by silica gel column chromatography (hexane:ethyl acetate = 4:1) gave the annulated product as a white solid in 54% yield (1.16 g, 5.4 mmol). ^1H NMR (CDCl_3): δ 2.33-2.63 (m, 4H, CH_2CH_2), 2.08 (s, 1H, OH), 1.62 (s, 3H, CH_3).

Preparation of 1,2-[1- CH_3 -($\text{C}=\text{CHCH}_2$)]-1,2- $\text{C}_2\text{B}_{10}\text{H}_{10}$ (I-6). Compounds 3-methyl-1,2-carboracyclopentan-3-ol (0.64 g, 3.0 mmol) and $p\text{-TsOH}$ (0.52 g, 3.0

mmol) were mixed in a glass tube. The tube was sealed and heated at 180 °C for 6 hours. The resulting black residue was dissolved in diethyl ether (15 mL). The solution was washed with water (20.0 mL), saturated NaHCO₃ aqueous solution (20.0 mL) and brine (20.0 mL), and then dried over anhydrous Na₂SO₄. Removal of the solvent afforded a pale brown solid. Column chromatographic separation (silicon gel, 230 – 400 mesh) using hexane as elute afforded **I-6** as a white solid (0.25 g, 42%). Mp. 48 - 49°C. ¹H NMR (CDCl₃): δ 5.53 (d, *J* = 2.1 Hz, 1H, CH=C), 3.05 (t, *J* = 2.1 Hz, 2H, CH₂), 1.88 (m, 3H, CH₃). ¹³C{¹H} NMR (CDCl₃): δ 140.4, 132.5 (CH=C), 87.51, 77.97 (cage C), 41.87 (CH₂), 14.24 (CH₃). ¹¹B{¹H} NMR (CDCl₃): δ -6.81 (s, 3B, BH), -7.72 (s, 1B, BH), -10.38 (s, 2B, BH), -11.54 (s, 2B, BH), -14.84 (s, 2B, BH). IR (KBr, cm⁻¹): ν_{BH} 2575 (vs). HRMS: *m/z* calcd for C₆H₁₆B₁₀⁺: 196.2250. Found: 196.2245.

Preparation of 1,2-[1-CH₃-3-Ph-(C=CHCH)]-1,2-C₂B₁₀H₁₀ (I-7**).** Compounds 3-methyl-5-phenyl-1,2-carboracyclopentan-3-ol (0.87 g, 3.0 mmol) and *p*-TsOH (0.52 g, 3.0 mmol) were mixed in a glass tube. The tube was sealed and heated at 180 °C for 6 hours. The resulting black residue was dissolved in diethyl ether (15.0 mL). The solution was washed with water (20.0 mL), saturated NaHCO₃ aqueous solution (20.0 mL) and brine (20.0 mL), and then dried over anhydrous Na₂SO₄. Removal of the solvent afforded a pale brown solid. Column chromatographic separation (silicon gel, 230 – 400 mesh) using hexane as elute afforded **I-7** as a white solid (0.66 g, 81%). Recrystallization from *n*-hexane gave X-ray-quality crystals of **I-7**. Mp. 119 - 120°C. ¹H NMR (CDCl₃): δ 7.35 (m, 3H, C₆H₅), 7.13 (m,

2H, C₆H₅), 5.74 (m, 1H, CH=C), 4.58 (t, *J* = 2.1 Hz, 1H, PhCH), 1.98 (t, *J* = 2.1 Hz, 3H, CH₃). ¹³C{¹H} NMR (CDCl₃): δ 140.9, 128.9, 128.6, 128.5 (C₆H₅), 135.9, 135.3 (CH=C), 87.03, 82.14 (cage C), 56.87 (PhCH), 14.45 (CH₃). ¹¹B{¹H} NMR (CDCl₃): δ -5.99 (s, 2B, BH), -7.43 (s, 1B, BH), -9.57 (s, 2B, BH), -10.51 (s, 1B, BH), -11.71 (s, 2B, BH), -14.42 (s, 1B, BH), -15.26 (s, 1B, BH). IR (KBr, cm⁻¹): ν_{BH} 2584 (vs). HRMS: *m/z* calcd for C₁₂H₂₀B₁₀⁺: 272.2563. Found: 272.2568.

Preparation of 1,2-{1',4'}-[EtC=C(Et)-C(Et)=CEt]-1,2-C₂B₁₀H₁₀ (I-8). This compound was prepared according to a literature method.⁵⁸ A 1.6 M solution of *n*-BuLi in *n*-hexane (14.0 mL, 22.4 mmol) was slowly added to a stirring solution of *o*-C₂B₁₀H₁₂ (1.44 g, 10.0 mmol) in THF (30 mL) at 0°C, and the mixture was stirred at room temperature for 1 h. The resulting Li₂C₂B₁₀H₁₀ suspension was then cooled to 0°C, to which was added (PPh₃)₂NiCl₂ (6.54 g, 10.0 mmol). The reaction mixture was then stirred for 0.5 h at room temperature, giving (η²-C₂B₁₀H₁₀)Ni(PPh₃)₂. Alkyne EtC≡CEt (30.0 mmol) was added and the reaction vessel was sealed and heated at 90°C for 4 d. The reaction mixture was then cooled to room temperature and quenched with aqueous NaHCO₃ solution. After extraction with Et₂O (50 mL × 2), the combined organic portions were dried over anhydrous Na₂SO₄. After removal of the solvent, the resulting solid was subjected to column chromatographic separation (SiO₂, 300 - 400 mesh) using hexane as eluent to give **I-8** as a white solid. Yield: 2.05 g, 67%, mp. 141 - 142 °C. ¹H NMR (CDCl₃): δ 2.42 (q, *J* = 7.5 Hz, 4H, CH₂), 2.01 (q, *J* = 7.5 Hz, 4H, CH₂), 1.02 (t, *J* = 7.5 Hz, 6H, CH₃), 0.78 (t, *J* = 7.5 Hz, 6H, CH₃). ¹³C{¹H} NMR (CDCl₃): δ 135.1, 134.0 (C=C), 76.26 (cage C), 26.31,

21.95 (CH₂CH₃), 14.99, 14.77 (CH₂CH₃). ¹¹B{¹H} NMR (CDCl₃): δ -7.29 (2B), -10.2 (6B), -13.1 (2B).

Preparation of 1,2-[1,8-C₁₀H₆(CH₂)₂]-1,2-C₂B₁₀H₁₀ (I-9). This compound was prepared according to a literature method.^{30c} This compound was prepared as a white solid from the reaction of *o*-C₂B₁₀H₁₂ (7.20 g, 50.0 mmol) with 1.60 M solution of BuⁿLi in *n*-hexane (62.5 mL, 100.0 mmol), followed by addition of 1,8-C₁₀H₆(CH₂Cl)₂ (11.3 g, 50.0 mmol) in toluene/Et₂O (2:1, 60 mL) using procedures similar to those used in the synthesis of **I-4**: yield 11.1 g (75%). ¹H NMR (CDCl₃): δ 7.80 (m, 2H, aryl *H*), 7.36 (m, 2H, aryl *H*), 7.22 (m, 2H, aryl *H*), 4.12 (s, 4H, ArCH₂). ¹¹B{¹H} NMR (CDCl₃): δ -7.71 (3B), -13.81 (5B), -16.48 (2B).

Preparation of 1,2-(1-methyl-2,5-cyclohexadiene-1,4-diyl)-1,2-C₂B₁₀H₁₀ (I-10). To a toluene solution (30 mL) of 1,2-C₂B₁₀H₁₂ (1.44 g, 10.0 mmol) was slowly added BuⁿLi (12.5 mL/1.6 M in hexane, 20.0 mmol) under N₂ atmosphere at 0 °C and the mixture was allowed to stir at room temperature for 2 hours. I₂ (2.54 g, 10.0 mmol) was then added, and the resulting mixture was stirred at room temperature for another 2 hours, before refluxing overnight under N₂ atmosphere. The reaction was quenched by water and extracted by diethyl ether (50 mL × 3). Removal of solvents gave a solid. Chromatographic separation (SiO₂, 300 ~ 400 mesh, *n*-hexane as eluent) afforded **I-10** as a white solid (1.45 g, 62%). ¹H NMR (CDCl₃): δ 6.67 (m, 2H, CH=CH), 6.22 (m, 1H, CH=CCH₃), 4.03 (m, 1H, CHCCH₃), 3.78 (m, 1H, CH), 1.87 (d, *J* = 1.8 Hz, 3H, CH₃). ¹³C{¹H} NMR (CDCl₃): δ 150.6, 141.7, 140.1, 135.8 (olefinic carbon), 50.01, 44.56 (alkyl carbon),

19.96 (CH₃), the cage carbons were not observed. ¹¹B NMR (CDCl₃): δ -2.06 (d, *J*_{BH} = 134 Hz, 3B, *BH*), -2.81 (d, *J*_{BH} = 107 Hz, 1B, *BH*), -12.45 (d, *J*_{BH} = 154 Hz, 6B, *BH*). IR (KBr, cm⁻¹): ν_{BH} 2591 (vs). HRMS: *m/z* calcd for C₉H₁₈B₁₀⁺: 234.2406. Found: 234.2409.

Preparation of 1,2-(CH₂)₃-1,2-C₂B₁₁H₁₁ (II-1). This compound was prepared according to a literature method.^{40a} To a THF (30 mL) solution of 1,2-(CH₂)₃-1,2-C₂B₁₀H₁₀ (**I-1**; 1.84 g, 10.0 mmol) was added finely cut Na metal (0.50 g, 21.7 mmol) and a catalytic amount of naphthalene (0.10 g, 0.78 mmol), and the mixture was stirred at room temperature for four days, giving a deep green solution. Removal of THF afforded a brown solid, presumably [*nido*-(CH₂)₃C₂B₁₀H₁₀][Na₂(THF)_x]. Toluene (30 mL) was then added, giving a yellow suspension. HBBBr₂·SMe₂ (20.0 mL of 1.0 M in dichloromethane, 20.0 mmol) was slowly added to the suspension at -78°C, the mixture was stirred at this temperature for 1 h, and then at room temperature for 6 h. Chromatographic separation (SiO₂, 300 ~ 400 mesh, *n*-hexane as eluent) afforded **I-1** (0.06 g, 3%) and **II-1** (0.73 g, 37%) both as a white solid. Mp. 60 - 61°C. ¹H NMR (CDCl₃): δ 3.26 (t, *J* = 7.5 Hz, 4H, CH₂CH₂CH₂), 2.18 (m, 2H, CH₂CH₂CH₂). ¹³C{¹H} NMR (CDCl₃): δ 49.11 (CH₂CH₂CH₂), 25.55 (CH₂CH₂CH₂), the cage carbons were not observed. ¹¹B NMR (CDCl₃): δ 3.52 (d, *J*_{BH} = 186 Hz, 1B, *BH*), 0.96 (d, *J*_{BH} = 186 Hz, 5B, *BH*), -1.19 (d, *J*_{BH} = 186 Hz, 5B, *BH*).

Preparation of 1,2-(CH₂)₃-3-Ph-1,2-C₂B₁₁H₁₀ (II-2). This compound was prepared according to a literature method.^{40a} Following the procedures described for

II-1, PhBCl_2 (2.60 mL, 20.0 mmol) was reacted with a suspension of $[\text{nido}-(\text{CH}_2)_3\text{C}_2\text{B}_{10}\text{H}_{10}][\text{Na}_2(\text{THF})_x]$ (10.0 mmol) in toluene (30 mL). Compounds **I-1** (0.12 g, 6%) and **II-2** (0.54 g, 20%) were obtained as a white solid. Mp. 97 - 98°C. ^1H NMR (CDCl_3): δ 7.42 (d, $J = 6.9$ Hz, 2H, C_6H_5), 7.32 (m, 3H, C_6H_5), 3.05 (t, $J = 7.2$ Hz, 4H, $\text{CH}_2\text{CH}_2\text{CH}_2$), 1.84 (m, 2H, $\text{CH}_2\text{CH}_2\text{CH}_2$). $^{13}\text{C}\{^1\text{H}\}$ NMR (CDCl_3): δ 134.1, 129.6, 128.1 (C_6H_5), 47.56 ($\text{CH}_2\text{CH}_2\text{CH}_2$), 25.57 ($\text{CH}_2\text{CH}_2\text{CH}_2$), the CB and cage carbons were not observed. ^{11}B NMR (CDCl_3): δ 3.31 (s, 1B, BPh), 1.18 (d, $J_{\text{BH}} = 186$ Hz, 1B, BH), -2.32 (d, $J_{\text{BH}} = 146$ Hz, 3B, BH), -3.30 (d, $J_{\text{BH}} = 128$ Hz, 2B, BH), -7.06 (d, $J_{\text{BH}} = 166$ Hz, 4B, BH).

Preparation of 1,2-(CH₂)₄-1,2-C₂B₁₁H₁₁ (II-3). Following the procedures described for **II-1**, $\text{HBBBr}_2 \cdot \text{SMe}_2$ (20.0 mL of 1.0 M in dichloromethane, 20.0 mmol) was added to a suspension of $[\text{nido}-(\text{CH}_2)_4\text{C}_2\text{B}_{10}\text{H}_{10}][\text{Na}_2(\text{THF})_x]$ (10.0 mmol) in toluene (30 mL). Compound **II-3** (0.37 g, 17.5%) was obtained as a white solid. Mp. 62 - 63°C. ^1H NMR (CDCl_3): δ 3.05 (t, $J = 6.6$ Hz, 4H, $\text{CH}_2\text{CH}_2\text{CH}_2\text{CH}_2$), 1.78 (m, 4H, $\text{CH}_2\text{CH}_2\text{CH}_2\text{CH}_2$). $^{13}\text{C}\{^1\text{H}\}$ NMR (CDCl_3): δ 44.58 ($\text{CH}_2\text{CH}_2\text{CH}_2\text{CH}_2$), 20.89 ($\text{CH}_2\text{CH}_2\text{CH}_2\text{CH}_2$), the cage carbons were not observed. ^{11}B NMR (CDCl_3): δ 4.58 (d, $J_{\text{BH}} = 148$ Hz, 1B, BH), 0.89 (d, $J_{\text{BH}} = 163$ Hz, 5B, BH), -0.54 (d, $J_{\text{BH}} = 180$ Hz, 5B, BH). IR (KBr, cm^{-1}): ν_{BH} 2568 (vs). HRMS: m/z calcd for $\text{C}_6\text{H}_{19}\text{B}_{11}^+$: 209.2499. Found: 209.2499.

Preparation of 1,2-(CH₂)₄-3-Ph-1,2-C₂B₁₁H₁₀ (II-4). Following the procedures described for **II-1**, PhBCl_2 (2.60 mL, 20.0 mmol) was reacted with a suspension of $[\text{nido}-(\text{CH}_2)_4\text{C}_2\text{B}_{10}\text{H}_{10}][\text{Na}_2(\text{THF})_x]$ (10.0 mmol) in toluene (30 mL). Compound

II-4 (0.88 g, 31%) was obtained as a white solid. X-ray-quality crystals of **II-4** were grown from a saturated *n*-hexane solution at room temperature. Mp. 126 - 128°C. ^1H NMR (CDCl_3): δ 7.38 (m, 5H, C_6H_5), 3.04 (t, $J = 6.6$ Hz, 4H, $\text{CH}_2\text{CH}_2\text{CH}_2\text{CH}_2$), 1.49 (m, 4H, $\text{CH}_2\text{CH}_2\text{CH}_2\text{CH}_2$). $^{13}\text{C}\{^1\text{H}\}$ NMR (CDCl_3): δ 148.3, 135.2, 130.8, 129.2 (C_6H_5), 44.09 ($\text{CH}_2\text{CH}_2\text{CH}_2\text{CH}_2$), 20.82 ($\text{CH}_2\text{CH}_2\text{CH}_2\text{CH}_2$), the cage carbons were not observed. ^{11}B NMR (CDCl_3): δ 7.05 (s, 1B, *BPh*), 5.96 (d, $J_{\text{BH}} = 207$ Hz, 1B, *BH*), 4.36 (d, $J_{\text{BH}} = 165$ Hz, 2B, *BH*), 1.94 (d, $J_{\text{BH}} = 165$ Hz, 2B, *BH*), 0.52 (d, $J_{\text{BH}} = 175$ Hz, 2B, *BH*), -1.07 (d, $J_{\text{BH}} = 206$ Hz, 2B, *BH*), -4.36 (d, $J_{\text{BH}} = 148$ Hz, 1B, *BH*). IR (KBr, cm^{-1}): ν_{BH} 2566 (vs). HRMS: m/z calcd for $\text{C}_{12}\text{H}_{23}\text{B}_{11}^+$: 284.2734. Found: 284.2734.

Preparation of 1,2-(CH₂CH=CHCH₂)-1,2-C₂B₁₁H₁₁ (II-5). Following the procedures described for **II-1**, $\text{HBBBr}_2 \cdot \text{SMe}_2$ (20.0 mL of 1.0 M in dichloromethane, 20.0 mmol) was added to a suspension of [*nido*-(CH₂CH=CHCH₂)C₂B₁₀H₁₀][Na₂(THF)_x] (10.0 mmol) in toluene (30 mL). Compound **II-5** (0.19 g, 9%) was obtained as a white solid. Mp. 67 - 69°C. ^1H NMR (CDCl_3): δ 3.57 (d, $J = 2.1$ Hz, 4H, $\text{CH}_2\text{CH}=\text{CHCH}_2$), 6.01 (t, $J = 2.1$ Hz, 2H, $\text{CH}_2\text{CH}=\text{CHCH}_2$). $^{13}\text{C}\{^1\text{H}\}$ NMR (CDCl_3): δ 45.41 ($\text{CH}_2\text{CH}=\text{CHCH}_2$), 123.47 ($\text{CH}_2\text{CH}=\text{CHCH}_2$), 138.81 (cage C). ^{11}B NMR (CDCl_3): δ 4.65 (d, $J_{\text{BH}} = 146$ Hz, 1B, *BH*), 0.96 (d, $J_{\text{BH}} = 160$ Hz, 5B, *BH*), -0.48 (d, $J_{\text{BH}} = 180$ Hz, 5B, *BH*). IR (KBr, cm^{-1}): ν_{BH} 2568 (vs). HRMS: m/z calcd for $\text{C}_6\text{H}_{17}\text{B}_{11}^+$: 206.2265. Found: 206.2269.

Preparation of 1,2-(CH₂CH=CHCH₂)-3-Ph-1,2-C₂B₁₁H₁₀ (II-6). Following the procedures described for **II-1**, PhBCl_2 (2.60 mL, 20.0 mmol) was reacted with a

suspension of [*nido*-(CH₂CH=CHCH₂)C₂B₁₀H₁₀][Na₂(THF)_x] (10.0 mmol) in toluene (30 mL). Compound **II-6** (0.17 g, 6%) was obtained as a white solid. X-ray-quality crystals of **II-6** were grown from a saturated *n*-hexane solution at room temperature. Mp. 135 - 136°C. ¹H NMR (CDCl₃): δ 7.35 (m, 5H, C₆H₅), 5.75 (t, *J* = 2.1 Hz, 2H, CH₂CH=CHCH₂), 3.59 (d, *J* = 2.1 Hz, 4H, CH₂CH=CHCH₂). ¹³C{¹H} NMR (CDCl₃): δ 144.4, 135.6, 130.8, 129.3 (C₆H₅), 45.36 (CH₂CH=CHCH₂), 124.02 (CH₂CH=CHCH₂), the cage carbons were not observed. ¹¹B NMR (CDCl₃): δ 7.29 (s, 1B, BPh), 6.05 (d, *J*_{BH} = 157 Hz, 1B, BH), 3.95 (d, *J*_{BH} = 159 Hz, 2B, BH), 1.63 (d, *J*_{BH} = 133 Hz, 2B, BH), 0.74 (d, *J*_{BH} = 134 Hz, 2B, BH), -1.32 (d, *J*_{BH} = 171 Hz, 2B, BH), -3.95 (d, *J*_{BH} = 143 Hz, 1B, BH). IR (KBr, cm⁻¹): ν_{BH} 2560 (vs). HRMS: *m/z* calcd for C₁₂H₂₁B₁₁⁺: 282.2578. Found: 282.2576.

Preparation of 1,2-[*o*-C₆H₄(CH₂)₂]-1,2-C₂B₁₁H₁₁ (II-7**).** This compound was prepared according to a literature method.^{40a} Following the procedures described for **II-1**. HBBBr₂·SMe₂ (25.0 mL of 1.0 M in dichloromethane, 25.0 mmol) was reacted with [*nido*-{1,2-C₆H₄(CH₂)₂-1,2-C₂B₁₀H₁₀}][Na₂(THF)_x] (5.0 mmol) in toluene (30 mL). **I-4** (0.21 g, 8%) and **II-7** (0.42 g, 17%) were obtained both as a white solid. Mp. 106 - 108°C. ¹H NMR (CDCl₃): δ 7.53 (m, 2H, C₆H₄), 7.45 (m, 2H, C₆H₄), 4.35 (s, 4H, CH₂). ¹³C{¹H} NMR (CDCl₃): δ 130.8, 128.5, 126.6 (C₆H₄), 50.81 (CH₂), the cage carbons were not observed. ¹¹B NMR (CDCl₃): δ 4.98 (d, *J*_{BH} = 128 Hz, 1B, BH), 2.11 (d, *J*_{BH} = 128 Hz, 5B, BH), -0.10 (d, *J*_{BH} = 146 Hz, 5B, BH).

Preparation of 1,2-Me₂Si(CH₂)₂-1,2-C₂B₁₁H₁₁ (II-8**).** This compound was prepared according to a literature method.⁴⁴ To a THF (30 mL) solution of

1,2-Me₂Si(CH₂)₂-1,2-C₂B₁₀H₁₀ (**I-5**) (2.28 g, 10.0 mmol) was added finely cut Na metal (1.00 g, 43.5 mmol), and the mixture was stirred at room temperature for 3 days. After removal of excess Na metal and THF, toluene (20 mL) was then added. HBBBr₂·SMe₂ (20.0 mL of 1.0 M in CH₂Cl₂, 20.0 mmol) was slowly added to the above suspension at -78 °C, and the mixture was stirred at this temperature for 1 h and at room temperature overnight. The precipitate was filtered off and washed with *n*-hexane (3 x 30 mL). The combined organic solutions were concentrated to yield **II-8** as a white solid (0.937 g, 39%). ¹H NMR (300 MHz, CDCl₃): δ 2.55 (s, 4H, CH₂), 0.31 (s, 6H, CH₃). ¹³C{¹H} NMR (100 MHz, CDCl₃): δ 144.3 (cage C), 40.5 (CH₂), -3.1 (CH₃). ¹¹B NMR (128 MHz, CDCl₃): δ 4.5 (*J*_{B-H} = 150 Hz, 1B), 0.6 (*J*_{B-H} = 148 Hz, 10B).

Preparation of 1,2-Me₂-1,2-C₂B₁₁H₁₁ (II-9) and 1,6-Me₂-1,6-C₂B₁₁H₁₁ (II-10).

These compounds were prepared according to a literature method.⁴⁴ Compound **II-8** (0.72 g, 3.0 mmol) was subjected to column chromatographic separation (SiO₂, 300-400 mesh, *n*-hexane) affording **II-9** (0.33 g, 60%) and **II-10** (0.17 g, 30%) as white solids. **II-9**: ¹H NMR (300 MHz, CDCl₃): δ 2.73 (s, 6H, CH₃). ¹³C{¹H} NMR (100 MHz, CDCl₃): δ 140.6 (cage C), 34.8 (CH₃). ¹¹B NMR (128 MHz, CDCl₃): δ 4.4 (*J*_{B-H} = 153 Hz, 1B), 1.7 (*J*_{B-H} = 150 Hz, 5B), 0.0 (*J*_{B-H} = 168 Hz, 5B). **II-10**: ¹H NMR (300 MHz, CDCl₃): δ 2.63 (s, 3H, CH₃), 1.89 (s, 3H, CH₃). ¹³C{¹H} NMR (100 MHz, CDCl₃): δ 120.7 (cage C), 83.0 (cage C), 35.6 (CH₃), 27.3 (CH₃). ¹¹B NMR (128 MHz, CDCl₃): δ 13.6 (*J*_{B-H} = 163 Hz, 1B), -5.3 (*J*_{B-H} = 160 Hz, 3B), -6.4 (*J*_{B-H} = 163 Hz, 7B).

Preparation of 1,2-Me₂-3-Ph-1,2-C₂B₁₁H₁₀ (II-11). To a THF (30 mL) solution of 1,2-Me₂Si(CH₂)₂-1,2-C₂B₁₀H₁₀ (**I-5**, 2.28 g, 10.0 mmol) was added finely cut Na metal (1.00 g, 43.5 mmol), and the mixture was stirred at room temperature for 6 days. After removal of excess Na metal and THF, toluene (20 mL) was then added. PhBCl₂ (2.60 mL, 20.0 mmol) was slowly added to the above suspension at -78 °C, and the mixture was stirred at this temperature for 1 h and at room temperature overnight. The precipitate was filtered off and washed with *n*-hexane (3 x 30 mL). The combined organic solutions were concentrated to yield a white solid, assumably 1,2-Me₂Si(CH₂)₂-3-Ph-1,2-C₂B₁₁H₁₀ which was subjected to column chromatographic separation (SiO₂, 300-400 mesh, *n*-hexane) affording **II-11** (0.54 g, 21%) as a white solid. ¹H NMR (300 MHz, CDCl₃): δ 2.67 (s, 6H, CH₃), 7.35 (m, 5H, C₆H₅). ¹³C{¹H} NMR (CDCl₃): δ 146.9, 135.1, 130.7, 129.2 (C₆H₅), 34.59 (CH₃), the cage carbons were not observed. ¹¹B NMR (128 MHz, CDCl₃): δ 6.69 (s, 1B, BPh), 5.89 (d, *J*_{BH} = 114 Hz, 1B, BH), 5.09 (d, *J*_{BH} = 211 Hz, 2B, BH), 3.35 (d, *J*_{BH} = 153 Hz, 2B, BH), 1.29 (d, *J*_{BH} = 151 Hz, 2B, BH), -0.68 (d, *J*_{BH} = 159 Hz, 2B, BH), -4.19 (d, *J*_{BH} = 154 Hz, 1B, BH). IR (KBr, cm⁻¹): ν 2573 (vs) (BH). HRMS (EI): *m/z* calcd for C₁₀H₂₁B₁₁⁺: 258.2578. Found: 258.2575.

Preparation of [1,2-(CH₂)₃-1,2-C₂B₁₁H₁₁][Na(18-crown-6)(THF)₂] (III-1). A THF (15 mL) suspension of 1,2-(CH₂)₃-1,2-C₂B₁₁H₁₁ (**II-1**; 0.196 g, 1.00 mmol) and finely cut Na metal (0.023 g, 1.00 mmol) was stirred at room temperature for 48 h. After addition of 18-crown-6 ether (0.264 g, 1.00 mmol), the mixture was stirred for

48 h to give a dark brown solution. Removal of the solvent afforded a brown solid. Recrystallization from a mixed THF/hexane solution at room temperature produced **III-1** as brown crystals (0.502 g, 80%). IR (KBr, cm^{-1}): ν 2900 (s), 2521 (s), 1343 (w), 1252 (w), 1105 (vs), 1027 (m), 961 (m), 805 (w). UV-Vis (nm): 360. Anal. Calcd for $\text{C}_{25}\text{H}_{57}\text{B}_{11}\text{NaO}_8$: C, 47.84; H, 9.15. Found: C, 47.69; H 9.31.

Preparation of [1,2-(CH₂)₃-3-Ph-1,2-C₂B₁₁H₁₀][Na(18-crown-6)(THF)₂] (III-2**).** A THF (15 mL) suspension of 1,2-(CH₂)₃-3-Ph-1,2-C₂B₁₁H₁₀ (**II-2**; 0.270 g, 1.00 mmol) and finely cut Na metal (0.023 g, 1.00 mmol) was stirred at room temperature for 48 h. After addition of 18-crown-6 ether (0.264 g, 1.00 mmol), the mixture was stirred for 48 h to give a dark brown solution. Removal of the solvent afforded a brown solid. Recrystallization from a mixed THF/hexane solution at room temperature produced **III-2** as brown crystals (0.598 g, 85%). IR (KBr, cm^{-1}): ν 2903 (s), 2516 (s), 1352 (w), 1247 (w), 1111 (vs), 1054 (m), 967 (m), 838 (w). UV-Vis (nm): 360, 220. Anal. Calcd for $\text{C}_{31}\text{H}_{61}\text{B}_{11}\text{NaO}_8$: C, 52.91; H, 8.74. Found: C, 53.24; H 8.91.

Preparation of [1,2-(CH₂)₄-1,2-C₂B₁₁H₁₁][Na(18-crown-6)(THF)₂] (III-3**).** A THF (15 mL) suspension of 1,2-(CH₂)₄-1,2-C₂B₁₁H₁₁ (**II-3**; 0.209 g, 1.00 mmol) and finely cut Na metal (0.023 g, 1.00 mmol) was stirred at room temperature for 48 h. After addition of 18-crown-6 ether (0.264 g, 1.00 mmol), the mixture was stirred for 48 h to give a dark brown solution. Removal of the solvent afforded a brown solid. Recrystallization from a mixed THF/hexane solution at room temperature produced **III-3** as brown crystals (0.532 g, 83%). IR (KBr, cm^{-1}): ν 2913 (s), 2521 (s), 1353

(w), 1251 (w), 1105 (vs), 1027 (m), 963 (m), 836 (w). UV-Vis (nm): 337, 258, 218. Anal. Calcd for $C_{20}H_{47}B_{11}NaO_{6.5}$ (**III-3** - 1.5THF): C, 45.03; H, 8.88. Found: C, 45.18; H 8.92.

Preparation of [1,2-(CH₂)₄-3-Ph-1,2-C₂B₁₁H₁₀][Na(18-crown-6)(THF)₂] (III-4**).** A THF (15 mL) suspension of 1,2-(CH₂)₄-3-Ph-1,2-C₂B₁₁H₁₀ (**II-4**; 0.284 g, 1.00 mmol) and finely cut Na metal (0.023 g, 1.00 mmol) was stirred at room temperature for 48 h. After addition of 18-crown-6 ether (0.264 g, 1.00 mmol), the mixture was stirred for 48 h to give a dark brown solution. Removal of the solvent afforded a brown solid. Recrystallization from a mixed THF/hexane solution at room temperature produced **III-4** as brown crystals (0.495 g, 69%). IR (KBr, cm⁻¹): ν 2916 (s), 2516 (s), 1353 (w), 1250 (w), 1108 (vs), 1053 (m), 963 (m), 837 (w). UV-Vis (nm): 340, 230. Anal. Calcd for $C_{28}H_{55}B_{11}NaO_7$ (**III-4** - 1THF): C, 52.09; H, 8.59. Found: C, 52.00; H 8.88.

Preparation of [1,2-{*o*-C₆H₄(CH₂)(CH)}-1,2-C₂B₁₁H₁₁][Li(THF)₄] (IV-7**).** A THF (15 mL) suspension of 1,2-[*o*-C₆H₄(CH₂)₂]-1,2-C₂B₁₁H₁₁ (**II-7**; 0.256 g, 1.00 mmol) and finely cut Li metal (0.007 g, 1.00 mmol) was stirred at room temperature for 48 h to give a bright yellow solution. Removal of the solvent afforded a yellow solid. Recrystallization from a mixed THF/hexane solution at room temperature produced **IV-7** as yellow crystals (0.458 g, 83%). Mp. 117 - 119°C. ¹H NMR (THF-D₈): δ 6.87 (m, 2H, C₆H₄), 6.68 (d, J = 7.2 Hz, 1H, C₆H₄), 6.56 (d, J = 7.2 Hz, 1H, C₆H₄), 6.04 (s, 1H, CH), 3.47 (s, 2H, CH₂). ¹³C{¹H} NMR (THF-D₈): δ 143.1, 127.8, 127.1, 126.9 (C₆H₄), 122.4 (CH), 46.41 (CH₂), the cage carbons were not

observed. $^{11}\text{B}\{^1\text{H}\}$ NMR (THF- D_8): δ 7.48 (s, 1B, BH), 0.31 (s, 5B, BH), -17.41 (s, 5B, BH). IR (KBr, cm^{-1}): ν 2963 (m), 2880 (m), 2526 (s), 1463 (w), 1378 (w), 1043 (m), 893 (m). Anal. Calcd for $\text{C}_{20}\text{H}_{38}\text{B}_{11}\text{LiO}_{2.5}$ (**IV-7** - 1.5THF): C, 54.06; H, 8.62. Found: C, 54.18; H 8.95.

Attempts to prepare 13-vertex carboranes from I-6, I-7 and I-8, respectively. Reaction of **I-7** (1.36 g, 5.0 mmol) with 3 equiv of sodium in THF gave, after 6 hours, a red suspension, and the ^{11}B NMR had peaks at δ -3.88, -6.99, -12.69, -16.93, -18.84, -22.94, -30.95, -42.51 and -44.19 ppm, and after 16 days, a red suspension with a deeper color, and the ^{11}B NMR had peaks at -7.87, -13.88, -18.87, -35.29, -44.85 and -54.97 ppm, respectively. After removal of excess Na metal and THF, toluene (20 mL) was then added. $\text{HBBBr}_2\cdot\text{SMe}_2$ (20.0 mL of 1.0 M in CH_2Cl_2 , 20.0 mmol) was slowly added to the above suspension at -78°C , and the mixture was stirred at this temperature for 1 h and at room temperature overnight. Quenched by water and extracted with diethyl ether, the ^{11}B NMR of the combined organic solvents had peaks at δ 5.02, 1.99, and -1.69 ppm with a pattern of 1:5:5, probably 13-vertex supercarborane. After column chromatography (hexane as elute), a white solid was obtained (0.39 g). The corresponding 13-vertex product of **I-7** should have a formula $\text{C}_{12}\text{H}_{21}\text{B}_{11}$ and HRMS (EI): m/z calcd for $\text{C}_{12}\text{H}_{21}\text{B}_{11}^+$: 282.2578. Found: 282.2581. However, the ^1H NMR of this white solid in CDCl_3 could not be explained as the corresponding 13-vertex carborane, which was complicated and didn't match with the HRMS result. Reaction of compounds **I-6** and **I-8** were conducted in the same manner as **I-7**, and in both cases, new

compound could be found in the ^{11}B NMR after the addition of dihaloborane reagents, δ 1.02, -0.51 and -1.64 ppm with a pattern of 1:5:5 for **I-6** and δ -0.02, and -2.77 ppm with a pattern of 1:10: for **I-8**. However, after column chromatography separation (hexane as elute), no new compound was obtained.

X-ray Structure Determination. All single crystals were immersed in Paraton-N oil and sealed under N_2 in thin-walled glass capillaries. Data were collected at 293 K on a Bruker SMART 1000 CCD diffractometer using $\text{Mo-K}\alpha$ radiation. An empirical absorption correction was applied using the SADABS program.⁵⁹ All structures were solved by direct methods and subsequent Fourier difference techniques and refined anisotropically for all non-hydrogen atoms by full-matrix least squares calculations on F^2 using the SHELXTL program package.⁶⁰ For noncentrosymmetric structures, the appropriate enantiomorph was chosen by refining Flack's parameter x toward zero.⁶¹ All hydrogen atoms were geometrically fixed using the riding model. Crystal data and details of data collection and structure refinements are given in Appendix II. CIF files are given in Appendix III in electronic format.

References

- (1) (a) Shapiro, I.; Good, C. D.; Williams, R. E. *J. Am. Chem. Soc.* **1962**, *84*, 3837. (b) Shapiro, I.; Keilin, B.; Williams, R. E.; Good, C. D. *J. Am. Chem. Soc.* **1963**, *85*, 3167.
- (2) (a) Wade, K., in *Adv. Inorg. Chem. Radiochem.*, **1976**, *18*, 1. (b) O'Neill, M. E.; Wade, K. in *Comprehensive Organometallic Chemistry*, Eds., Wilkinson, G.; Stone, F. G. A.; Abel, E. W. Pergamon: N. Y., **1982**, Vol. 1, Chap. 1, p.1. (c) Williams, R. E. *Adv. Inorg. Chem. Radiochem.*, **1976**, *18*, 67; *Chem. Rev.*, **1992**, *92*, 177.
- (3) *Boron Hydrides* Lipscomb, W. N., Ed.; Benjamin: New York, 1963.
- (4) (a) *Carboranes* Grimes, R. N., Ed.; Academic Press: New York, 1970. (b) Onak, T. Polyhedral Carbaboranes. In *Comprehensive Organometallic Chemistry II*; Abel, E. W., Stone, F. G. A., Wilkinson, G., Eds. Pergamon: New York, 1995; Vol. 1, pp 217. (c) Grimes, R. N. Metallacarboranes. In *Comprehensive Organometallic Chemistry II*; Abel, E. W.; Stone, F. G. A.; Wilkinson, G., Eds. Pergamon: New York, 1995; Vol. 1, pp 373. (d) Davidson, M.; Hughes, A. K.; Marder, T. B.; Wade, K. *Contemporary Boron Chemistry*; Royal Society of Chemistry: Cambridge, UK, 2000. (e) Bubnov, Y. N. *Boron Chemistry at the Beginning of the 21st Century*; Russian Academy of Sciences: Moscow, Russia, 2002.
- (5) (a) Štíbr, B. *Chem. Rev.* **1992**, *92*, 225. (b) Siebert, W.; Maier, C.-J.; Maier,

- A.; Greiwe, P.; Bayer, M. J.; Hofmann, M.; Pritzkow, H. *Pure Appl. Chem.* **2003**, 75, 1277. (c) Grimes, R. N. *Pure Appl. Chem.* **2003**, 75, 1211. (d) Hosmane, N. S.; Maguire, J. A. *Organometallics* **2005**, 24, 1356.
- (6) (a) Grimes, R. N. *J. Am. Chem. Soc.* **1966**, 88, 1070. (b) Grimes, R. N. *J. Am. Chem. Soc.* **1966**, 88, 1895. (c) Grimes, R. N. *J. Organomet. Chem.* **1967**, 8, 45. (d) Grimes, R. N.; Bramlett, C. L. *J. Am. Chem. Soc.* **1967**, 89, 2557. (e) Grimes, R. N.; Bramlett, C. L.; Vance, R. L. *Inorg. Chem.* **1969**, 8, 55.
- (7) (a) Scott, J. E., Jr.; Spielman, J. R. *U. S. Clearinghouse Fed. Sci. Tech. Inform.* **1968**, AD 666314. (b) Seklemian, H. V.; Williams, R. E. *Inorg. Nuc. Chem. Lett.* **1967**, 3, 289. (c) Spielman, J. R.; Scott, J. E., Jr. *J. Am. Chem. Soc.* **1965**, 87, 3512.
- (8) (a) Köster, R.; Rotermund, G. W. *Tetrahedron Lett.* **1964**, 5, 1667. (b) Köster, R.; Rotermund, G. W. *Tetrahedron Lett.* **1965**, 6, 777.
- (9) (a) Köster, R.; Grassberger, M. A. *Angew. Chem., Int. Ed. Engl.* **1966**, 5, 580. (b) Köster, R.; Grassberger, M. A. *Angew. Chem., Int. Ed. Engl.* **1967**, 6, 218. (c) Köster, R.; Grassberger, M. A.; Hoffmann, E. G.; Rotermund, G. W. *Tetrahedron Lett.* **1966**, 7, 905.
- (10) (a) Heying, T. L.; Ager, J. W., Jr.; Clark, S. L.; Mangold, D. J.; Goldstein, H. L.; Hillman, M.; Polak, R. J.; Szymanski, J. W. *Inorg. Chem.* **1963**, 2, 1089. (b) Fein, M. M.; Bobinski, J.; Mayes, N.; Schwartz, N. N.; Cohen, M. S. *Inorg. Chem.* **1963**, 2, 1111. (c) Fein, M. M.; Grafstein, D.; Paustian, J. E.; Bobinski, J.; Lichstein, B. M.; Mayes, N.; Schwartz, N. N.; Cohen, M. S. *Inorg. Chem.* **1963**,

- 2, 1115.
- (11) (a) Garrett, P. M.; Tebbe, F. N.; Hawthorne, M. F. *J. Am. Chem. Soc.* **1964**, *86*, 5016. (b) Tebbe, F. N.; Garrett, P. M.; Hawthorne, M. F. *J. Am. Chem. Soc.* **1964**, *86*, 4222. (c) Tebbe, F. N.; Garrett, P. M.; Hawthorne, M. F. *J. Am. Chem. Soc.* **1968**, *90*, 869.
- (12) (a) Dunks, G. B.; Hawthorne, M. F. *Inorg. Chem.* **1969**, *8*, 2667. (b) Dunks, G. B.; Hawthorne, M. F. *Inorg. Chem.* **1970**, *9*, 893. (c) Garrett, P. M.; Smart, J. C.; Ditta, G. S.; Hawthorne, M. F. *Inorg. Chem.* **1969**, *8*, 1907.
- (13) (a) Plešek, J.; Heřmánek, S. *Collect. Czech. Chem. Commun.* **1974**, *39*, 821. (b) Štíbr, B.; Plešek, J.; Heřmánek, S. *Collect. Czech. Chem. Commun.* **1973**, *38*, 338.
- (14) Kusari, U.; Li, Y.; Bradley, M. G.; Sneddon, L. G. *J. Am. Chem. Soc.* **2004**, *126*, 8662.
- (15) Burke, A.; Ellis, D.; Giles, B. T.; Hodson, B. E.; MacGregor, S. A.; Rosair, G. M.; Welch, A. J. *Angew. Chem. Int. Ed.* **2003**, *42*, 225.
- (16) (a) Grafstein, D.; Bobinski, J.; Dvorak, J.; Smith, H. F.; Schwartz, N. N.; Cohen, M. S.; Fein, M. M. *Inorg. Chem.* **1963**, *2*, 1120. (b) Heying, T. L.; Ager, J. W.; Clark, S. L.; Alexander, R. P.; Papetti, S.; Reid, J. A.; Trotz, S. I. *Inorg. Chem.* **1963**, *2*, 1097.
- (17) Gomez, F. A.; Johnson, S. E.; Hawthorne, M. F. *J. Am. Chem. Soc.* **1991**, *111*, 5915.
- (18) King, R. B. *Chem. Rev.* **2001**, *101*, 1119.

- (19) Kongpricha, S.; Schroeder, H. *Inorg. Chem.* **1969**, *8*, 2449.
- (20) (a) Schroeder, H.; Heying, T. L.; Reiner, J. R. *Inorg. Chem.* **1963**, *2*, 1092. (b) Sieckhaus, J. F.; Semenuk, N. S.; Knowles, T. A.; Schroeder, H. *Inorg. Chem.* **1969**, *8*, 2452.
- (21) Potenza, J. A.; Lipscomb, W. N. *Inorg. Chem.* **1966**, *5*, 1483.
- (22) Zakharkin, L. I.; Kalinin, V. N. *Izv. Akad. Nauk. SSSR, Ser. Khim.* **1966**, *3*, 575.
- (23) Srivastava, R. R.; Hamlin, D. K.; Wilbur, D. S. *J. Org. Chem.* **1996**, *61*, 9041.
- (24) Herzog, A.; Maderna, A.; Harakas, G. N.; Knobler, C. B.; Hawthorne, M. F. *Chem. Eur. J.* **1999**, *5*, 1212.
- (25) Wiesboeck, R. A.; Hawthorne, M. F. *J. Am. Chem. Soc.* **1964**, *86*, 1642.
- (26) (a) Hawthorne, M. F.; Young, D. C.; Wegner, P. A. *J. Am. Chem. Soc.* **1965**, *87*, 1818. (b) Zakharkin, L. I.; Kukulina, E. I.; Podvisotskaya, L. S. *Izv. Akad. Nauk. SSSR, Ser. Khim.* **1966**, 1866. (c) Roscoe, J. S.; Kongpricha, S.; Papetti, S. *Inorg. Chem.* **1970**, *9*, 1561.
- (27) Hawthorne, M. F.; Wegner, P. A.; Stafford, R. C. *Inorg. Chem.* **1965**, *4*, 1675.
- (28) (a) Getman, T. D.; Knobler, C. B.; Hawthorne, M. F. *J. Am. Chem. Soc.* **1990**, *112*, 4593. (b) Getman, T. D.; Knobler, C. B.; Hawthorne, M. F. *Inorg. Chem.* **1992**, *31*, 101.
- (29) (a) Dunks, G. B.; Wiersema, R. J.; Hawthorne, M. F. *J. Am. Chem. Soc.* **1973**, *95*, 3174. (b) Tolpin, E. I.; Lipscomb, W. N. *Inorg. Chem.* **1973**, *12*, 2257. (c) Churchill, M. R.; DeBoer, B. G. *Inorg. Chem.* **1973**, *12*, 2674. (d) Chui, K.; Li,

- H.-W.; Xie, Z. *Organometallics* **2000**, *19*, 5447.
- (30) (a) Zi, G.; Li, H.-W.; Xie, Z. *Organometallics* **2001**, *20*, 3836. (b) Zi, G.; Li, H.-W.; Xie, Z. *Chem. Commun.* **2001**, 1110. (c) Zi, G.; Li, H.-W.; Xie, Z. *Organometallics* **2002**, *21*, 5415. (d) Xie, Z. *Pure Appl. Chem.* **2003**, *75*, 1335.
- (31) (a) Grafstein, D.; Dvorak, J. *Inorg. Chem.* **1963**, *2*, 1128. (b) Papetti, S.; Obenland, C. O.; Heying, T. L. *Ind. Eng. Chem., Prod. Res. Develop.* **1966**, *5*, 334.
- (32) Lipscomb, W. N. *Science* **1966**, *153*, 373.
- (33) (a) Hodson, B. E.; McGrath, T. D.; Stone, F. G. A. *Organometallics* **2005**, *24*, 3386. (b) Hodson, B. E.; McGrath, T. D.; Stone, F. G. A. *Organometallics* **2005**, *24*, 14. (c) Burke, A.; Ellis, D.; Ferrer, D.; Ormsby, D. L.; Rosair, G. M.; Welch, A. J. *Dalton Trans.* **2005**, 1716. (d) Hodson, B. E.; McGrath, T. D.; Stone, F. G. A. *Organometallics* **2005**, *24*, 1638. (e) Wang, S.; Li, H.-W.; Xie, Z. *Organometallics* **2004**, *23*, 3780. (f) Wang, S.; Li, H.-W.; Xie, Z. *Organometallics* **2004**, *23*, 2469. (g) Hodson, B. E.; McGrath, T. D.; Stone, F. G. A. *Dalton Trans.* **2004**, 2570. (h) Wang, S.; Wang, Y.; Cheung, M.-S.; Chan, H.-S.; Xie, Z. *Tetrahedron* **2003**, *59*, 52. (i) Laguna, M. A.; Ellis, D.; Rosair, G. M.; Welch, A. J. *Inorg. Chim. Acta* **2003**, *347*, 161. (j) Garrioch, R. M.; Kuballa, P.; Low, K. S.; Rosair, G. M.; Welch, A. J. *J. Organomet. Chem.* **1999**, *575*, 57.
- (34) For recent reviews, see: (a) Grimes, R. N. *Coord. Chem. Rev.* **2000**, *200/202*, 773. (b) Saxena, A. K.; Hosmane, N. S. *Chem. Rev.* **1993**, *93*, 1081. (c) Saxena, A. K.; Maguire, J. A.; Hosmane, N. S. *Chem. Rev.* **1997**, *97*, 2421. (d) Xie, Z.

- Coord. Chem. Rev.* **2002**, 231, 23. (e) Xie, Z. *Pure Appl. Chem.* **2001**, 73, 361.
- (f) Xie, Z. *Acc. Chem. Res.* **2003**, 36, 1. (g) Hosmane, N. S.; Maguire, J. A. *Organometallics* **2005**, 24, 1356.
- (35) Wong, K.-H.; Chan, H.-S.; Xie, Z. *Organometallics* **2003**, 22, 1775.
- (36) (a) McIntosh, R.; Ellis, D.; Gil-Lostes, J.; Dalby, K. J.; Rosair, G. M.; Welch, A. J. *Dalton Trans.* **2005**, 1842. (b) Kwong, W.-C.; Chan, H.-S.; Tang, Y.; Xie, Z. *Organometallics* **2004**, 23, 3098.
- (37) Deng, L.; Cheung, M.-S.; Chan, H.-S.; Xie, Z. *Organometallics* **2005**, 24, 6244.
- (38) Grimes, R. N. *Angew. Chem. Int. Ed.* **2003**, 42, 1198.
- (39) Zakharkin, L. I. *Izv. Akad. Nauk. SSSR, Ser. Khim.* **1965**, 1114.
- (40) (a) Deng, L.; Chan, H.-S.; Xie, Z. *J. Am. Chem. Soc.* **2006**, 128, 5219. (b) Deng, L.; Xie, Z. *Coord. Chem. Rev.* **2007**, 251, 2452-2476. (c) Deng, L.; Xie, Z. *Organometallics* **2007**, 26, 1832-1845. (d) Deng, L.; Zhang, J.; Chan, H.-S.; Xie, Z. *Angew. Chem. Int. Ed.* **2006**, 45, 4309.
- (41) For $B_{12}H_{12}^{2-}$, see: (a) Peymann, T.; Knobler, C. B.; Hawthorne, M. F. *J. Am. Chem. Soc.* **1999**, 121, 5601. (b) Peymann, T.; Knobler, C. B.; Khan, S. I.; Hawthorne, M. F. *Angew. Chem. Int. Ed.* **2001**, 40, 1664. (c) Peymann, T.; Knobler, C. B.; Khan, S. I.; Hawthorne, M. F. *J. Am. Chem. Soc.* **2001**, 123, 2182. (d) Sivaev, I. B.; Bregadze, V. I.; Sjöberg, S. *Collect. Czech. Chem. Commun.* **2002**, 67, 679. (e) Farha, O. K.; Julius, R. L.; Lee, M. W.; Huertas, R. E.; Knobler, C. B.; Hawthorne, M. F. *J. Am. Chem. Soc.* **2005**, 127, 18243.

- (42) For $\text{CB}_{11}\text{H}_{12}^-$, see: (a) Jelinek, T.; Plešek, J.; Heřmánek, S.; Štíbr, B. *Collect. Czech. Chem. Commun.* **1986**, *51*, 819. (b) Jelinek, T.; Baldwin, P.; Scheidt, W. R.; Reed, C. A. *Inorg. Chem.* **1993**, *32*, 1982. (c) Xie, Z.; Jelinek, T.; Bau, R.; Reed, C. A. *J. Am. Chem. Soc.* **1994**, *116*, 1907. (d) King, B. T.; Janousek, Z.; Gruener, B.; Trammell, M.; Noll, B. C.; Michl, J. *J. Am. Chem. Soc.* **1996**, *118*, 3313. (e) Xie, Z.; Manning, J.; Reed, R. W.; Mathur, R.; Boyd, P. D. W.; Benesi, A.; Reed, C. A. *J. Am. Chem. Soc.* **1996**, *118*, 2922. (f) Xie, Z.; Tsang, C. W.; Xue, F.; Mak, T. C. W. *Inorg. Chem.* **1997**, *36*, 2246. (g) Ivanov, S. V.; Rockwell, J. J.; Polyakov, O. G.; Gaudinski, C. M.; Anderson, O. P.; Solntsev, K. A.; Strauss, S. H. *J. Am. Chem. Soc.* **1998**, *120*, 4224. (h) Xie, Z.; Tsang, C. W.; Sze, E. T. P.; Yang, Q.; Chan, D. T. W.; Mak, T. C. W. *Inorg. Chem.* **1998**, *37*, 6444. (i) Tsang, C. W.; Xie, Z. *Chem. Commun.* **2000**, 1839. (j) Clarke, A. J.; Ingleson, M. J.; Kociok-Köhn, G.; Mahon, M. F.; Patmore, N. J.; Rourke, J. P.; Ruggiero, G. D.; Weller, A. S. *J. Am. Chem. Soc.* **2004**, *126*, 1503.
- (43) For $\text{C}_2\text{B}_{10}\text{H}_{12}$, see: ref. 19 to 24 and: (a) Bregadze, V. I. *Chem. Rev.* **1992**, *92*, 209. (b) Jiang, W.; Knobler, C. B.; Mortimer, M. D.; Hawthorne, M. F. *Angew. Chem. Int. Ed.* **1995**, *34*, 1332. (c) Jiang, W.; Knobler, C. B.; Hawthorne, M. F. *Angew. Chem. Int. Ed.* **1996**, *35*, 2536. (d) Herzog, A.; Knobler, C. B.; Hawthorne, M. F. *Angew. Chem. Int. Ed.* **1998**, *37*, 1552. (e) Herzog, A.; Callahan, R. P.; Macdonald, C. L. B.; Lynch, V. M.; Hawthorne, M. F.; Lagow, R. J. *Angew. Chem. Int. Ed.* **2001**, *40*, 2121. (f) Herzog, A.; Knobler, C. B.; Hawthorne, M. F. *J. Am. Chem. Soc.* **2001**, *123*, 12791. (g) Barberà, G.; Teixidor,

- F.; Viñas, C.; Sillanpää, R.; Kivekäs, R. *Eur. J. Inorg. Chem.* **2003**, 8, 1511. (h)
- Teixidor, F.; Barberà, G.; Vaca, A.; Kivekäs, R.; Sillanpää, R.; Oliva, J.; Viñas, C. *J. Am. Chem. Soc.* **2005**, 127, 10158.
- (44) Zhang, J.; Deng, L.; Chan, H.-S.; Xie, Z. *J. Am. Chem. Soc.* **2007**, 129, 18.
- (45) Minkin V. I. *Pure Appl. Chem.* **1999**, 71(10), 1919.
- (46) Williams, R. E. *Inorg. Chem.* **1971**, 10, 210; Williams, R. E. *Adv. Inorg. Chem. Radiochem.* **1976**, 18, 67.
- (47) (a) Einholz, W.; Vaas, K.; Wieloch, C.; Speiser, B.; Wizemann, T.; Strobele, M.; Meyer, H.-J. *Z. Anorg. Allg. Chem.* **2002**, 628, 258. (b) Binder, H.; Kellner, R.; Vaas, K.; Hein, M.; Baumann, F.; Wanner, M.; Winter, R.; Kaim, W.; Honle, W.; Grin, Y.; Wedig, U.; Schultheiss, M.; Kremer, R. K.; Schnering, H. G. Von; Groeger, O.; Engelhardt, G. *Z. Anorg. Allg. Chem.* **1999**, 625, 1638. (c) Speiser, B.; Tittel, C.; Einholz, W.; Schafer, R. *J. Chem. Soc., Dalton Trans.*, **1999**, 1741. (d) Heinrich, A.; Keller, H.-L.; Preetz, W. *Z. Naturforsch B* **1990**, 45, 184. (e) Lorenzen, V.; Preetz, W. *Z. Naturforsch B* **1997**, 52, 565. (f) Speiser, B.; Wizemann, T.; Wurde, M. *Inorg. Chem.* **2003**, 42, 4018.
- (48) (a) Peymann, T.; Knobler, C. B.; Hawthorne, M. F. *Chem. Commun.* **1999**, 2039. (b) Farha, O. K.; Julius, R. L.; Lee, M. W.; Huertas, R. E.; Knobler, C. B.; Hawthorne, M. F. *J. Am. Chem. Soc.* **2005**, 127, 18243.
- (49) King, B. T.; Noll, B. C.; McKinley, A. J.; Michl, J. *J. Am. Chem. Soc.* **1996**, 118, 10902.
- (50) For reviews, see: (a) Hosmane, N. S.; Maguire, J. A. In *Comprehensive*

- Organometallic Chemistry III*; Crabtree, R. H., Mingos, D. M. P., Eds.; Elsevier: Oxford, 2006; Vol. 4, Chapter 3.05, p 175. (b) Fox, M. A. In *Comprehensive Organometallic Chemistry III*; Crabtree, R. H., Mingos, D. M. P., Eds.; Elsevier: Oxford, 2006; Vol. 4, Chapter 3.02, p 49. (c) Grimes, R. N. Metallocarboranes. In *Comprehensive Organometallic Chemistry II*; Abel, E. W.; Stone, F. G. A.; Wilkinson, G., Eds. Pergamon: New York, 1995; Vol. 1, p 373. (d) Xie, Z. *Coord. Chem. Rev.* **2002**, *231*, 23.
- (51) For examples, see: (a) Zakharkin, L. I. *Pure Appl. Chem.* **1972**, *29*, 513. (b) Morris, J. H.; Gysling, H. J.; Reed, D. *Chem. Rev.* **1985**, *85*, 51. (c) Yarosh, M. V.; Baranova, T. V.; Shirokii, V. L.; Erdman, A. A.; Maier, N. A. *Elektrokhimiya* **1994**, *30*, 406. (d) Fox, M. A.; Nervi, C.; Crivello, A.; Low, P. *J. Chem. Commun.* **2007**, 2372.
- (52) Chui, K.; Li, H.-W.; Xie, Z. *Organometallics* **2000**, *19*, 5447.
- (53) Hermansson, K.; Wojcik, M.; Sjöberg, S. *Inorg. Chem.* **1999**, *38*, 6039.
- (54) Hota, N. K.; Matteson, D. S. *J. Am. Chem. Soc.* **1968**, *90*, 3570.
- (55) Matteson, D. S.; Davis, R. A. *Inorg. Chem.* **1974**, *13*, 859.
- (56) Heying, T. L.; Ager, J. W., Jr.; Clark, S. L.; Alexander, R. P.; Papetti, S.; Reid, J. A.; Trotz, S. I. *Inorg. Chem.* **1963**, *2*, 1097.
- (57) Nakamura, H.; Aoyagi, K.; Yamamoto Y. *J. Am. Chem. Soc.* **1998**, *120*, 1167.
- (58) Deng, L.; Chan, H.-S.; Xie, Z. *J. Am. Chem. Soc.* **2006**, *128*, 7728.
- (59) Sheldrick, G. M. SADABS: Program for Empirical Absorption Correction of Area Detector Data. University of Göttingen: Germany, 1996.

- (60) Sheldrick, G. M. SHELXTL 5.10 for Windows NT: Structure Determination Software Programs. Bruker Analytical X-ray systems, Inc.: Madison, Wisconsin, USA, 1997.
- (61) Flack, H. D. *Acta Cryst.* **1983**, *A39*, 876.
- (62) Fu, X.; Chan, H. S.; Xie, Z. *J. Am. Chem. Soc.* **2007**, *129*, 8964.
- (63) Deng, L.; Chan, H. S.; Xie, Z. *Angew. Chem., Int. Ed.* **2005**, *44*, 2128.
- (64) Morris, J. H.; Gysling, H. J.; Reed, D. *Chem. Rev.* **1985**, *85*, 51.

Appendix I. Publications Based on the Research Findings

1. Xiaodu Fu, Hoi-Shan Chan, and Zuowei Xie. "Synthesis and Crystal Structure of a 13-Vertex Carborane Radical Anion with $2n+3$ Framework Electrons" *J. Am. Chem. Soc.* **2007**, *129*, 8964 - 8965.

Appendix II. Crystal Data and Summary of Data Collection and Refinement

	I-7	II-4	II-6	III-1
formula	C ₁₂ H ₂₀ B ₁₀	C ₁₂ H ₂₃ B ₁₁	C ₁₂ H ₂₁ B ₁₁	C ₂₅ H ₅₇ B ₁₁ NaO ₈
crystal size (mm)	0.50 x 0.50 x 0.40	0.50 x 0.40 x 0.30	0.50 x 0.50 x 0.40	0.50 x 0.40 x 0.20
fw	272.4	286.2	284.2	627.6
crystal system	monoclinic	orthorhombic	monoclinic	monoclinic
space group	<i>P</i> 2 ₁ / <i>n</i>	<i>P</i> ca2 ₁	<i>P</i> 2 ₁ / <i>n</i>	<i>C</i> 2/ <i>m</i>
<i>a</i> , Å	10.039(3)	18.109(1)	10.617(2)	30.551(2)
<i>b</i> , Å	14.627(4)	13.101(1)	14.741(3)	11.514(8)
<i>c</i> , Å	11.432(3)	14.468(1)	10.829(2)	10.562(7)
α , deg	90	90	90	90
β , deg	96.92(1)	90	99.09(1)	97.58(1)
γ , deg	90	90	90	90
<i>V</i> , Å ³	1666.4(9)	3432.5(3)	1673.7(5)	3683(4)
<i>Z</i>	4	8	4	4
<i>D</i> _{calcd} , Mg/m ³	1.086	1.108	1.128	1.132
radiation (λ), Å	Mo (0.71073)	K α Mo (0.71073)	K α Mo (0.71073)	K α Mo (0.71073)
2 θ range, deg	4.54 to 56.20	3.84 to 55.96	4.70 to 56.14	2.68 to 50.00
μ , mm ⁻¹	0.052	0.052	0.053	0.084
<i>F</i> (000)	568	1200	592	1348
no. of obsd rflns	4046	7981	4050	3383
no. of params refnd	199	415	208	260
goodness of fit	1.021	0.996	1.001	1.093
R1	0.0651	0.0726	0.0590	0.0881
wR2	0.1655	0.1900	0.1394	0.2227

	III-3	III-4	IV-7
formula	C ₂₆ H ₅₉ B ₁₁ NaO ₈	C ₃₂ H ₆₃ B ₁₁ NaO ₈	C ₂₆ H ₅₀ B ₁₁ LiO ₄
crystal size (mm)	0.40 x 0.30 x 0.20	0.40 x 0.30 x 0.20	0.20 x 0.10 x 0.10
fw	641.6	717.7	552.5
crystal system	monoclinic	orthorhombic	orthorhombic
space group	C2/m	P2 ₁ 2 ₁ 2 ₁	Pna2 ₁
a, Å	31.940(2)	9.806(2)	19.642(2)
b, Å	11.552(5)	12.167(2)	15.127(2)
c, Å	10.369(5)	34.318(4)	11.638(2)
α, deg	90	90	90
β, deg	102.00(2)	90	90
γ, deg	90	90	90
V, Å ³	3742(3)	4094.1(7)	3457.6(6)
Z	4	4	2
D _{calcd} , Mg/m ³	1.139	1.164	1.061
radiation (λ), Å	Mo Kα (0.71073)	Mo Kα (0.71073)	Mo Kα (0.71073)
2θ range, deg	2.60 to 50.00	3.56 to 50.00	3.40 to 50.00
μ, mm ⁻¹	0.084	0.084	0.062
F(000)	1380	1540	1184
no. of obsd rflns	3477	6958	6059
no. of params refnd	229	577	383
goodness of fit	1.956	1.014	1.036
R1	0.1337	0.0952	0.0960
wR2	0.4293	0.2563	0.2637

CUHK Libraries



004561485